

AD

AD 747807

USAAMRDL TECHNICAL REPORT 72-49
SPRAG OVERRIDING AIRCRAFT CLUTCH

By

P. Lynwander
A. G. Meyer
S. Chachakis

July 1972

EUSTIS DIRECTORATE
U. S. ARMY AIR MOBILITY RESEARCH AND DEVELOPMENT LABORATORY
FORT EUSTIS, VIRGINIA

CONTRACT DAAJ02-71-C-0028
AVCO LYCOMING DIVISION
STRATFORD, CONNECTICUT

Approved for public release;
distribution unlimited.



Reproduced by
**NATIONAL TECHNICAL
INFORMATION SERVICE**
U S Department of Commerce
Springfield VA 22151

D D C
RECEIVED
SEP 5 1972
REGISTERED
B

166

DISCLAIMERS

The findings in this report are not to be construed as an official Department of the Army position unless so designated by other authorized documents.

When Government drawings, specifications, or other data are used for any purpose other than in connection with a definitely related Government procurement operation, the United States Government thereby incurs no responsibility nor any obligation whatsoever; and the fact that the Government may have formulated, furnished, or in any way supplied the said drawings, specifications, or other data is not to be regarded by implication or otherwise as in any manner licensing the holder or any other person or corporation, or conveying any rights or permission, to manufacture, use, or sell any patented invention that may in any way be related thereto.

Trade names cited in this report do not constitute an official endorsement or approval of the use of such commercial hardware or software.

DISPOSITION INSTRUCTIONS

Destroy this report when no longer needed. Do not return it to the originator.

PROCESSED BY		
110	White Section	<input checked="" type="checkbox"/>
110	Blue Section	<input type="checkbox"/>
110	Other Section	<input type="checkbox"/>
AUTHORITY		
BY		
DISTRIBUTION/AVAILABILITY CODES		
Dist.	AVAIL. ORG. or SPECIAL	
A		

Unclassified
Security Classification

DOCUMENT CONTROL DATA - R & D

(Security classification of title, body of abstract and indexing annotation must be entered when the overall report is classified)

1. ORIGINATING ACTIVITY (Corporate author) Avco Lycoming Division Stratford, Connecticut		2a. REPORT SECURITY CLASSIFICATION Unclassified	
		2b. GROUP	
3. REPORT TITLE SPRAG OVERRIDING AIRCRAFT CLUTCH			
4. DESCRIPTIVE NOTES (Type of report and inclusive dates) Final Report			
5. AUTHOR(S) (First name, middle initial, last name) P. Lynwander A. G. Meyer S. Chachakis			
6. REPORT DATE July 1972	7a. TOTAL NO. OF PAGES 164	7b. NO. OF REFS 3	
8a. CONTRACT OR GRANT NO. DAAJ02-71-C-0028		8b. ORIGINATOR'S REPORT NUMBER(S) USAAMRDL Technical Report 72-49	
9. PROJECT NO. 1G162207AA72		9c. OTHER REPORT NO(S) (Any other numbers that may be assigned this report) Avco Lycoming Report No. 105.7.11	
10. DISTRIBUTION STATEMENT Approved for public release; distribution unlimited.			
11. SUPPLEMENTARY NOTES		12. SPONSORING MILITARY ACTIVITY Eustis Directorate U.S. Army Air Mobility R&D Laboratory Fort Eustis, Virginia	
13. ABSTRACT The purpose of this program was to investigate the performance of high-speed overrunning clutch assemblies for use in a multiengine helicopter. The design operating conditions were 3,570 inch-pounds torque transmitted at 26,500 rpm. Two clutch configurations with differing design philosophies were evaluated. One design utilizes inner and outer sprag retainers with a central energizing ribbon spring. The other design positions the sprags with one retainer and incorporates garter springs at the sprag edges. An extensive test program was conducted as follows: 1. Full-Speed Dynamic Clutch Override Test - Operation at zero input speed and 26,500 rpm output speed for 5-hour runs at various oil flows 2. Differential-Speed Dynamic Clutch Override Test - Operation at output speed of 26,500 rpm and input speeds of 13,250 (50 percent normal rated), 17,755 (67 percent normal rated) and 19,875 (75 percent normal rated) rpm 3. Dynamic Engagement Test - Simulated high-speed engagements 4. Static Cyclic Torque Fatigue Test - Operation at 7,140 ± 900 inch-pounds for 10 ⁷ cycles 5. Static Overload Test - Torque application to failure Drag torque and metal and oil temperatures were measured during the dynamic testing. Results of the test program indicated that the most severe operating condition was differential speed operation and that both clutch configurations would require design modifications to operate successfully in this mode. An analysis of high-speed sprag clutch operation was performed, and a computer program was developed as an initial step to provide a mathematical model of clutch operation reflecting modern, high-speed mechanical technology.			

DD FORM 1473

REPLACES DD FORM 1473, 1 JAN 66, WHICH IS OBSOLETE FOR ARMY USE.

Unclassified
Security Classification

1



**DEPARTMENT OF THE ARMY
U. S. ARMY AIR MOBILITY RESEARCH & DEVELOPMENT LABORATORY
EUSTIS DIRECTORATE
FORT EUSTIS, VIRGINIA 23004**

The research described herein was conducted by AVCO/Lycoming Division, under the terms of contract DAAJ02-71-C-0028. The work was performed under the technical management of Mr. E. R. Givens, assisted by Mr. D. P. Lubrano, Propulsion Division, Eustis Directorate.

VTOL drive systems must incorporate an overrunning (free-wheel) clutch unit so that in the event of engine malfunction, the aircraft can safely autorotate or, in the case of multiengines, proceed on single-engine operation. Current overrunning speeds are limited to approximately 12,000 rpm or less, depending on the torque transmitted. The objective of this program was to evaluate sprag type clutches operating at engine input conditions of 26,500 rpm and 1500 hp.

Appropriate technical personnel of this Directorate have reviewed this report and concur with the conclusions contained herein.

Project IG162207AA72
Contract DAAJ02-71-C-0028
USAAMRDL Technical Report 72-49
July 1972

SPRAG OVERRIDING
AIRCRAFT CLUTCH

Final Report

Avco Lycoming Report No. 105. 7. 11

By

P. Lynwander
A. G. Meyer
S. Chachakis

Prepared by

Avco Lycoming Division
Stratford, Connecticut

for

EUSTIS DIRECTORATE
U. S. ARMY AIR MOBILITY RESEARCH
AND DEVELOPMENT LABORATORY
FORT EUSTIS, VIRGINIA

iv

Approved for public release; distribution unlimited.

SUMMARY

The purpose of this program was to investigate the performance of high-speed overrunning clutch assemblies for use in a multiengine helicopter. The design operating conditions were 3, 570 inch-pounds torque transmitted at 26, 500 rpm. Two clutch configurations with differing design philosophies were evaluated. One design utilizes inner and outer sprag retainers with a central energizing ribbon spring. The other design positions the sprags with one retainer and incorporates garter springs at the sprag edges.

An extensive test program was conducted as follows:

1. Full-Speed Dynamic Clutch Override Test - Operation at zero input speed and 26, 500 rpm output speed for 5-hour runs at various oil flows
2. Differential Speed Dynamic Clutch Override Test - Operation at output speed of 26, 500 rpm and input speeds of 13, 250 (50 percent normal rated), 17, 755 (67 percent normal rated) and 19, 875 (75 percent normal rated) rpm
3. Dynamic Engagement Test - Simulated high-speed engagements
4. Static Cyclic Torque Fatigue Test - Operation at $7, 140 \pm 900$ inch-pounds for 10^7 cycles
5. Static Overload Test - Torque application to failure

Drag torque and metal and oil temperatures were measured during the dynamic testing. Results of the test program indicated that the most severe operating condition was differential speed operation and that both clutch configurations would require design modifications to operate successfully in this mode.

An analysis of high-speed sprag clutch operation was performed, and a computer program was developed as an initial step to provide a mathematical model of clutch operation reflecting modern, high-speed mechanical component technology.

✓

FOREWORD

This program was conducted for the U. S. Army Air Mobility Research and Development Laboratory under Contract DAAJ02-71-C-0028, Project 1G162207AA72. The period of performance was 15 March through 15 December 1971.

U. S. Army technical direction was provided by Mr. R. Givens and Mr. D. Lubrano.

Acknowledgement is made to the engineering staffs of the following organizations for their assistance in the design, fabrication, and evaluation of the clutches used in this program:

Spring Division, Borg-Warner Corporation, Bellwood, Illinois

Formsprag Company, Warren, Michigan

TABLE OF CONTENTS

	<u>Page</u>
SUMMARY.....	iii
FOREWORD.....	v
LIST OF ILLUSTRATIONS.....	viii
LIST OF TABLES.....	xiii
LIST OF SYMBOLS.....	xiv
INTRODUCTION.....	1
DESIGN AND ANALYSIS.....	3
TEST FACILITY.....	18
TEST PROCEDURE.....	31
TEST RESULTS AND DISCUSSION.....	43
METALLURGICAL STUDY.....	82
CONCLUSIONS.....	87
APPENDIXES	
I. Analysis of Clutch Operation.....	89
II. Computer Program.....	109
III. Raw Data, Override Test.....	139
DISTRIBUTION.....	145

LIST OF ILLUSTRATIONS

<u>Figure</u>		<u>Page</u>
1	Principle of Sprag Clutch Operation	4
2	Clutch Modes of Operation	5
3	Clutch Designs A and B	7
4	Clutch Design A Details	8
5	Clutch Design B Details	10
6	Clutch Lubrication Details	13
7	Inner Race Lubrication Hole Pattern	14
8	Overall Rig Arrangement	19
9	Test Rig Installation	21
10	Test Cartridge Details	22
11	Lubrication Schematic	23
12	Console and Instrument Panel	24
13	Clutch Instrumentation Schematic	26
14	Cyclic Fatigue Test Schematic	27
15	Cyclic Fatigue Test Installation	29
16	Static Overload Test Installation	30
17	Typical Log Sheet	32
18	Indi-Ron	38
19	Proficorder	39

<u>Figure</u>		<u>Page</u>
20	Typical Proficorder Chart	40
21	Typical Indi-Ron Chart	41
22	Sprag Wear Following Override Test, Design A	44
23	Inner and Outer Races Following Override Test, Design A.	45
24	Sprag Wear Versus Hours of Operation, Design A Full- Speed Override (Input Stationary).	46
25	Sprag Condition Following Override Test, Design B.	47
26	Inner Race Following Override Test, Design B	48
27	Outer Race Following Override Test, Design B	49
28	Reaction Torque Versus Oil Flow, Design A Full- Speed Override (Input Stationary).	51
29	Reaction Torque Versus Oil Flow, Design B Full- Speed Override (Input Stationary).	52
30	Oil Leakage Paths.	53
31	Oil ΔT Versus Flow, Design A Full-Speed Override (Input Stationary).	55
32	Oil ΔT Versus Flow, Design B Full-Speed Override (Input Stationary).	56
33	Clutch Race Temperature Versus Oil Flow, Override Test, Design A	57
34	Clutch Race Temperature Versus Oil Flow, Override Test, Design B	58
35	Bearing Race Temperature Versus Oil Flow, Override Test, Design A	59
36	Bearing Race Temperature Versus Oil Flow, Override Test, Design B	60

<u>Figure</u>		<u>Page</u>
37	Design Modifications	61
38	Sprag Wear Following Differential Speed Test, Design A	63
39	Inner Race Following Differential Speed Test, Design A	64
40	Outer Race Following Differential Speed Test, Design B	65
41	Plot of Clutch Engagement, Design B	67
42	Sprag Wear Following Differential Speed Test, Design B	69
43	Inner Race Following Differential Speed Test, Design B	70
44	Outer Race Following Differential Speed Test, Design B	71
45	Methods of Decreasing Centrifugal Energizing Moment	73
46	Plot of Dynamic Engagement Test, Design A	75
47	Typical Clutch Race Condition Following Cyclic Fatigue Test	76
48	Bearing Fretting in Cyclic Fatigue Test	78
49	Sprag Rollover Failure	80
50	Diametral Growth of Outer Race	83
51	Angular Displacement of Outer Race	84
52	Sprag Microstructure	85
53	Sprag Case Hardness Versus Depth	86

<u>Figure</u>		<u>Page</u>
54	Sprag Cam Positions for Various Operating Conditions	90
55	Relationship Between Sprag Rotation Angle and Sprag Height for Parallel Flat Plates	92
56	Relationship Between Sprag Rotation Angle and Strut Angles for Curved Surface Raceways	94
57	Sprag Forces for the Torque Transmittal Mode of Operation	95
58	Sprag Forces for the Override or Differential Speed Modes of Operation	100
59	Spring Forces Acting on Sprag for Override or Differential Speed Modes of Operation	102
60	Computer Program Input Cards 3 and 4	112
61	Computer Program Input Card 5	113
62	Computer Program Input Card 6	115
63	Computer Program Input Card 7	116
64	Computer Program Input Card 8A	118
65	Computer Program Input Card 8B	119
66	Computer Program Output Data - Clutch Design A .	121
67	Computer Program Output Data - Clutch Design B .	122
68	Strut Angle Versus Sprag Height for Clutch Design A	123
69	Strut Angle Versus Sprag Height for Clutch Design B	124
70	Reaction Torque Versus Oil Flow at Various Speeds, Design A Full-Speed Override (Input Stationary). . .	141

<u>Figure</u>		<u>Page</u>
71	Reaction Torque Versus Oil Flow at Various Speeds, Design B Full-Speed Override (Input Stationary).	142
72	Oil ΔT Versus Flow at Various Speeds, Design A Full-Speed Override (Input Stationary).	143
73	Oil ΔT Versus Flow at Various Speeds, Design B Full-Speed Override (Input Stationary)	144

LIST OF TABLES

<u>Table</u>		<u>Page</u>
I	Clutch Geometry	9
II	Test Clutch Materials	11
III	Clutch Design Parameters	15
IV	Full-Speed Dynamic Clutch Override Oil Flows and Pressures	33
V	Full-Speed Override Test, Sprag Wear, Design A.	43
VI	Differential Speed Test Results, Design A.	56
VII	Conditions at Maximum Cyclic Fatigue Torque, 8,040 Inch-Pounds	77
VIII	Metallurgical Results, Case-Carburized Races	82

LIST OF SYMBOLS

b_i	half width of inner race contact area, override mode - in.
b_{iL}	half width of inner race contact area, torque transmittal mode - in.
b_{oL}	half width of outer race contact area, torque transmittal mode - in.
$\angle CG$	angle between lines connecting inner race contact point to center of clutch - deg
$\angle CB_S$	angle between a radial line to the spring contact point at the sprag back face and a line passing through the inner race contact point and the center of the clutch - deg
$\angle CF_S$	angle between a radial line to the spring contact point at the sprag front face and a line passing through the inner race contact point and the center of the clutch - deg
C_p	specific heat = .46 Btu/lb - °F
D	as-assembled spring diameter at the point of contact - in.
D_f	free spring diameter - in.
D_o	outer race inside diameter corresponding to outer strut angle α'_o - in.
D_{of}	outer race inside diameter resulting from radial growth due to rotation and pressure loading effects - in.
F_{CG}	sprag centrifugal force - lb
F_{SP}	total spring force for clutch design A - lb
$F_{SP'}$	spring deflection force for clutch design A - lb
$F_{SP''}$	spring centrifugal force - lb

$F_{SP'B}$	spring force acting normal to the back face of the sprag - lb
$F_{SP'F}$	spring force acting normal to the front face of the sprag - lb
F_{SRF}	spring deflection force for clutch design B - lb
F_{STB}	spring tangential component at the sprag back face - lb
F_{STF}	spring tangential component at the sprag front face - lb
G	materials parameter for film thickness calculations
g	acceleration due to gravity = 386.4 - in./sec ²
h_{EHD}	elastohydrodynamic film thickness at inner race contact point - in.
h_{HYD}	hydrodynamic film thickness at inner race contact point - in.
J	sprag height between parallel flat plates - in.
K_S	spring constant - lb/in.
K_{Wt}	conversion factor = 2.205×10^{-3} - lb/gm
L	sprag effective length - in.
M	oil flow - lb/hr
M_B	moment arm to back face at spring contact point in.
M_F	moment arm to front face at spring contact point - in.
m_G	sprag mass - lb-sec ² /in.
m_S	spring mass - lb-sec ² /in.

N	number of sprags
N_S	number of springs
\overline{OL}	distance between centers of sprag cam inner and outer radii of curvature - in.
P_i	external pressure at inner race outside diameter for override mode - psi
P_o	internal pressure at outer race inside diameter for torque transmittal mode - psi
Q	heat loss - Btu/hr
R	equivalent radius - in.
R_i	inner race outside radius - in. (engineering drawing)
R_{N_i}	normal force at inner race for override mode - lb
R_{N_o}	normal force at outer race for override mode - lb
R_{T_i}	tangential force at inner race for override mode - lb
R_{T_o}	tangential force at outer race for override mode - lb
$R_{N_{iL}}$	normal force at inner race for torque transmittal mode - lb
$R_{N_{oL}}$	normal force at outer race for torque transmittal mode - lb
$R_{T_{iL}}$	tangential force at inner race for torque transmittal mode - lb
$R_{T_{oL}}$	tangential force at outer race for torque transmittal mode - lb
RES_B	total spring force at sprag back face for clutch design B - lb

RES_F	total spring force at sprag front face for clutch design B - lb
RES_{TB}	spring combined tangential component at the sprag back face - lb
RES_{TF}	spring combined tangential component at the sprag front face - lb
r	radius to any point on inner or outer race - in.
r_1	outer race inside radius - in. (engineering drawing)
r_2	outer race outside radius - in. (engineering drawing)
r_{11}	outer race inside radius due to rotation - in.
r_{22}	outer race outside radius due to rotation - in.
r_{CG}	radius to sprag's center of gravity - in.
SC_I	compressive stress at inner race contact point - psi
SC_O	compressive stress at outer race contact point - psi
S_{rp}	radial stress due to pressure loading - psi
S_{rR}	radial stress due to rotation - psi
S_{tp}	tangential stress due to pressure loading - psi
S_{tR}	tangential stress due to rotation - psi
S_h	maximum hoop stress - psi
$\angle SP$	angle between lines connecting inner race contact point to center of clutch for clutch design B - deg
$\angle SP_B$	angle between a line that is tangent to the spring contact point at the sprag back face and a line passing through the inner race contact point and the center of the clutch for clutch design B - deg

$\angle SP_F$	angle between a line that is tangent to the spring contact point at the sprag front face and a line passing through the inner race contact point and the center of the clutch for clutch design B - deg
T	transmitted torque - in. -lb
U	velocity parameter for film thickness calculations
V_G	tangential velocity of sprag at the inner race contact point - fps
V_R	tangential velocity of the inner race at the contact point - fps
W	load parameter for film thickness calculations
W_G	sprag weight - lb
W_S	spring weight - lb
Y	difference between free and deflected position of the spring tang - in.
α	inner or outer strut angle for parallel flat plates - deg
α_i	inner strut angle for parallel flat plates - deg
α_o	outer strut angle for parallel flat plates - deg
α'_i	inner strut angle for curved surface raceways - deg
α'_o	outer strut angle for curved surface raceways - deg
α_L	lubricant pressure-viscosity coefficient = 95×10^{-6} - in. ² /lb
β	angle between lines connecting inner race contact point to center of clutch - deg
Δr_I	deflection of inner race contact points due to compression - in.

Δr_o	deflection of outer race contact points due to compression - in.
Δr_p	total radial growth of outer race inside radius - in.
Δr_R	radial growth due to rotation - in.
Δr_{R1}	radial growth of outer race inside radius due to rotation - in.
Δr_{R2}	radial growth of outer race outside radius due to rotation - in.
ΔT	change in oil temperature - $^{\circ}F$
δ	weight density constant = .282 - lb/in. ³
E	modulus of elasticity = 29×10^6 - psi
E'	materials factor - psi
η	design point speed - rpm
η_i	inner race speed - rpm
η_o	outer race speed - rpm
θ	sprag rotation angle - deg
μ_I	inner race traction coefficient of friction
μ_k	sliding coefficient of friction
μ_O	outer race traction coefficient of friction
μ_o	absolute viscosity of the lubricant = 73×10^{-8} reyns
ν	Poisson's ratio - 0.25
π	constant = 3.14159263

ρ_i sprag cam inner race radius of curvature - in.
 ρ_o sprag cam outer race radius of curvature - in.
 Σ sprag rotation angle as measured from 'X' coordinate axis - deg
 τ_d drag torque - in.-lb
 ω angular velocity - rad/sec

INTRODUCTION

The purpose of this program was to advance the technology of overrunning sprag clutch units to allow for reliable and efficient operation at speeds and loads commensurate with advanced aircraft gas turbine engines. The design operating conditions for this program were 26, 500 rpm and 3, 570 inch-pounds torque.

The overrunning clutch is a critical helicopter component that transmits engine torque in normal operation and allows the rotors to autorotate in case of engine malfunction. With the advent of multiple engine configurations, the overrunning clutch assumes an even greater role since the aircraft must be capable of operation with an engine shut down or with engines operating at different speeds.

Current transmission designs locate the clutch after the first or second gear reduction stage from the engine in order to eliminate problems associated with high-speed operation; however, this practice is costly in terms of component size, weight, and oil flow. To achieve the lightest configuration, the overrunning clutch must be located on the high-speed shaft before or in combination with the first gear reduction.

Difficulties associated with high-speed overrunning clutches fall into two categories:

1. Fatigue and overload capability
2. Problems associated with high-speed overrunning operation

The fatigue and overload capabilities of a clutch configuration are relatively easy to predict using established theory. Successful high-speed clutch operation depends upon the effect of clutch heat generation and deterioration during prolonged periods of freewheeling and differential speed. Also, clutch engagements and disengagements at high rates of speed and acceleration with attendant shock loads are a potential source of difficulties.

The approach taken to investigate these problems and to advance the technology of overrunning sprag clutches in the subject program follows:

1. An analytical study was conducted to arrive at the sprag clutch configuration best suited for high-speed aircraft operation. Two designs currently used in aircraft applications were considered. Design A features a sprag assembly positioned by outer and inner cages and a central energizing ribbon spring. Design B positions the sprags with one retainer and incorporates energizing garter springs at the sprag ends. Design B also incorporates a feature which prevents sprag rollover due to torque overload. Because both configurations have advantages, it was decided to evaluate the two designs both analytically and experimentally.
2. A computer program was developed to provide an analytical tool for the analysis of high-speed sprag clutches.
3. An extensive test program was conducted as follows:
 - a. Full-Speed Dynamic Clutch Override Test - Operation at zero input speed and 26,500 rpm output speed for 5-hour runs at various oil flows.
 - b. Differential Speed Dynamic Clutch Override Test - Operation at output speed of 26,500 rpm and input speeds of 13,250 (50 percent normal rated), 17,755 (67 percent normal rated) and 19,875 (75 percent normal rated) rpm.
 - c. Dynamic Engagement Test - Simulated high-speed engagements.
 - d. Static Cyclic Torque Fatigue Test - Operation at $7,140 \pm 900$ inch-pounds for 10^7 cycles.
 - e. Static Overload Test - Torque application to failure.

DESIGN AND ANALYSIS

DESCRIPTION OF CLUTCH OPERATION

The principle of sprag clutch operation is illustrated in Figure 1. The sprag component is designed with cross-corner dimensions such that $a > b$. Assuming that an engine is driving counterclockwise through the outer race, the wedging action of the sprag (contact through dimension "a") will drive a gearbox through the inner race. If the engine is shut down and the gearbox continues to rotate, the clutch will overrun (sprags rotate clockwise toward dimension "b"), thus achieving the desired effect of disengaging the engine and its associated drag torque from the power drive system.

A section of the clutch has been enlarged (Figure 2) to illustrate the forces involved during the driving and overrunning modes of operation. The outer or inner operating surfaces of the sprag may be thought of as cams of circular form. If radial lines are drawn from the center of the clutch through the centers of the radii determining the sprag surfaces, the intersections of these lines with the race surfaces define the contact points of the sprag with the races. A line drawn between the inner and outer race sprag contact points is called a strut, and the angles between this strut and the radial lines through the centers of the cam radii are called strut angles.

The transmitted components of the driving load (R_{TIL} , R_{TO_L}) are functions of the strut angles (α'_i) and (α'_o), respectively, such that $R_{TIL} = R_{NIL} \tan \alpha'_i$ and $R_{TO_L} = R_{NOL} \tan \alpha'_o$. The traction force equals $\mu_I R_{NIL}$ at the inner race and $\mu_O R_{NOL}$ at the outer race where μ_I and μ_O are coefficients of friction. Therefore, to ensure that the strut will not slip on the raceways and the torque will be transmitted through the clutch, the tangential force must be less than the available traction force ($R_{NIL} \tan \alpha'_i < \mu_I R_{NIL}$), ($R_{NOL} \tan \alpha'_o < \mu_O R_{NOL}$). If all components are made of the same material, μ_I will equal μ_O ; since $\alpha'_i = \alpha'_o + \beta$, it follows that $\alpha'_i > \alpha'_o$, so that the available traction force at the inner race will govern. For steel on steel, therefore, the inner strut angle must be approximately 4 degrees or less, since the tangent of 4 degrees is 0.07, which is approximately the coefficient of friction for this type of contact.

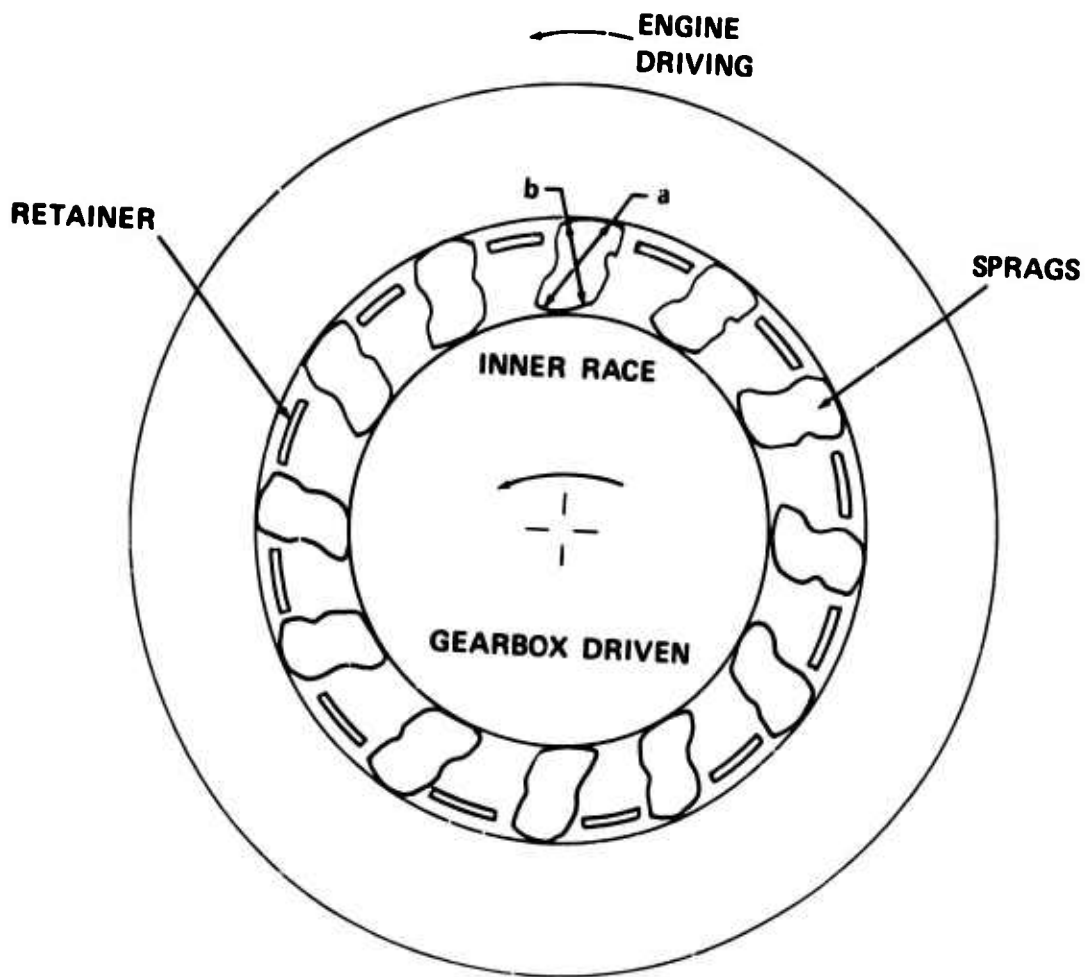


Figure 1. Principle of Sprag Clutch Operation.

A spring is normally added to the clutch to ensure traction (energizing) during driving, and to maintain raceway contact during overrunning. This spring force is designated by F_{sp} in Figure 2. To provide for equal load sharing (full phasing), a retainer is employed between the races, which keeps the sprags uniformly spaced. A centrifugal force F_{CG} , a result of the mass and rotation of the sprags, also acts to energize the clutch during the engine drive mode. No centrifugal force acts on the sprags during the overrunning mode because the tangential driving force component is greater at the inner race ($\alpha'_i > \alpha'_o$) so that slipping will occur initially at the inner race, and the sprags will remain stationary with the outer race.

An important feature of sprag cam design is the compounding of radii of curvature, especially at the inner race. When the clutch changes from the load to overrun mode of operation, called the release position, the radius of curvature at the inner race is greatly reduced, thus allowing the clutch to slip more easily into the overrun mode.

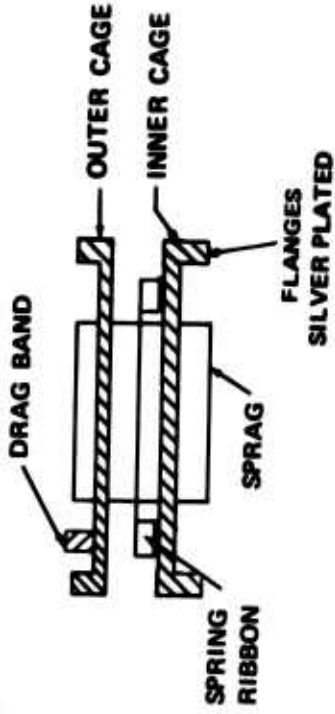
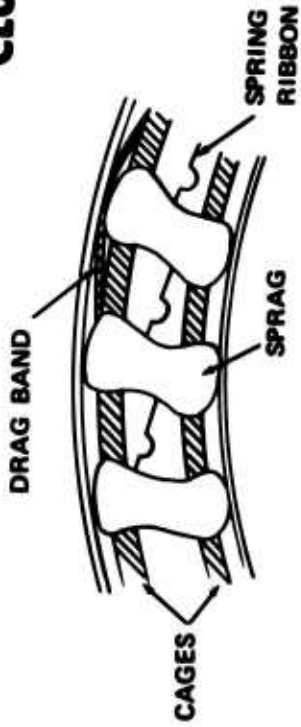
In addition to the conditions just described, drive and overrunning, a third mode of operation called "differential speed" must be evaluated. In a twinning application, if one engine is driving the gearbox, the clutch on the second engine is overrunning (inner race coupled to gearbox and rotating at speed of the first engine). If the second engine is started it cannot transmit torque to the gearbox until it accelerates to the first engine speed. During this time, however, centrifugal force of the sprags is acting to energize the clutch, and this condition is much more severe on the wear life of the clutch than pure overrunning. This mode of operation could occur during preflight checkout of the aircraft or during flight if one engine is driving and the other is maintained at idle for quick response to any need for reserve power.

DESCRIPTION OF TEST CLUTCHES

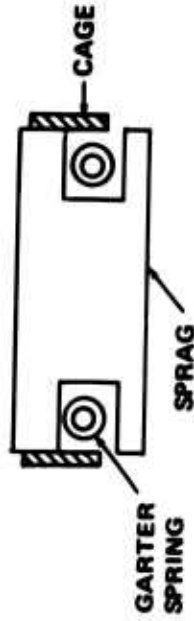
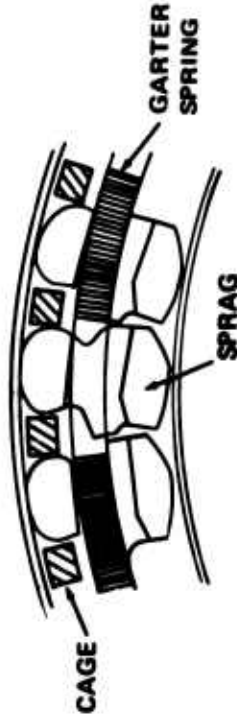
Two clutch designs currently used in aircraft applications were evaluated analytically and experimentally. The designs are designated "clutch design A" and "clutch design B." The difference in design philosophy is shown in Figure 3.

Clutch design A utilizes retainers (cages) both at the top and bottom of the sprags with a ribbon spring in between. The outer retainer pilots on the outer race and the inner retainer in turn pilots on the inner race. A stainless steel drag band was incorporated on the outer retainer to create frictional drag between the sprag assembly and the outer race. Clutch design A components are shown in Figure 4.

CLUTCH A



CLUTCH B



OVERLOADED CLUTCH
SHOWING FEATURE
THAT PREVENTS SPRAGS
FROM ROLLING OVER



Figure 3. Clutch Designs A and B.

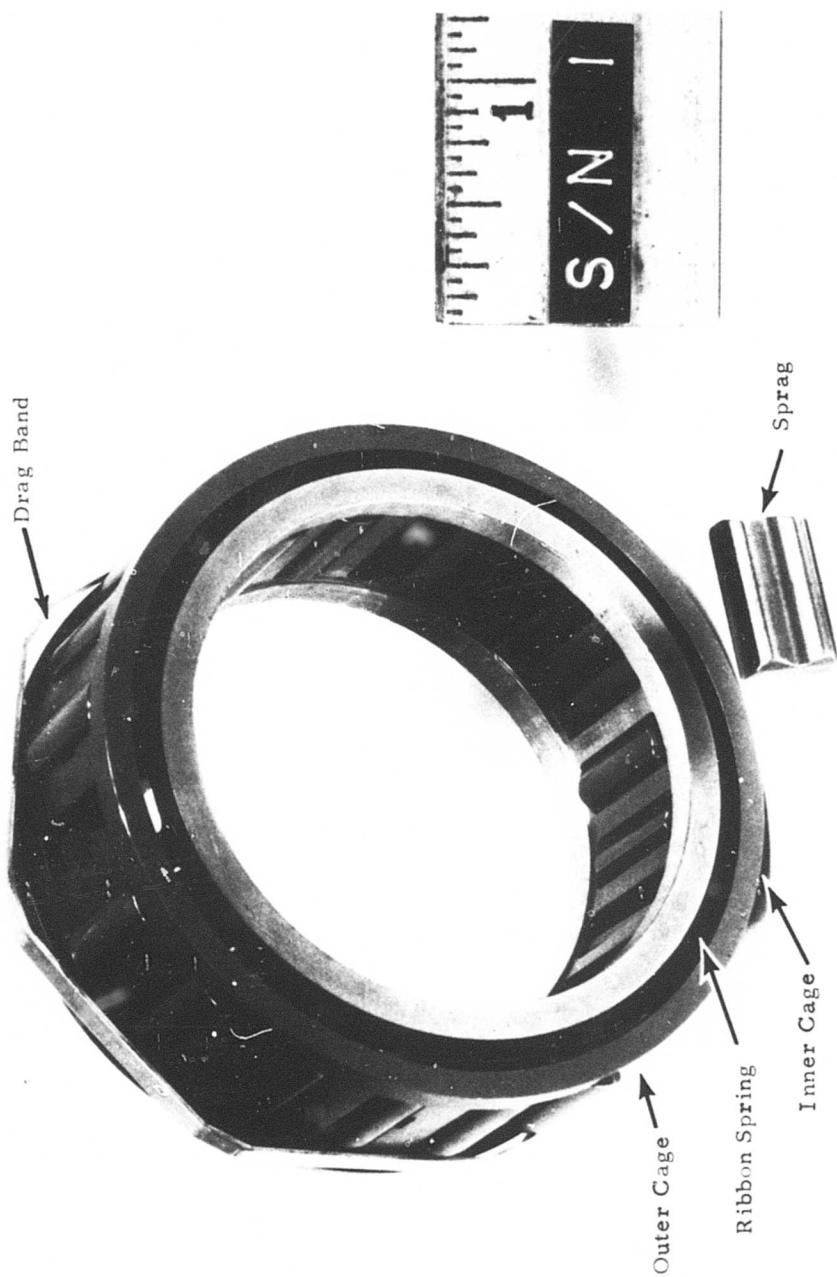


Figure 4. Clutch Design A Details.

Clutch design B utilizes a single retainer piloted by the outer race with garter springs at each end of the sprags. This design also incorporates a feature which prevents sprag rollover from torque overload. The sprags are designed to contact and lock up against one another when overloaded (Figure 3). Clutch design B components are shown in Figure 5.

Both clutch designs, in addition to energizing the sprags by springs, use centrifugal engaging. The center of gravity of the sprag is located to provide an engaging moment when the sprag assembly is rotating.

Pertinent dimensions for clutch designs A and B are listed in Table I, and materials data are listed in Table II.

TABLE I. CLUTCH GEOMETRY		
	Design A	Design B
Outer Race OD (in.)	3.7500	3.0950
Outer Race ID (in.)	2.9042	2.4060
Inner Race OD (in.)	2.1562	1.7500
Inner Race ID (in.)	1.0000	1.0000
Number of Sprags	20	24
Sprag Effective Length (in.)	0.665	0.880
Race Surface Finish (AA)	20 Max	20 Max
Sprag Surface Finish (AA)	12 Max	7 Max
Eccentricity of Races	0.0015 Max	0.0015 Max

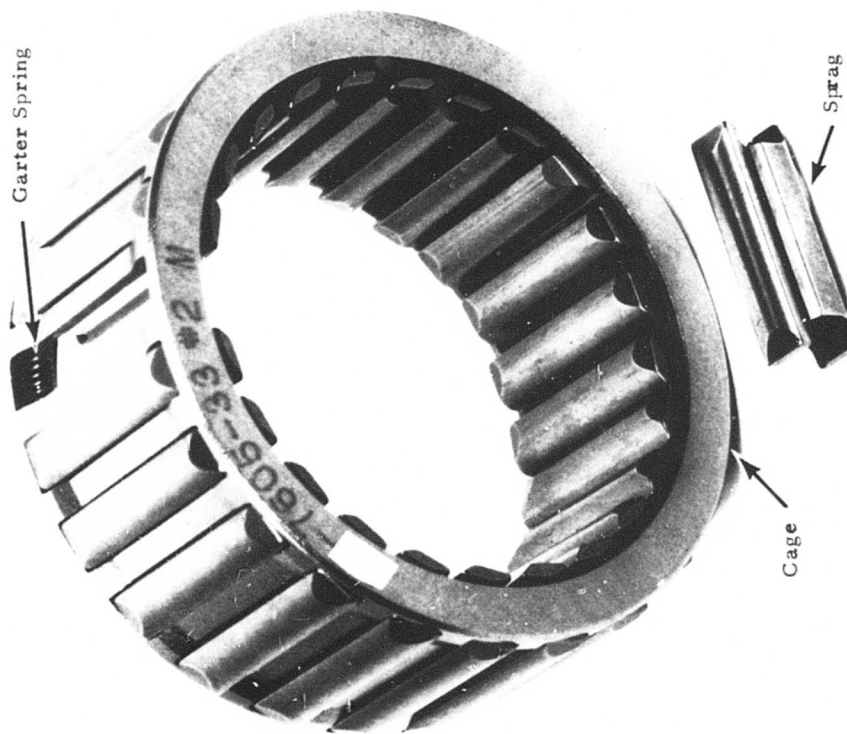


Figure 5. Clutch Design B Details.

TABLE II. TEST CLUTCH MATERIALS

	Design A	Design B
<u>Inner and Outer Races</u>		
Material Specification	AMS 6265	AMS 6265
Heat Treatment	Carburize	Carburize
Case Depth (in.)	.050-.065	.050-.065
Max. Stock Removal (After Heat Treatment) (in.)	.010	.010
Case Hardness	R _C 60-63	R _C 60-63
Core Hardness	R _C 32-40	R _C 32-40
<u>Sprags</u>		
Material Specification	M-50	SAE 52100
Heat Treatment	Thru hardened	Thru hardened
Surface Hardness	R _C 61 min	R _C 75
Core Hardness	R _C 58-62	R _C 58-62
Surface Treatment	Nitrided	Chromium carbide
<u>Retainers</u>		
Material Specification	SAE 4340	AMS 6274
Heat Treatment	Nitrided R _C 50 case R _C 38-42 core	Thru hardened R _C 40-47
Surface Treatment	Silver plated	Shot-peened
<u>Springs</u>		
Material Specification	17-7	AMS 5112E
Treatment	Stainless Cold drawn	Music wire Heat treated and normalized
<u>Drag Band</u>		
Material Specification	Stainless	
Treatment	Cold drawn	
<u>Oil</u>	MIL-L-23699	

Lubrication for both clutch designs is provided centrifugally via holes drilled through the inner races as shown in Figure 6. Dams are provided at each end of the sprag assembly to ensure operation in a flooded condition. The dams also trap some oil at shutdown to provide lubrication at subsequent startup.

Dams are also placed before the bearings, and the clutch scavenge flow is drained between the clutch and bearing dams. This arrangement keeps clutch particles from contaminating the bearings and eliminates oil churning in the bearings.

The lubrication hole pattern for clutch design B is shown in Figure 7. That for design A is similar. Axial grooves, machined in the inner race, extend to the bearing and sprag ends away from the feed oil so as not to starve this area in case of low oil flow.

The test program was designed to evaluate oil flows from 33 percent to 300 percent of design flow. A design oil flow of 0.8 gpm (376 pph) was selected as being reasonable for this type of transmission component. Twenty-one percent of the flow lubricates the clutch bearings, and the remainder lubricates the sprag assembly.

The bearings are 40x62x12 millimeter bronze cage angular contact, quality ABEC 7. Bearings are preloaded by a 40-pound spring (Figure 6) to take up end play. This is done to prevent bearing skidding at speed and eliminate axial shaft excursion at the rubbing surfaces.

Clutches were dynamically balanced to 0.25 inch-grams prior to operation. This procedure is standard for high-speed rotating components.

CLUTCH ANALYSIS

The successful design of a high-speed sprag overriding clutch requires consideration not only of the load-carrying capability but also the energy losses during overriding and differential speed operation.

The critical parameters for load-carrying capability are compressive stress at the inner race-sprag interface and hoop stress at the outer race inside diameter. These parameters are listed in Table III for both the A and B clutch configurations at the design point of 3,570 inch-pounds and 26,500 rpm.

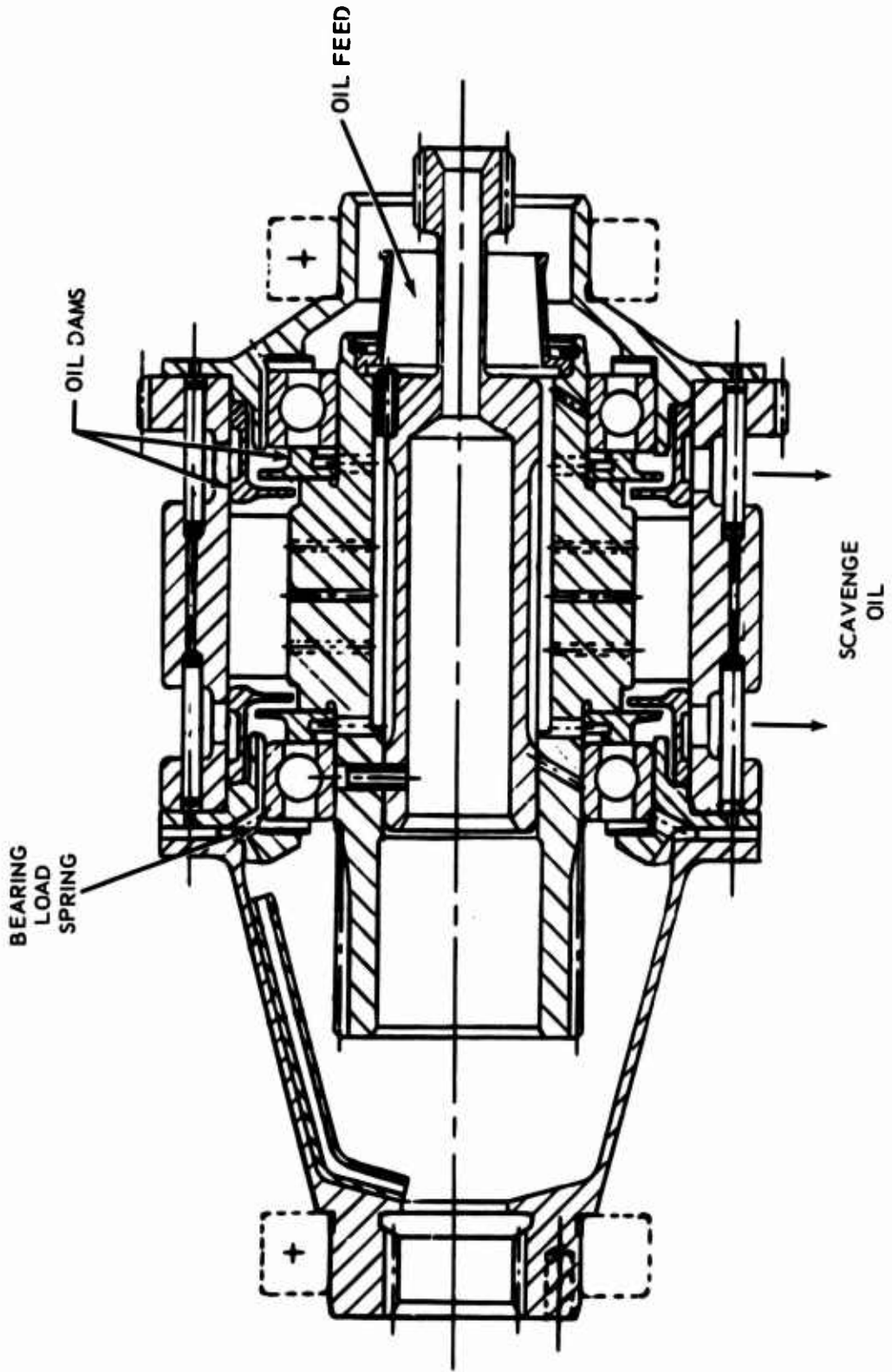


Figure 6. Clutch Lubrication Details.

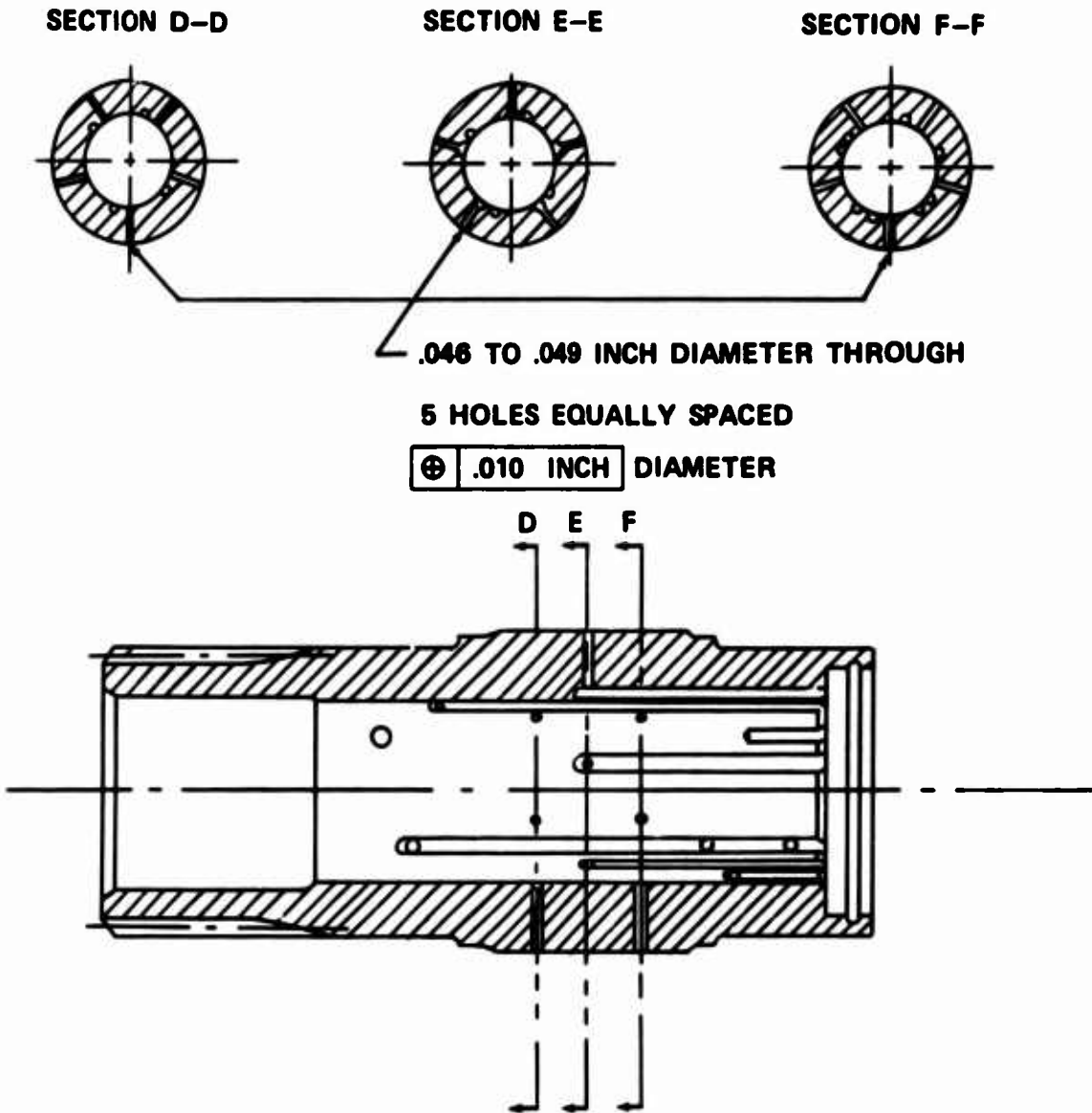


Figure 7. Inner Race Lubrication Hole Pattern.

TABLE III. CLUTCH DESIGN PARAMETERS (DESIGN POINT: 3, 570 IN. - LB AT 26, 500 RPM)

Parameters	Design A	Design B
<u>Driving Mode</u>		
Tangential stress due to rotation of outer race ID (psi)	18, 300	12, 500
Tangential stress due to pressure loading of outer race ID (psi)	35, 200	45, 700
Total tangential stress (hoop) of outer race ID (psi)	53, 500	58, 200
Compressive stress (Hertz) at inner race OD (psi) (max)	343, 500	347, 600
<u>Overrunning Mode</u>		
Oil film thickness (in.) ⁽¹⁾	.0003	.0003
Load/inch x velocity factor (lb/in. x fpm) ⁽²⁾	28, 800	25, 680
Interface pressure x velocity factor (psi x fps) ⁽³⁾	3.4x10 ⁶	2.7x10 ⁶
Sliding velocity (fpm) = $\frac{\pi (RPM) R_i}{6}$	14, 900	12, 150
<u>Differential Speed Mode</u>		
Load/inch x velocity factor (lb/in. x fpm) ⁽²⁾ at outer race speed (rpm) ⁽⁴⁾	259, 000 17, 436	137, 400 17, 265
Interface pressure x velocity factor (psi x fps) ⁽³⁾ at outer race speed (rpm) ⁽⁴⁾	6.8x10 ⁶ 13, 250	4.15x10 ⁶ 13, 250
<ol style="list-style-type: none"> 1. Refer to page 108. 2. Refer to page 107. 3. Refer to page 106. 4. Outer race speeds chosen are those which the computer analysis showed to give maximum values for the factor. 		

To develop a means of predicting wear and heat generation during over-running and differential speed operation, three indexes were investigated:

1. Elastohydrodynamic and hydrodynamic oil film thicknesses were calculated at the inner race-sprag contact.
2. A 'PRS-V' factor, interface pressure (psi) times velocity (fps), was calculated at the inner race-sprag contact.
3. A 'PV' factor used in the clutch industry, load per inch times velocity (fpm), was calculated at the inner race-sprag contact.

The usefulness of these indexes will depend on the accumulation of far more data than was generated in the test program.

These parameters are listed in Table III for the override condition. The last two factors are listed for the differential speed condition at the outer race speed for which they are a maximum.

A complete mathematical analysis of clutch operation was performed (Appendix I), and a computer program was developed (Appendix II). This initial effort was made to provide an analytical base that can be appropriately modified as data becomes available to incorporate new information. This base will provide a valuable analytical tool with which trade-off design studies can be efficiently conducted.

The initial computer results for the test clutches are immediately useful in the following areas:

1. Clutch Stresses - An iteration procedure is used to determine the proper position of the sprag, i. e., strut angle for any given value of torque. The critical stresses and deflections are then calculated:
 - a. Compressive (Hertz) stress and deflection at both inner and outer race contact points
 - b. Hoop stress and radial deflection at the outer race ID
2. Rollover Torque - Rollover or slippage of the sprags at the inner race due to excessive torque occurs when the inner strut angle exceeds approximately 4 degrees. Therefore, by running cases with increasing values of torque, this point can be determined.

3. **Strut Angle Curve** - Values for the strut angle versus sprag height are calculated assuming both flat plate and curved surface raceways. The flat plate values can be used to generate a strut angle curve that is commonly used in the industry along with an inspection instrument to functionally check sprag geometry. The curved surface values are used in the stress and deflection calculations.

4. **Sprag Centrifugal Force** - At each strut angle position, the location of the center of gravity is calculated in relation to the contact points. This value is then used to calculate the energizing moment due to the sprag.

TEST FACILITY

DYNAMIC TESTS

Test Rig

The dynamic tests were conducted on an existing rig especially fabricated for high-speed overrunning clutch development. The test vehicle (Figure 8) consists of two independently controlled 8-inch Barbour Stockwell 100 hp, 30,000-rpm steam turbine prime movers driving through 3:1 speed increasers. One turbine drives the clutch inner race and the second turbine drives the clutch outer race. A pad is provided on each speed increaser to accommodate slip ring assemblies that transmit data from the rotating shafts. A photograph of the test setup is presented in Figure 9.

The test cartridge is shown in Figure 10. The cartridge containing the test clutch has been designed to be installed between the supporting frames without moving either frame. This procedure ensures good alignment for each test increment and rapid turnaround between tests.

MIL-L-23699 lubricant as specified was employed in all tests. One batch of Hatco 3211 lubricant was used.

A schematic representation of the lubrication system is presented in Figure 11. Two independent pressure pumps were employed in the tests, one to feed the test clutch, and the other for the rig support bearings. A constant flow of 0.17 gpm was supplied to the rig support bearings. High quality ABEC 7 ball bearings with bronze retainers were utilized. The oil used in the dynamic tests was analyzed and found to be clean and in good condition. The viscosity at 100° F was found to be 25.71, and the acid number was 0.05. Wear metal was less than one part per million each for chromium, nickel, silver, copper, aluminum, and magnesium.

Instrumentation

A typical console and instrument panel for external control of rig operating environments is shown in Figure 12. Clutch rig instrumentation monitored from the panel included:

1. Oil flow and pressure
2. Oil temperature in and out
3. Rig vibration

A

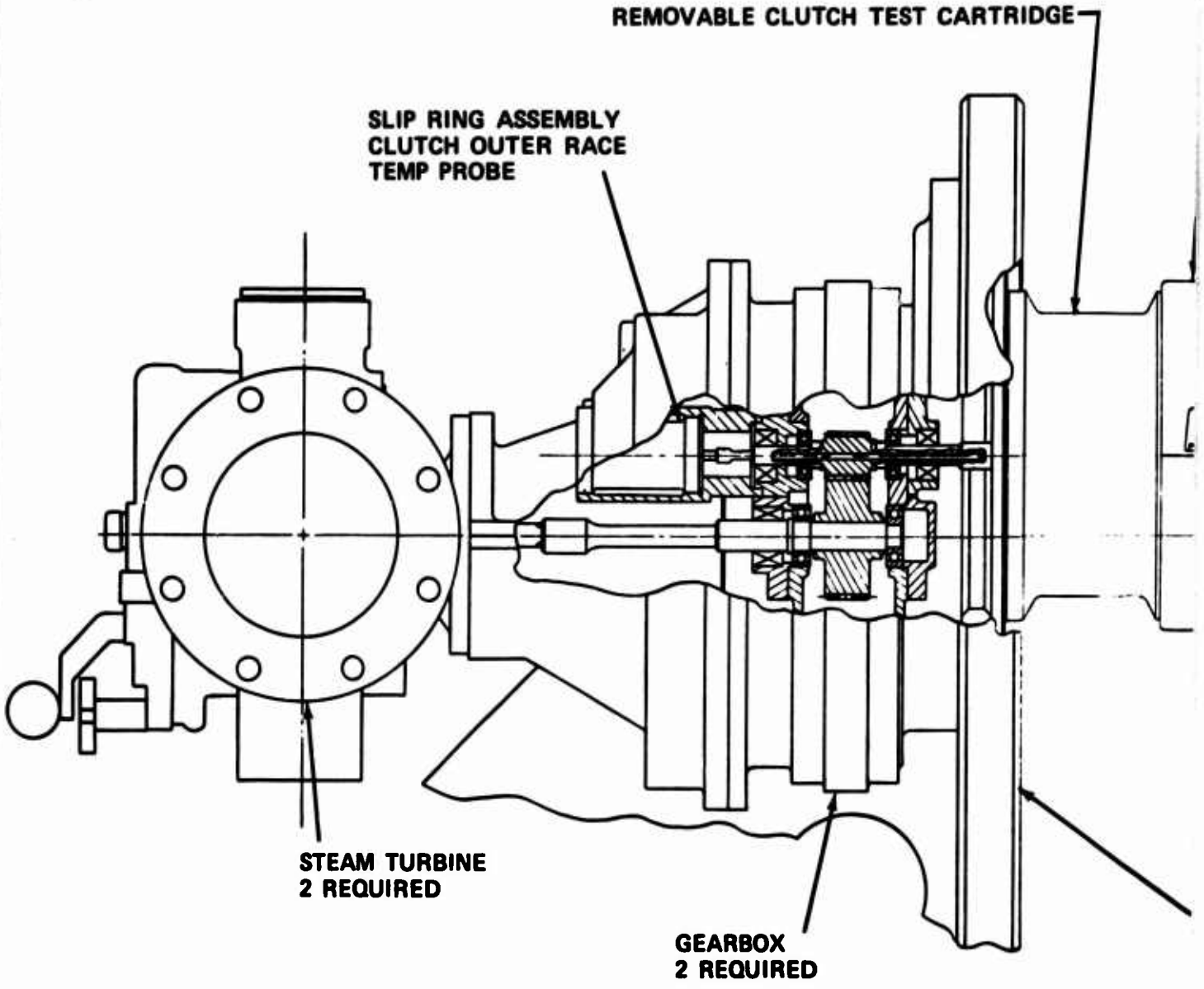
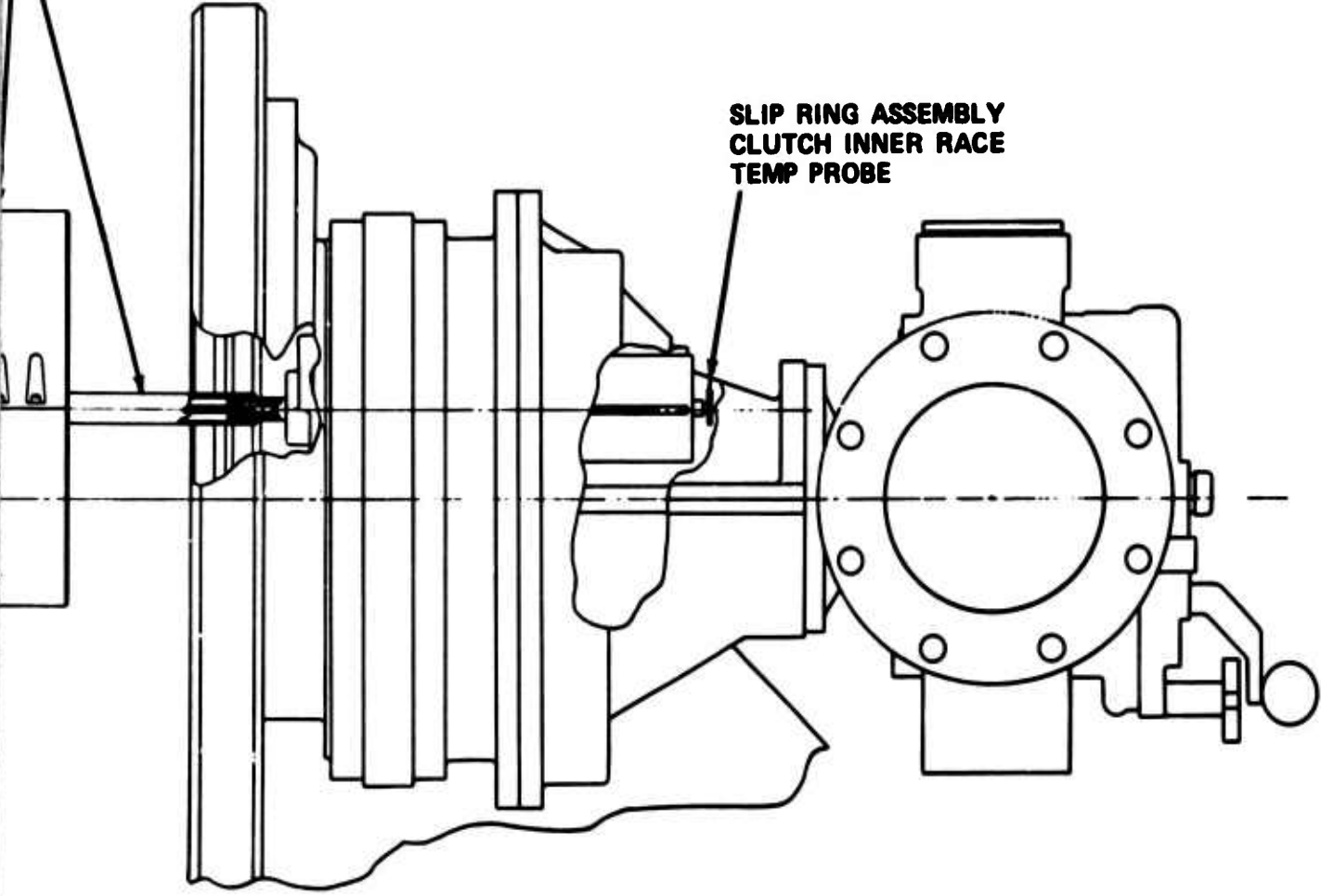


Figure 8. Overall Rig Arrangement.

B

**REMOVABLE COVER & SHAFT FOR EASY
REMOVAL OF CLUTCH TEST CARTRIDGE**

**SLIP RING ASSEMBLY
CLUTCH INNER RACE
TEMP PROBE**



**SUPPORT STAND
2 REQUIRED**

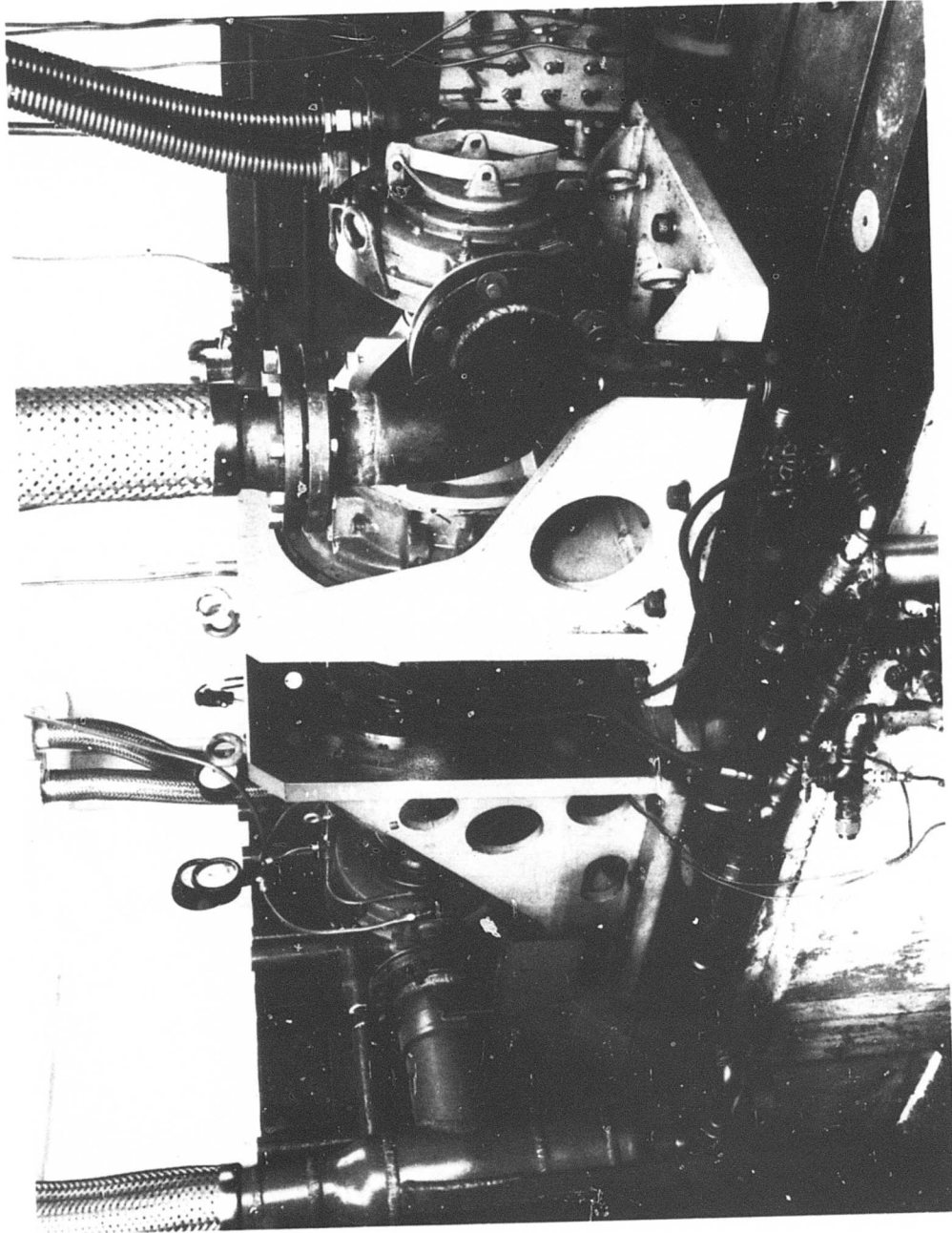


Figure 9. Test Rig Installation.

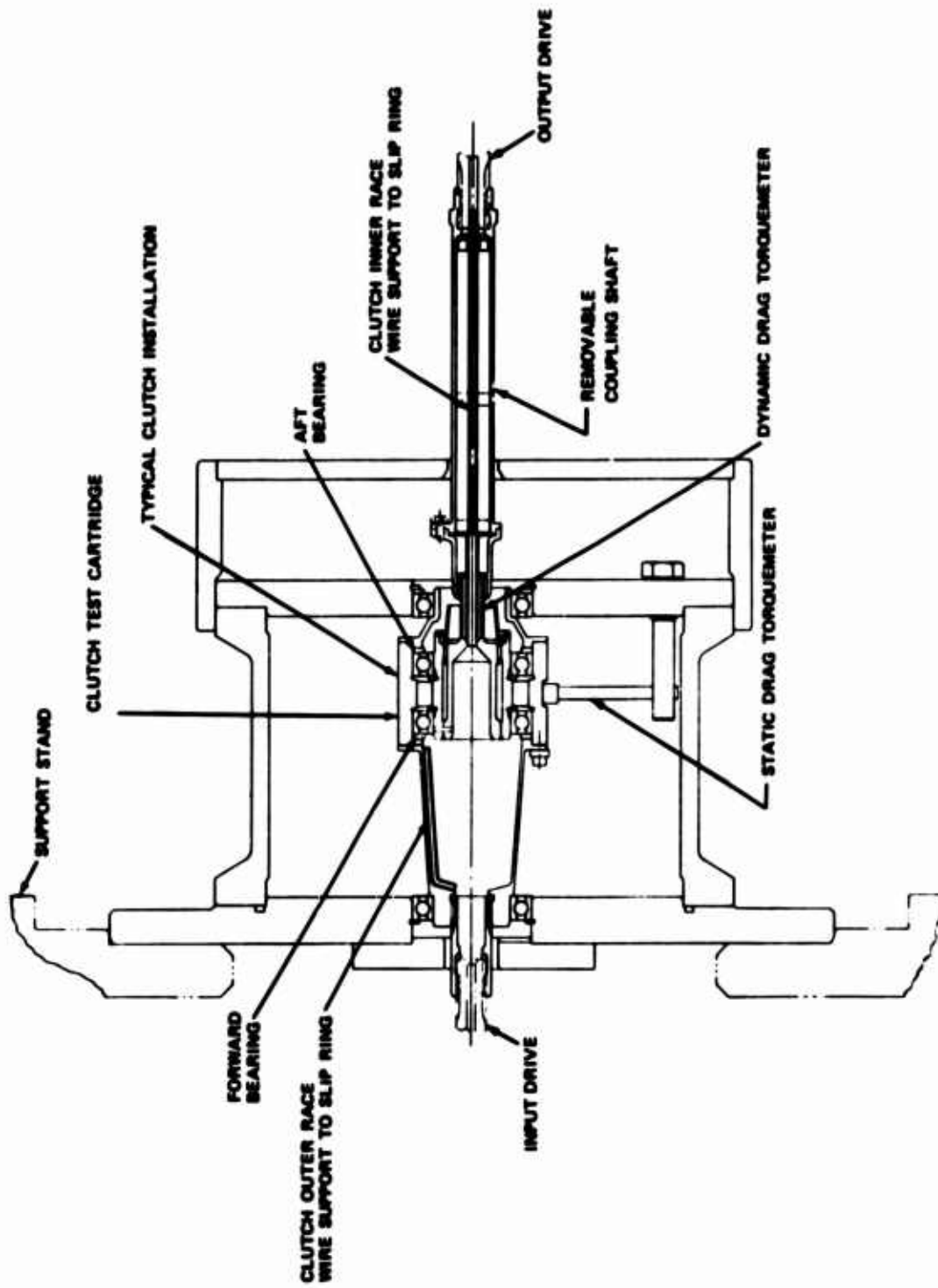


Figure 10. Test Cartridge Details.

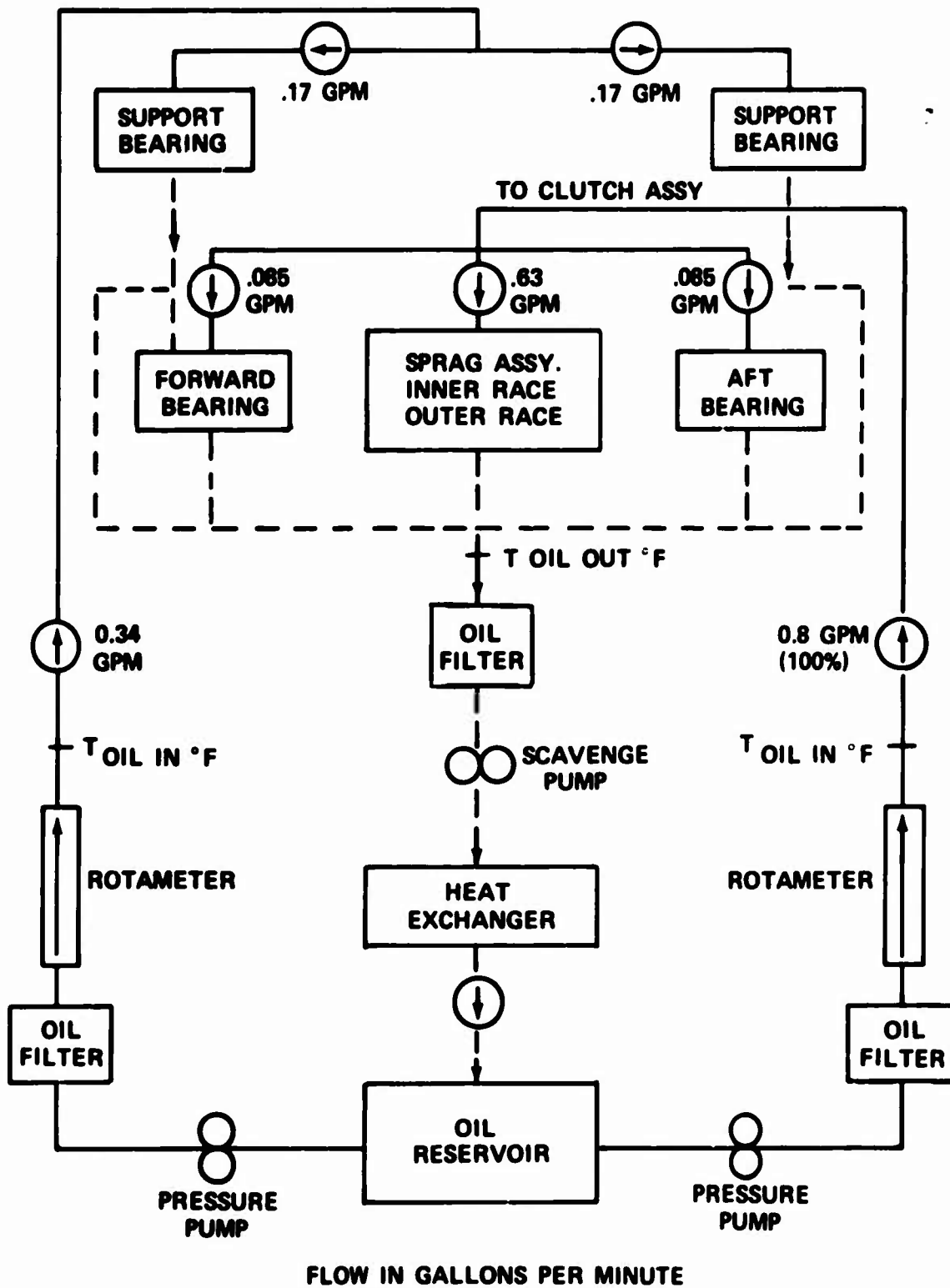


Figure 11. Lubrication Schematic.

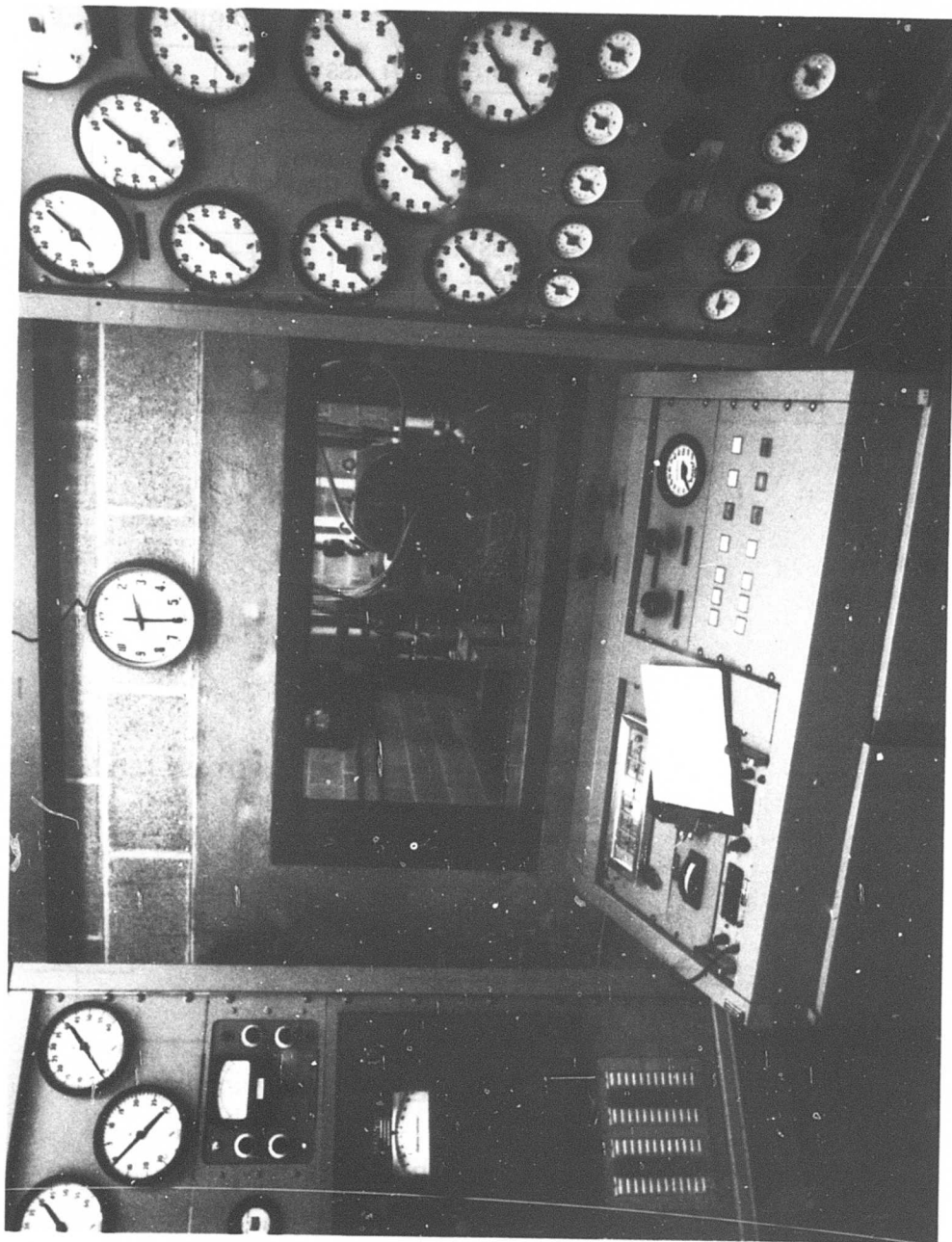


Figure 12. Console and Instrument Panel.

4. Rig speeds
5. Clutch inner and outer race temperatures
6. Bearing inner and outer race temperatures
7. Clutch drag torque
8. Chip detectors

The locations where measurements were obtained are shown schematically in Figure 13. Iron-Constantan thermocouples were employed throughout. Clutch scavenge oil temperature was measured at the test clutch oil ports rather than the rig scavenge port so that no heat would be lost to the rig housing.

Clutch torque was measured by two methods in the overrunning tests. One method measured driving shaft torque (Figure 13). Foil resistance strain gages were mounted on a reduced section of the inner race drive shaft. The gages were located to form a torque bridge at 45 degrees to the axis of the shaft. The shaft and gage installation was calibrated for torque versus bridge output over the expected torque range (0 to 250 inch-ounce). The calibration was accomplished through the application of weights on a specially constructed fixture. Corrections were made for extraneous loads and temperature effects.

The other method of measuring shaft torque was to restrain the outer race from rotating with an instrumented beam (Figure 10). Foil resistance strain gages were mounted on the beam to form a shear bridge. The beam was calibrated for point load versus bridge output over the expected load range. Corrections were made for extraneous loads and temperature effects. The shear bridge was chosen to eliminate any need to correct the calibration for variations in the point of load application relative to the strain gage locations. When the differential speed tests were conducted with both shafts rotating, only the drive shaft torque could be measured.

STATIC TESTS

Test Rig

The cyclic fatigue tests were conducted in the experimental mechanical laboratory using electrohydraulic closed-loop, servo controlled, rotary actuator systems. A cross section of a typical installation is shown in Figure 14. The system utilizes a rotary actuator and provides the

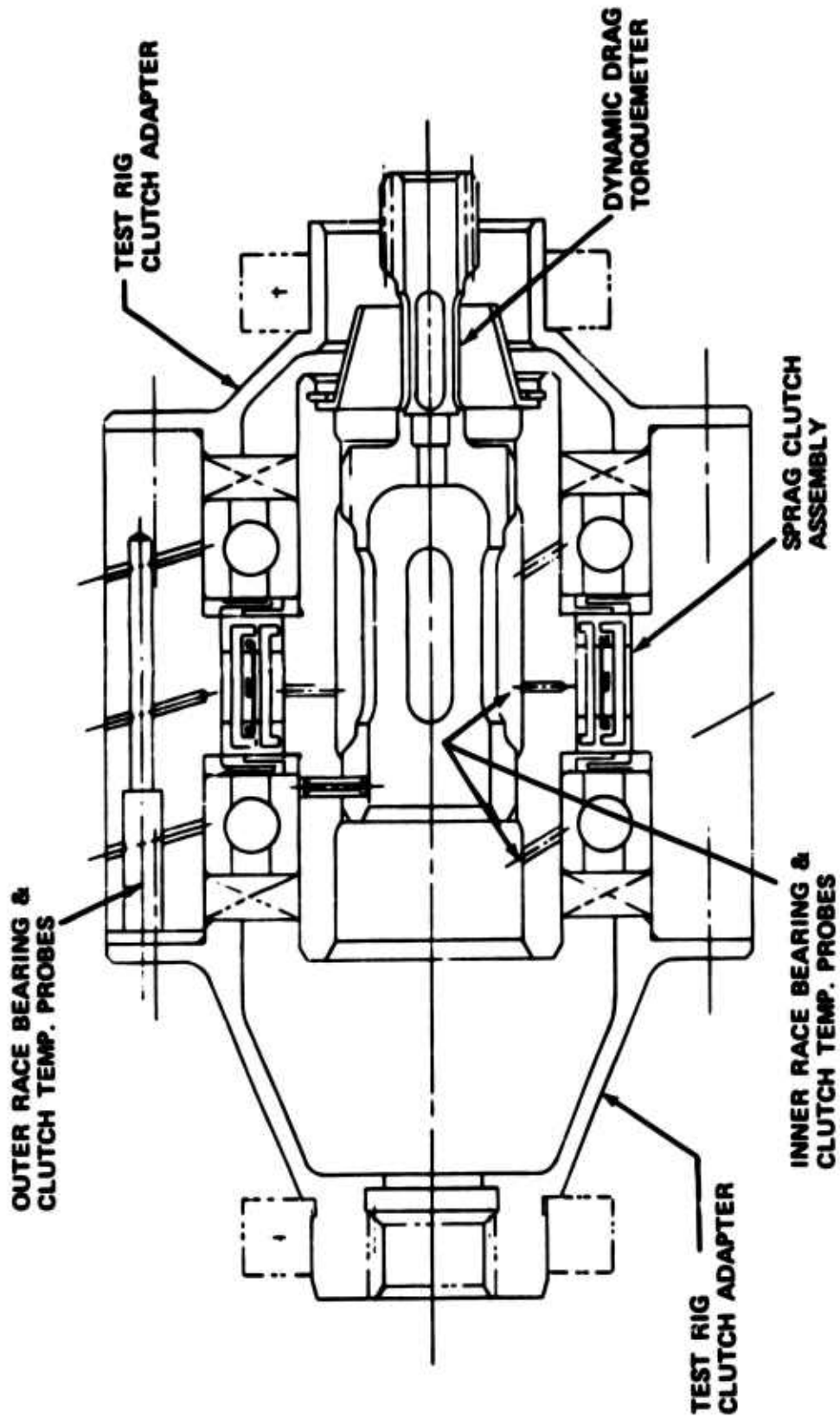


Figure 13. Clutch Instrumentation Schematic.

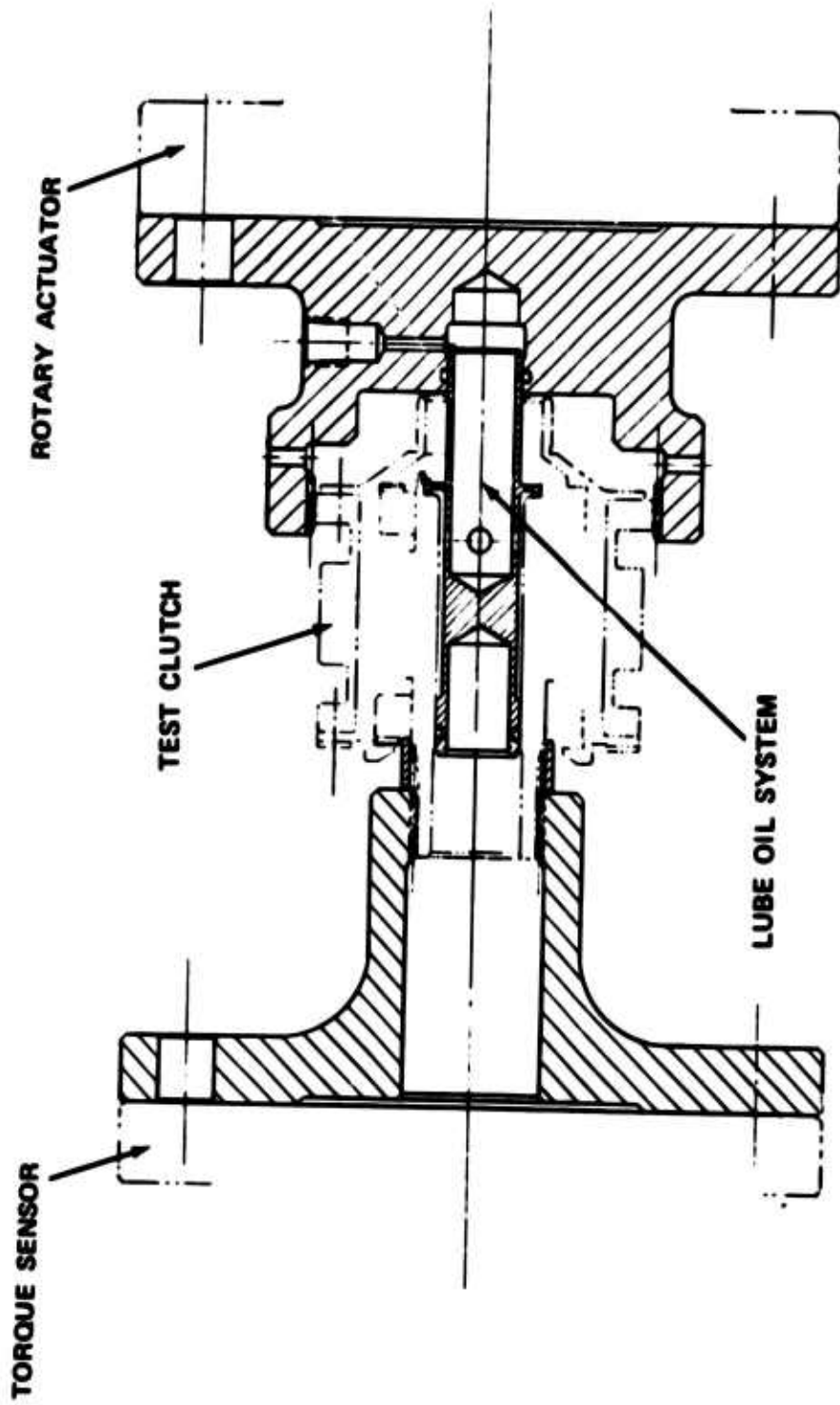


Figure 14. Cyclic Fatigue Test Schematic.

required torque load of $7,140 \pm 900$ inch-pounds at a frequency of 10 Hertz. The torque load was applied, using the hydraulic rotary actuator, through a bolted adaptor splined to the clutch outer race. This load was then reacted through a torque sensor bolted to an adaptor and splined to the clutch inner race. Continuous oil flow of 0.5 gpm was maintained within the clutch assembly at a pressure of 20 psig using MIL-L-23699 oil. The system uses a full-flow chip detector and is instrumented for an automatic shutdown in the event of chip detection or component failure. The equipment compares input and output torque and shuts down automatically if the difference is greater than 1/2 percent of full torque. Torque load, angular displacement between input and output races, and outer race radial deflections were monitored every 1-million cycles. The torque readouts were observed with an oscilloscope, digital voltmeter, and load amplitude measurement system. Angular displacement between outer and inner races was measured with graduated scales, located on the input and output adaptor flanges, and with pointers attached to ground. Outer race radial deflection was determined by averaging the output of eight strain gages tangentially oriented and equally spaced around the shaft circumference. The rig utilizes a rotary actuator that is rated at 8,020 inch-pounds dynamic and 12,000 inch-pounds static. Maximum travel is 90 degrees (± 45 degrees). A 10 gpm hydraulic power supply at 3,000 psi source pressure is employed. A photograph of the cyclic fatigue test installation is shown in Figure 15.

The overload tests were performed on a second rotary actuator that is rated at 72,000 inch-pounds static torque. Instrumentation utilized was the same as that in the cyclic fatigue test. A photograph of the overload test installation is shown in Figure 16.

required torque load of $7,140 \pm 900$ inch-pounds at a frequency of 10 Hertz. The torque load was applied, using the hydraulic rotary actuator, through a bolted adaptor splined to the clutch outer race. This load was then reacted through a torque sensor bolted to an adaptor and splined to the clutch inner race. Continuous oil flow of 0.5 gpm was maintained within the clutch assembly at a pressure of 20 psig using MIL-L-23699 oil. The system uses a full-flow chip detector and is instrumented for an automatic shutdown in the event of chip detection or component failure. The equipment compares input and output torque and shuts down automatically if the difference is greater than 1/2 percent of full torque. Torque load, angular displacement between input and output races, and outer race radial deflections were monitored every 1-million cycles. The torque readouts were observed with an oscilloscope, digital voltmeter, and load amplitude measurement system. Angular displacement between outer and inner races was measured with graduated scales, located on the input and output adaptor flanges, and with pointers attached to ground. Outer race radial deflection was determined by averaging the output of eight strain gages tangentially oriented and equally spaced around the shaft circumference. The rig utilizes a rotary actuator that is rated at 8,020 inch-pounds dynamic and 12,000 inch-pounds static. Maximum travel is 90 degrees (± 45 degrees). A 10 gpm hydraulic power supply at 3,000 psi source pressure is employed. A photograph of the cyclic fatigue test installation is shown in Figure 15.

The overload tests were performed on a second rotary actuator that is rated at 72,000 inch-pounds static torque. Instrumentation utilized was the same as that in the cyclic fatigue test. A photograph of the overload test installation is shown in Figure 16.

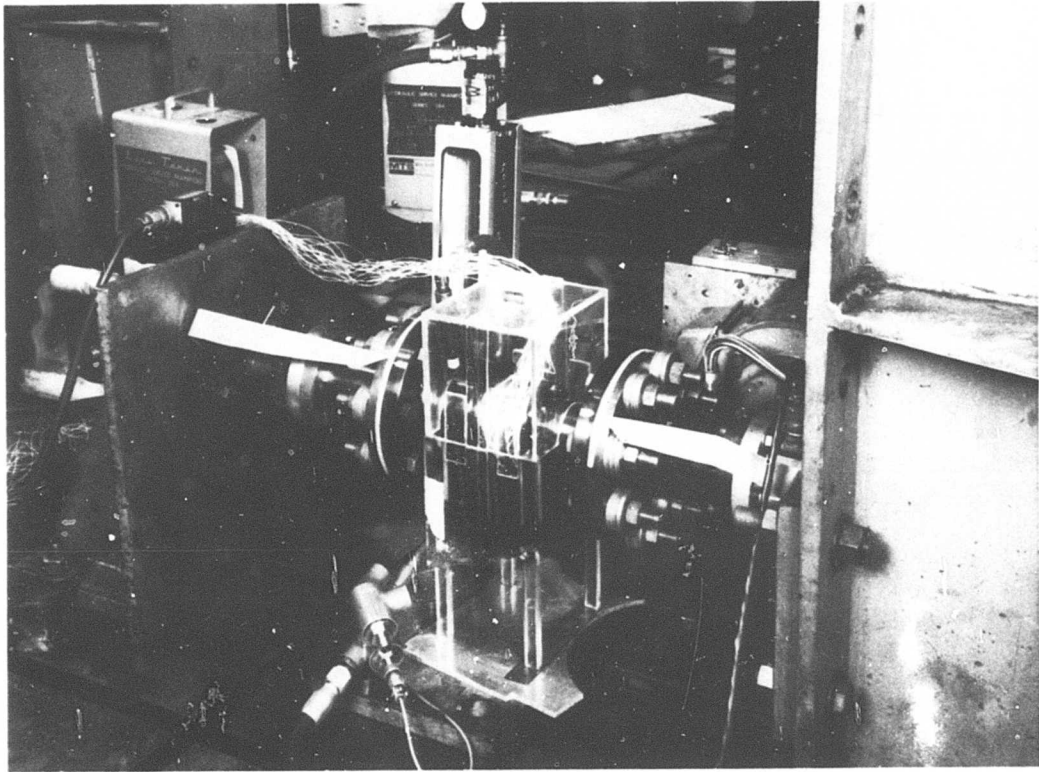


Figure 15. Cyclic Fatigue Test Installation.

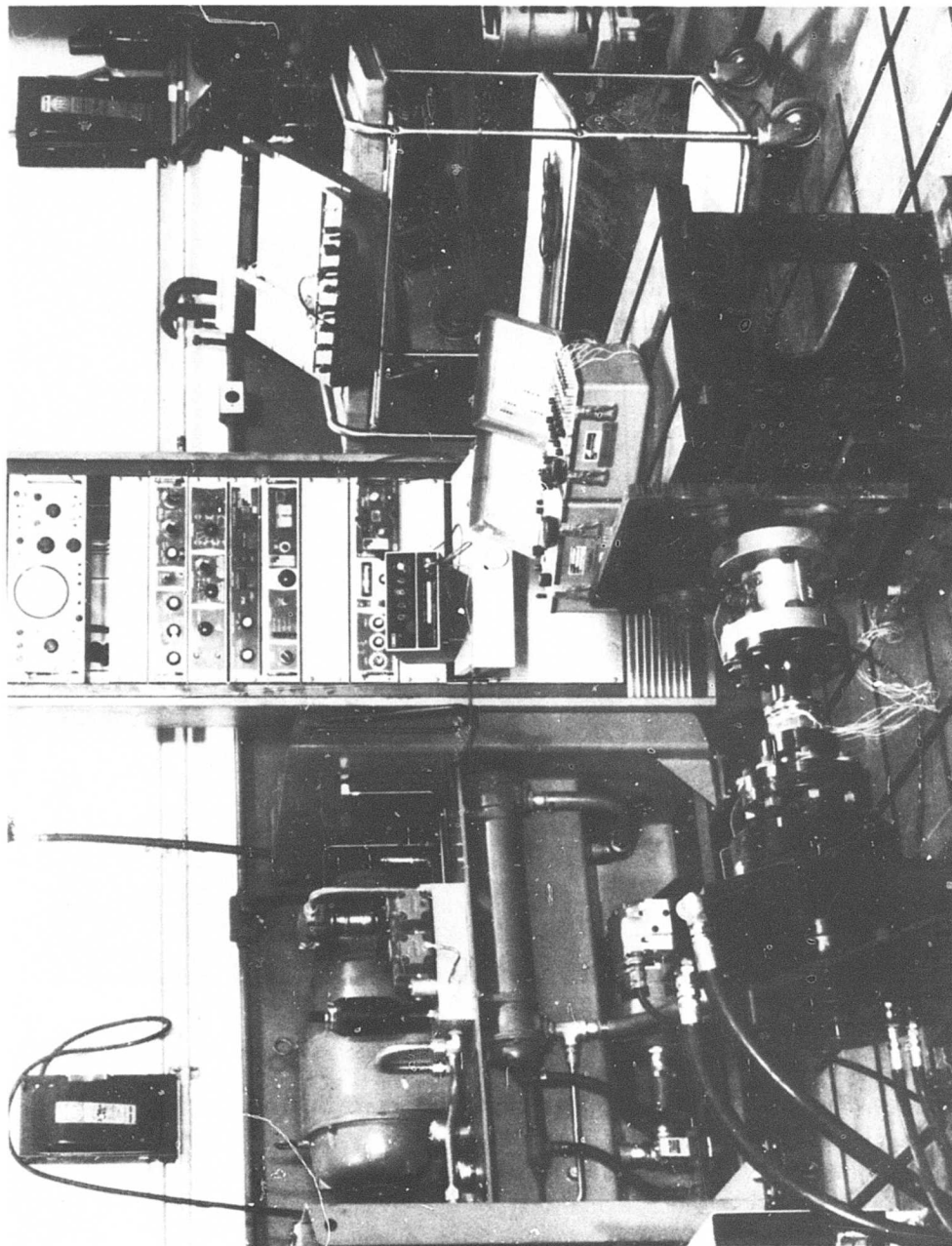


Figure 16. Static Overload Test Installation.

TEST PROCEDURE

GENERAL

Five series of tests were conducted as follows:

1. Full-speed dynamic clutch override test
2. Differential speed dynamic clutch override test
3. Dynamic engagement tests
4. Static cyclic torque fatigue test
5. Static overload test

One design A clutch and one design B clutch were subjected to tests 1 through 3. Two design A clutches and two design B clutches were subjected to tests 4 and 5. For the dynamic tests, data were recorded every 15 minutes. A typical log sheet is shown in Figure 17. Data points taken were averaged for presentation under "Test Results and Discussion."

FULL-SPEED DYNAMIC CLUTCH OVERRIDE TEST

The objective of this test was to determine the optimum clutch oil flow in terms of heat generation, drag torque, and component wear.

Prior to testing, the clutch rig was fully instrumented to monitor the following parameters, which were recorded every 15 minutes:

<u>Parameter</u>	<u>Number of Positions</u>
Outer race temperature of bearings - °F	4
Inner race temperature of bearings - °F	4
Clutch outer race temperature - °F	2
Clutch inner race temperature - °F	2
Temperature of clutch, oil in - °F	1
Clutch drag torque, dynamic measurement - in.-oz	1
Clutch drag torque, static measurement - in.-oz	1
Clutch assembly oil-out temperature - °F	1
Oil flow to clutch assembly - pph	1
Rig housing vibration (displacement and velocity)	2
Chip detectors	2
Oil pressure at rig housing for clutch assembly - psig	1
Output shaft speed - rpm	1

The clutch was operated at zero input speed and 26, 500 rpm output speed. Tests were conducted with oil flows of 300, 200, 100, 67, and 33 percent of design flow (design flow = 0.8 gpm). Each test was of 5 hours duration. The oil inlet temperature was held to a minimum of 195° F and did not go above 215° F. The oil inlet pressure did not exceed 100 psig, nor did it go below 45 psig throughout the dynamic test program. It must be remembered that this is the oil fed to the inside of the clutch inner race. Test oil flows and pressures are listed in Table IV.

TABLE IV. FULL-SPEED DYNAMIC CLUTCH OVERRIDE OIL FLOWS AND PRESSURES				
Test	Percent Design Flow	GPM	PPH	Feed Pressure
1	300	2.4	1125	98
2	200	1.6	750	85
3	100	.8	375	63
4	67	.54	250	48
5	33	.26	125	45

At the end of each oil flow level test, (300 percent oil flow, 200 percent oil flow, etc.) a speed rundown was conducted. For this portion of the test, the variable was clutch output speed and the operating oil flow was maintained at a steady state. The output speed levels selected are listed below:

Output Speed Level (rpm)

- 25,000
- 20,000
- 15,000
- 10,000

Each output speed level was maintained until steady-state temperature condition was achieved. Temperatures were stabilized for approximately 15 minutes at each speed level. After testing, the test rig was dismantled and the clutch components were inspected visually and analytically.

The entire test procedure for the full-speed override test, including the speed rundown, was repeated without the sprag assembly installed. The purpose was to resolve clutch drag force into individual components produced by bearings and shafts on one hand and the sprag assembly on the other hand.

One clutch each of designs A and B was subjected to the full-speed override test.

DIFFERENTIAL SPEED DYNAMIC CLUTCH OVERRIDE TEST

The objective of this test was to determine the maximum drag condition.

The test objective was accomplished by adjusting the clutch output speed to 26,500 rpm (100 percent normal rated) and then adjusting the clutch input speed to the values noted below:

<u>Output Speed (rpm)</u>	<u>Normal Rated (percent)</u>	<u>Input Speed (rpm)</u>	<u>Normal Rated (percent)</u>
26,500	100	13,250	50
26,500	100	17,667	67
26,500	100	19,875	75

The optimum oil flow rates established during the full-speed override test were used during this test. Oil inlet temperatures and pressures were maintained at 195° F minimum and 100 psig maximum, respectively. After conditions were stabilized, each speed condition was maintained for 1 hour and the following parameters were monitored every 15 minutes:

<u>Parameter</u>	<u>Number of Positions</u>
Outer race temperature of bearings - °F	4
Inner race temperature of bearings - °F	4
Clutch outer race temperature - °F	2
Clutch inner race temperature - °F	2
Temperature of clutch, oil out - °F	2
Clutch drag torque, dynamic measurement - in.-oz	1
Clutch assembly oil-in temperature - °F	1
Oil flow to clutch assembly - pph	1
Rig housing vibration (displacement and velocity)	2
Chip detectors	2
Oil pressure at rig housing for clutch assembly - psig	1
Output shaft speed - rpm	1
Input shaft speed - rpm	1

After completing the three 1-hour speed runs, i. e., clutch input speed adjusted to 50, 67, and 75 percent normal rated, the clutch input speed associated with the highest drag torque was selected as the next operating point, and a 5-hour test was conducted at the selected clutch input speed. All other test parameters were the same as before.

At the end of the differential speed dynamic override test, the clutch rig was dismantled and clutch components were visually and analytically inspected. One clutch each of designs A and B was subjected to the differential speed test.

DYNAMIC ENGAGEMENT TEST

The objective of this test was to investigate the engaging and disengaging characteristics of the clutch.

The test procedure employed was to adjust the output speed to the clutch to 13,250 rpm (50 percent normal rated). The input speed of the clutch was then accelerated to exceed 13,250 rpm, such that clutch engagement occurred. As the input speed increased, the output prime mover was shut down to impart a shock load to the clutch components, an operation that was accomplished twice.

The procedure was repeated at output speeds of 19,875 rpm (75 percent normal rated) for two engagements and of 26,500 rpm (100 percent) for five engagements. For this test series, the strain-gaged drive shaft, capable of monitoring clutch drag torque, was not used. The shaft was designed to measure only small values of drag torque and would fail if subjected to the shock loads. Accordingly, another drive shaft capable of withstanding shock loads was employed. The optimum oil flow established in the full-speed override test was utilized.

One clutch each of designs A and B was subjected to the dynamic engagement test.

Following the test, clutch components were visually and analytically inspected.

STATIC CYCLIC TORQUE FATIGUE TEST

The objective of this test was to determine the fatigue characteristics of the clutch.

A torque load of $7,140 \pm 900$ inch-pounds was applied for 10^7 cycles. The cyclic fatigue test program was conducted at twice the design torque, reflecting safety factors commonly used in the aircraft industry to account for torsionals, shock loads, etc. Load application frequency was 10 Hertz using sine wave excitation. The following parameters were monitored:

Torque - in.-lb
Angular Displacement - deg
Outer Shaft Radial Deflection - in.

A continuous oil flow of 0.5 gpm at 20 psig and room temperature was maintained within the clutch assembly with the use of special fixtures.

Two clutches each of designs A and B were subjected to the cyclic fatigue test.

Following the test, clutch components were visually and analytically inspected.

STATIC OVERLOAD TEST

The objective of this test was to determine the clutch's ultimate capacity and the overload mode of failure.

Static torque load, in increasing increments of 500 inch-pounds, was applied until slippage or component failure occurred. The following parameters were monitored:

Torque - in.-lb
Angular Displacement - deg
Outer Shaft Radial Deflection - in.

Internal clutch components were lubricated with MIL-L-23699 oil prior to testing.

Two clutches each of designs A and B were subjected to the static overload test.

Following the test, clutch components were visually and analytically inspected.

INSPECTION

Prior to testing, all clutch components were completely dimensionally inspected. Clutch races were measured on the Indi-Ron (Figure 18) to determine race roundness to 1.5×10^{-6} inch and on the Proficorder (Figure 19) to determine surface texture to 3×10^{-6} inch. Proficorder traces were also taken on the sprags in both the axial and circumferential directions. A typical Proficorder chart, which provides a permanent record of component surface texture, is shown in Figure 20. An Indi-Ron chart of an inner race permanently recording roundness and squareness of all critical surfaces with respect to a reference surface is shown in Figure 21.

These measurements were taken following each test run in order to determine component deterioration during operation. In addition, magnaflux inspections were performed after testing to determine crack initiation, if any.

In practice, measurement of sprag wear by use of the Proficorder was not successful. The inner cam surface of the sprag is made up of two radii of curvature, one for load transmittal and the other for overriding. Wear occurred during dynamic tests at the transition between these two curves, which made it extremely difficult to set up the Proficorder, since it is set to a radius and then zeroed out at each end of the curve defined by the radius. It was found that the best sprag wear indication was to measure the width of the wear band.

The wear was manifested as a flat on the cam surface, so knowing the width and the radius of curvature enabled calculation of wear depth.

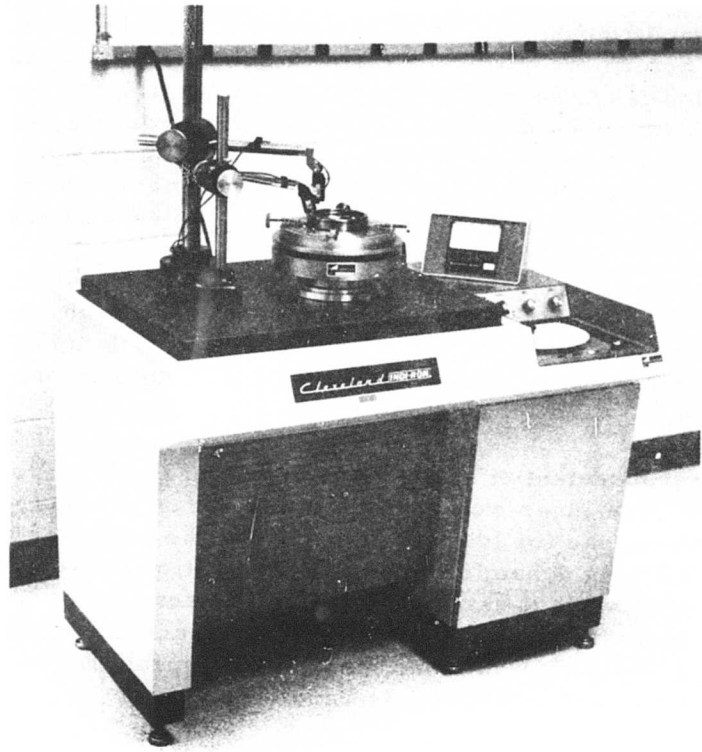


Figure 18. Indi-Ron.

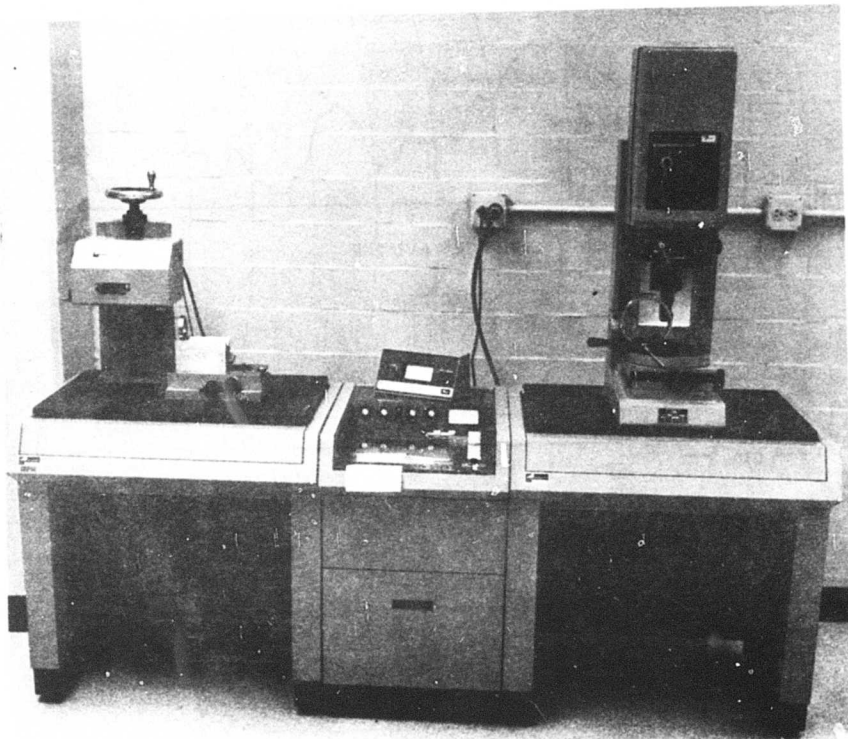


Figure 19. Proficorder.

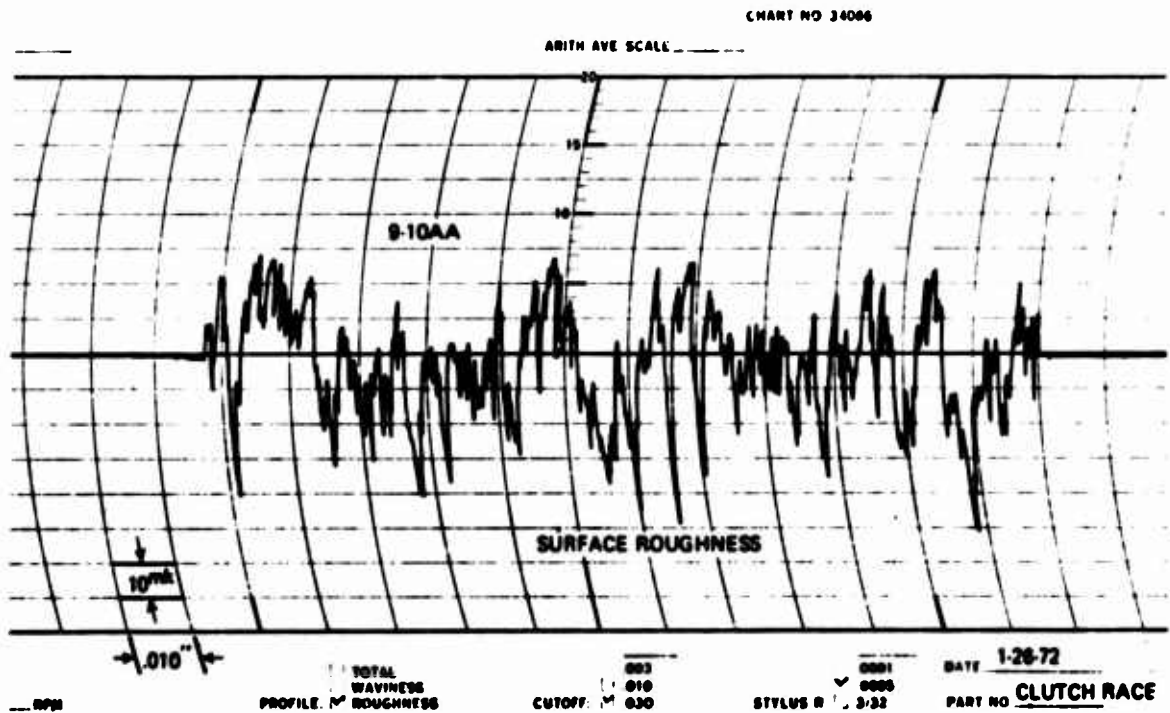
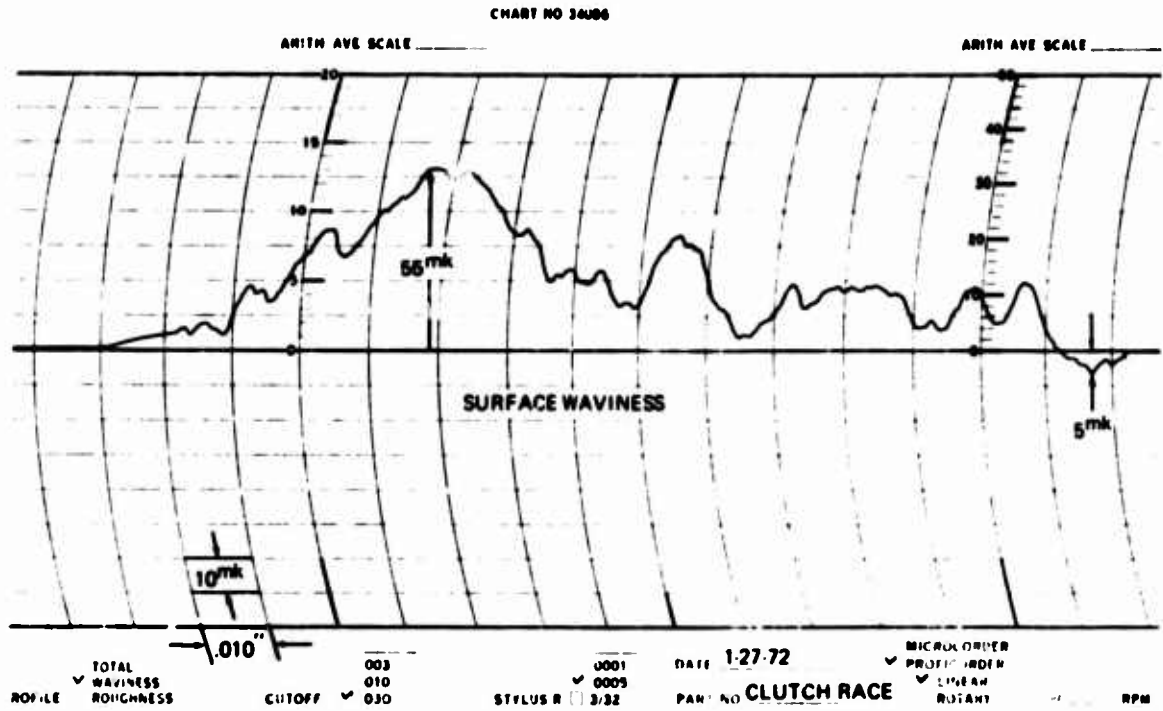


Figure 20. Typical Proficorder Chart.

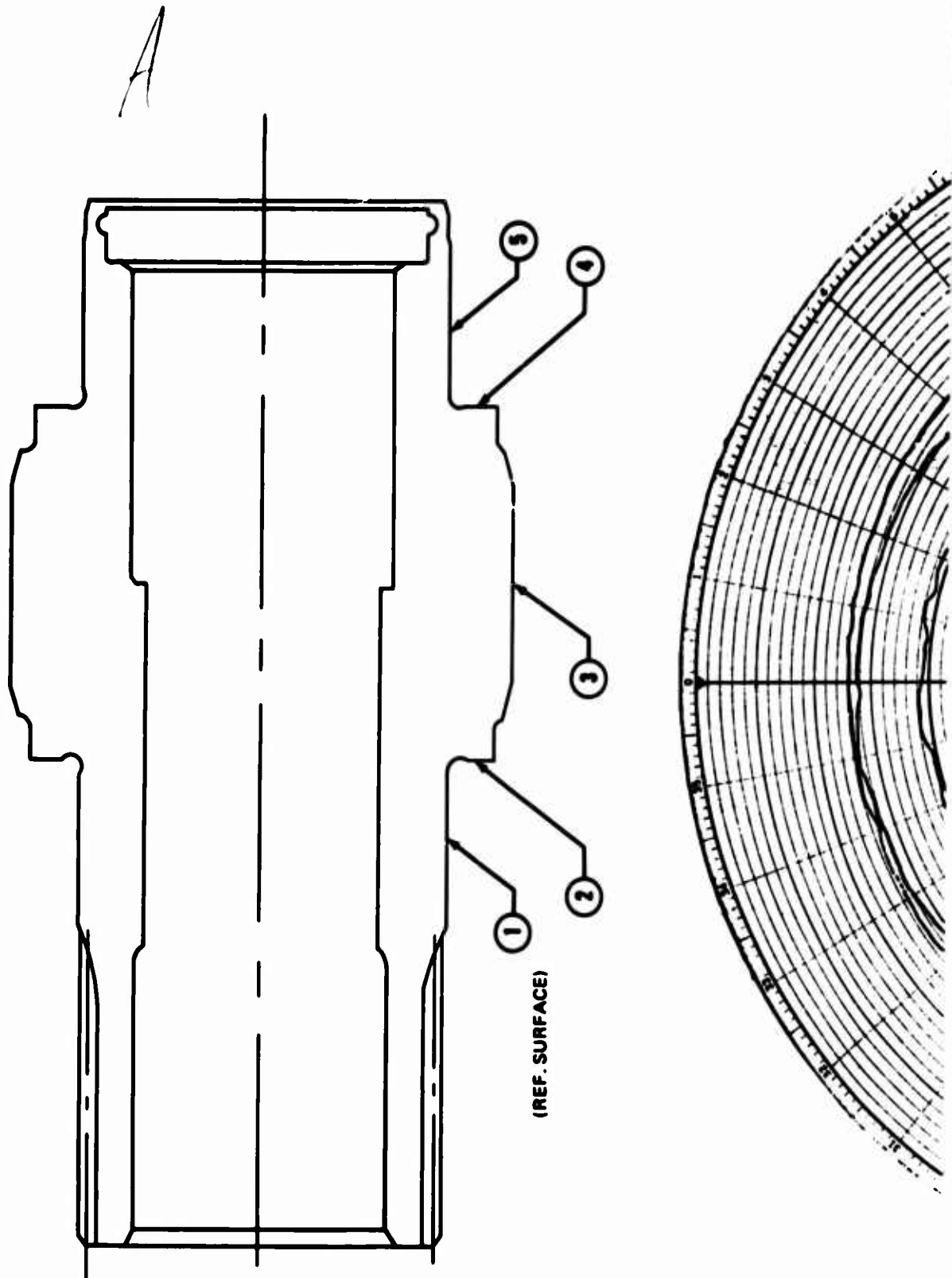
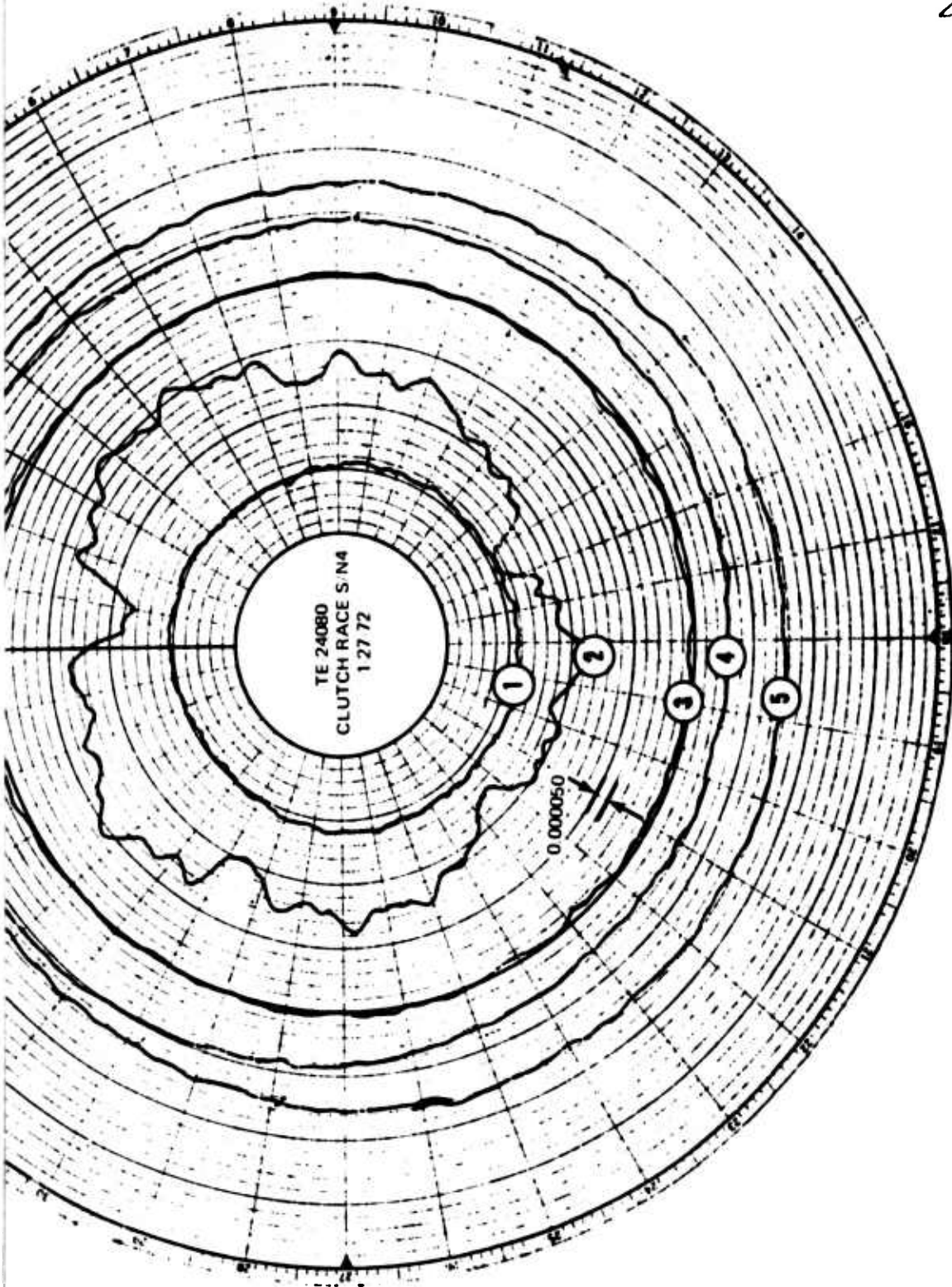


Figure 21. Typical Indi-Ron Chart.

B



TEST RESULTS AND DISCUSSION

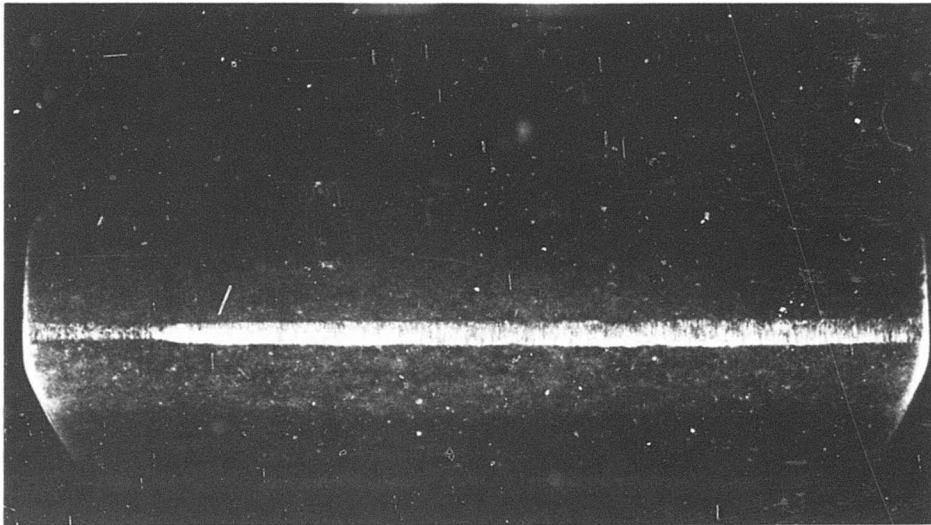
FULL SPEED DYNAMIC CLUTCH OVERRIDE TEST

Design A clutch testing was terminated at 67 percent design oil flow (0.54 gpm) because of wear at the sprag inner surface where the inner race overrides. The sprag wear pattern after the 100 and the 67 percent oil flow runs is shown in Figure 22. The inner and outer races exhibited no measurable wear, but there was slight scuffing on the inner race following the 67 percent oil flow run as shown in Figure 23. The width and depth of the sprag wear band after each oil flow run are listed in Table V.

TABLE V. FULL SPEED OVERRIDE TEST, SPRAG WEAR, DESIGN A		
Oil Flow (percent)	Wear After 5 Hours (in.)	
	Width of Band	Depth of Wear
300	.005	.00002
200	.008	.00005
100 (.8 gpm)	.015	.00017
67	.031	.00071

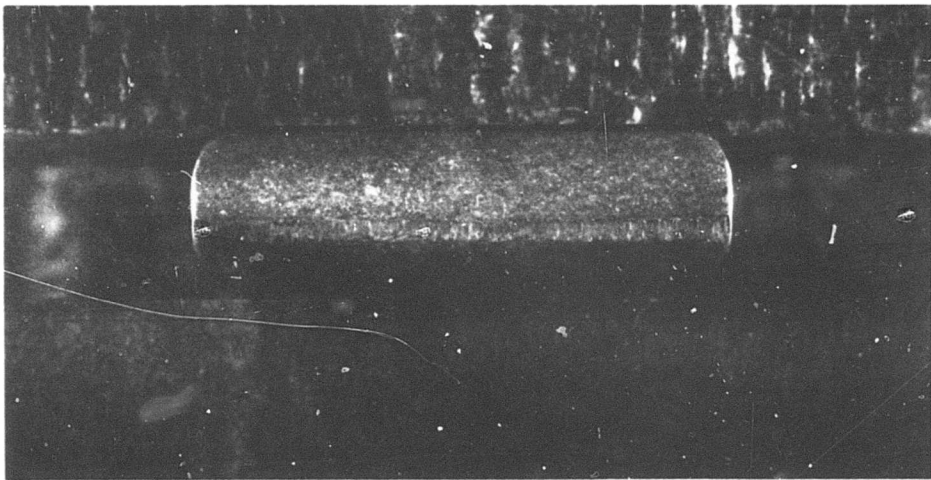
The width of the wear band versus hours of operation is plotted in Figure 24, which shows an increasing wear rate as oil flow was reduced. Wear was apparent on the drag band where it contacts the outer race following testing. Also, some of the silver plating on the retainers had flaked and some silver was deposited in the sprag pockets.

The design B clutch survived all oil flow runs down to 33 percent (0.26 gpm) in excellent condition without measurable wear. Clutch component condition following the override testing is shown in Figures 25 through 27.



100 Percent Oil Flow

Mag: 9.5X



67 Percent Oil Flow

Mag: 5X

Figure 22. Sprag Wear Following Override Test, Design A.

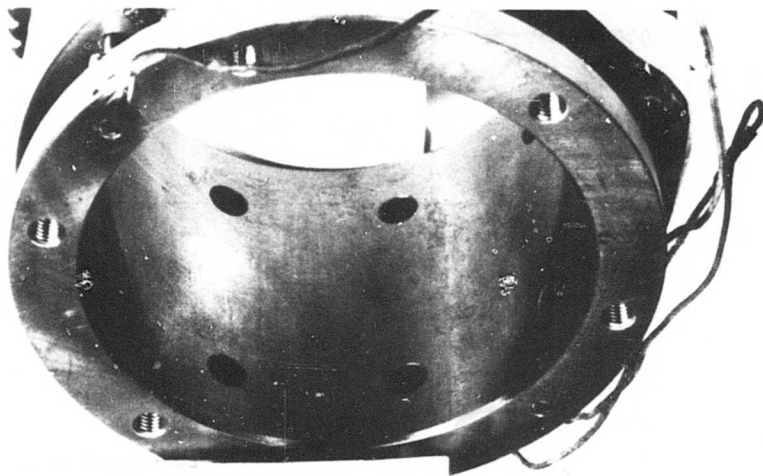
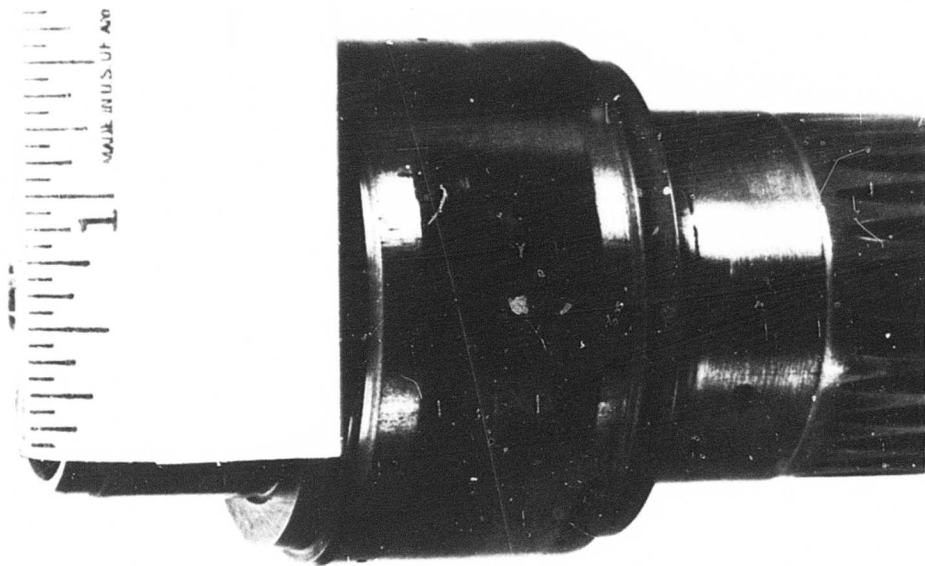


Figure 23. Inner and Outer Races Following Override Test, Design A.

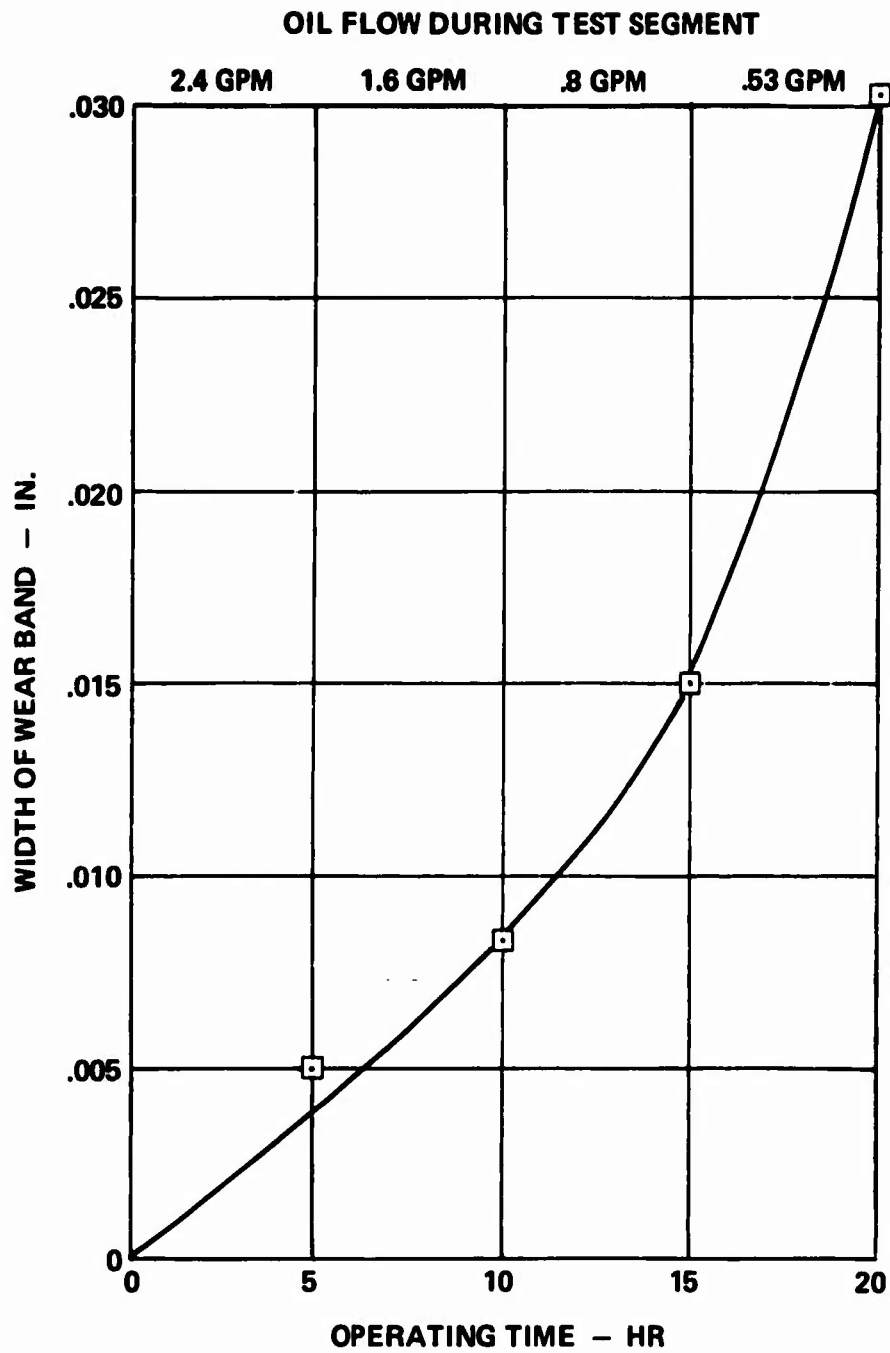


Figure 24. Sprag Wear Versus Hours of Operation, Design A Full-Speed Override (Input Stationary).

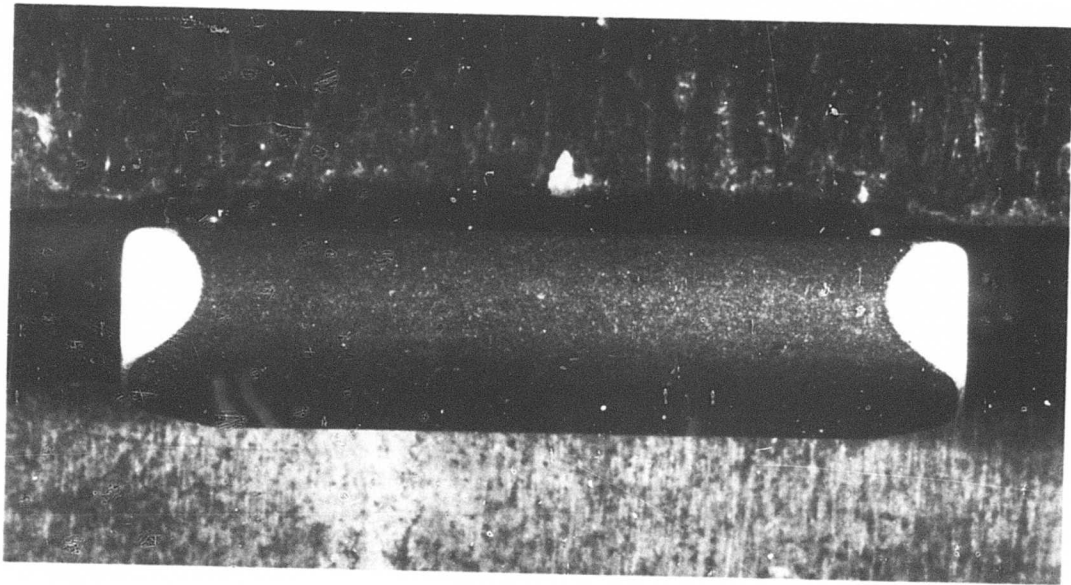


Figure 25. Sprag Condition Following Override Test, Design B.

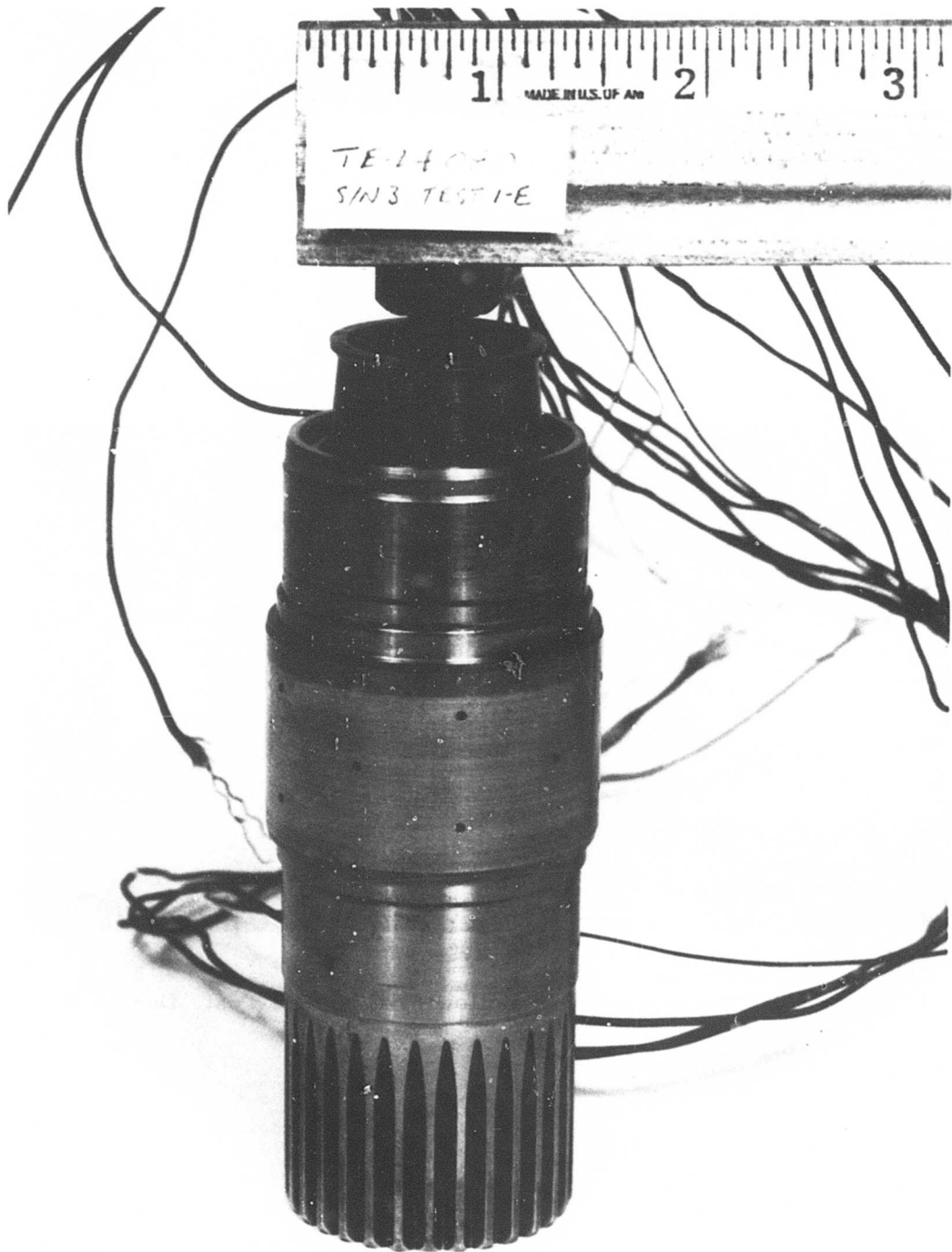


Figure 26. Inner Race Following Override Test, Design B.

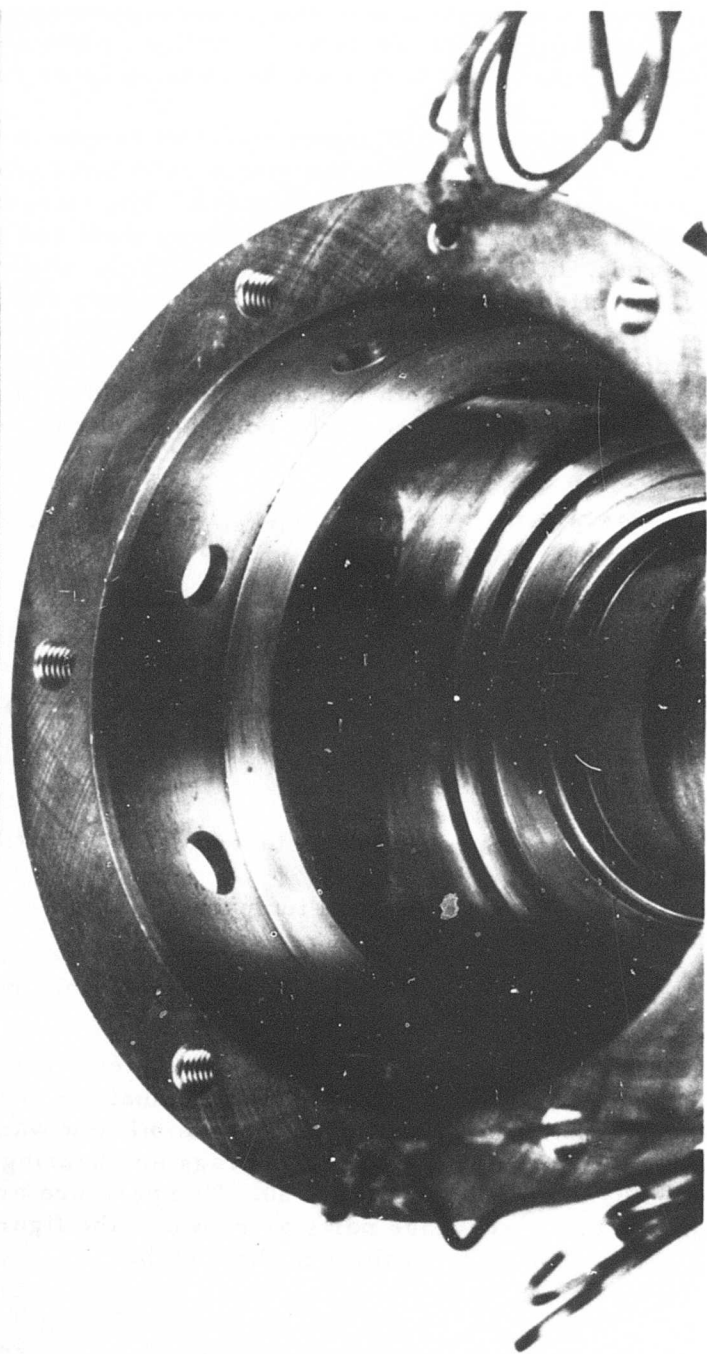
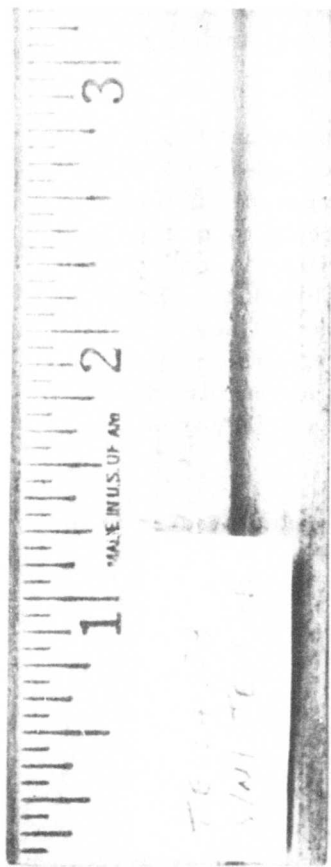


Figure 27. Outer Race Following Override Test, Design B.

The energy loss in the clutch due to overriding was measured in three ways: oil temperature increase, reaction torque on the stationary outer race, and shaft torque on the rotating inner race.

Theoretically, one would expect the shaft torque to be equal to the reaction torque and also to the torque calculated from oil-in and oil-out temperature differential and speed. The measurements obtained showed a reasonable correlation between shaft and beam torques. In some runs, difficulty was experienced with the slip ring readout; therefore, reaction torque was taken to be the more reliable data. These data for designs A and B are plotted in Figures 28 and 29 respectively. In order to determine the energy loss due to the sprag assembly alone, the rig was operated both with and without the sprag assembly installed. The results are reflected in the solid and dotted lines in Figures 28 and 29.

Energy loss using oil-in and -out temperatures was calculated as follows:

$$Q = MC_p \Delta T$$

where

Q = Heat loss - Btu/hr

M = Flow - pph

C_p = Specific heat - taken as .46 Btu/lb-°F

ΔT = Change in oil temperature - °F

$$\text{Torque} = \frac{24.8 Q}{\text{rpm}} \quad (\text{in. - lb})$$

At the higher oil flows, the torque calculated from oil-in and -out temperatures was significantly higher than shaft or reaction torque, which indicates that a large percentage of the oil flow was lost in leakage and was not passing through the sprags and bearings. Potential oil leakage paths are shown in Figure 30. Temperature probes were placed adjacent to the scavenge ports as shown in the figure, therefore measuring only the oil passing through the clutch.

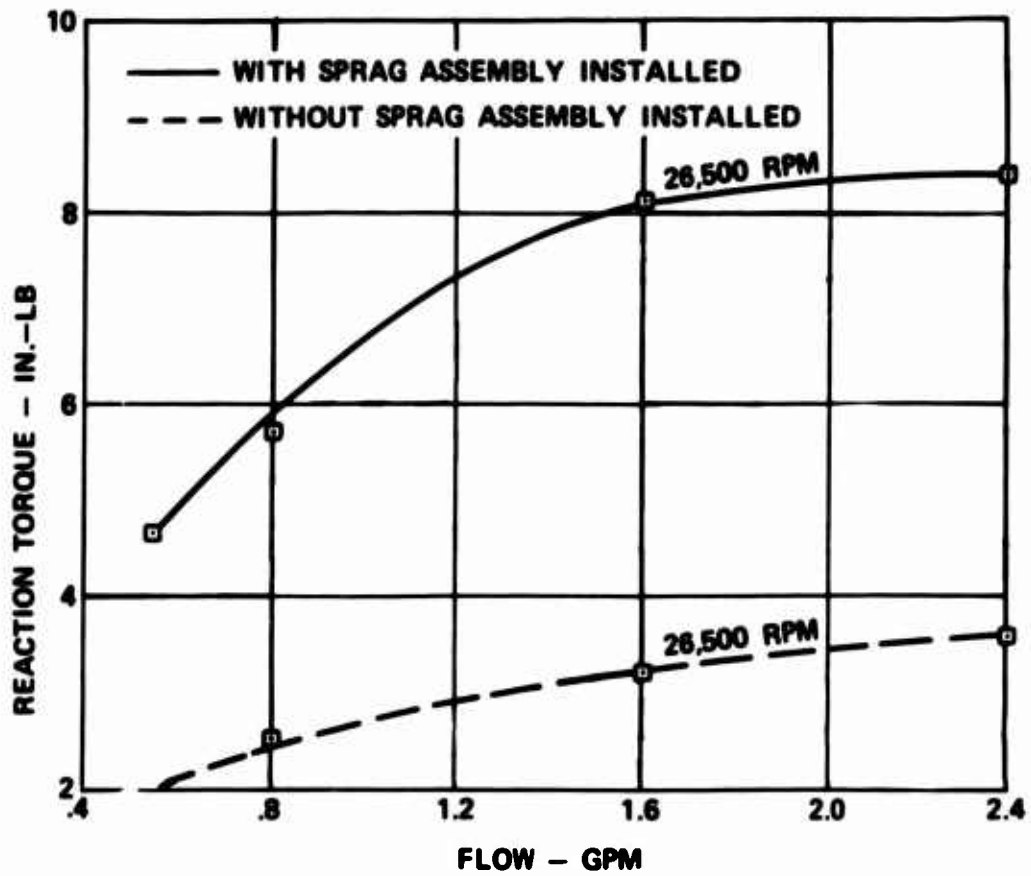


Figure 28. Reaction Torque Versus Oil Flow, Design A Full-Speed Override (Input Stationary).

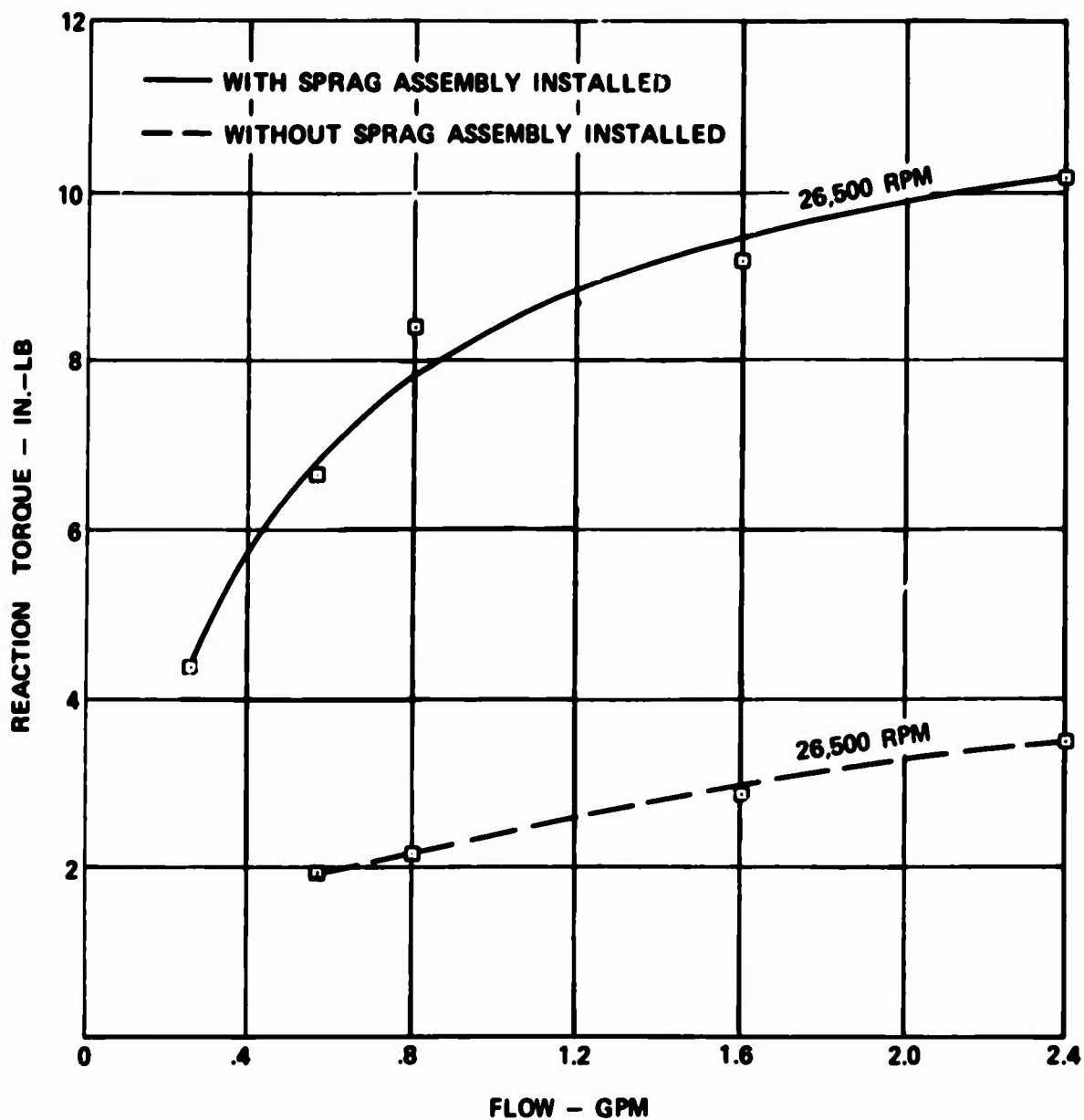


Figure 29. Reaction Torque Versus Oil Flow, Design B Full-Speed Override (Input Stationary).

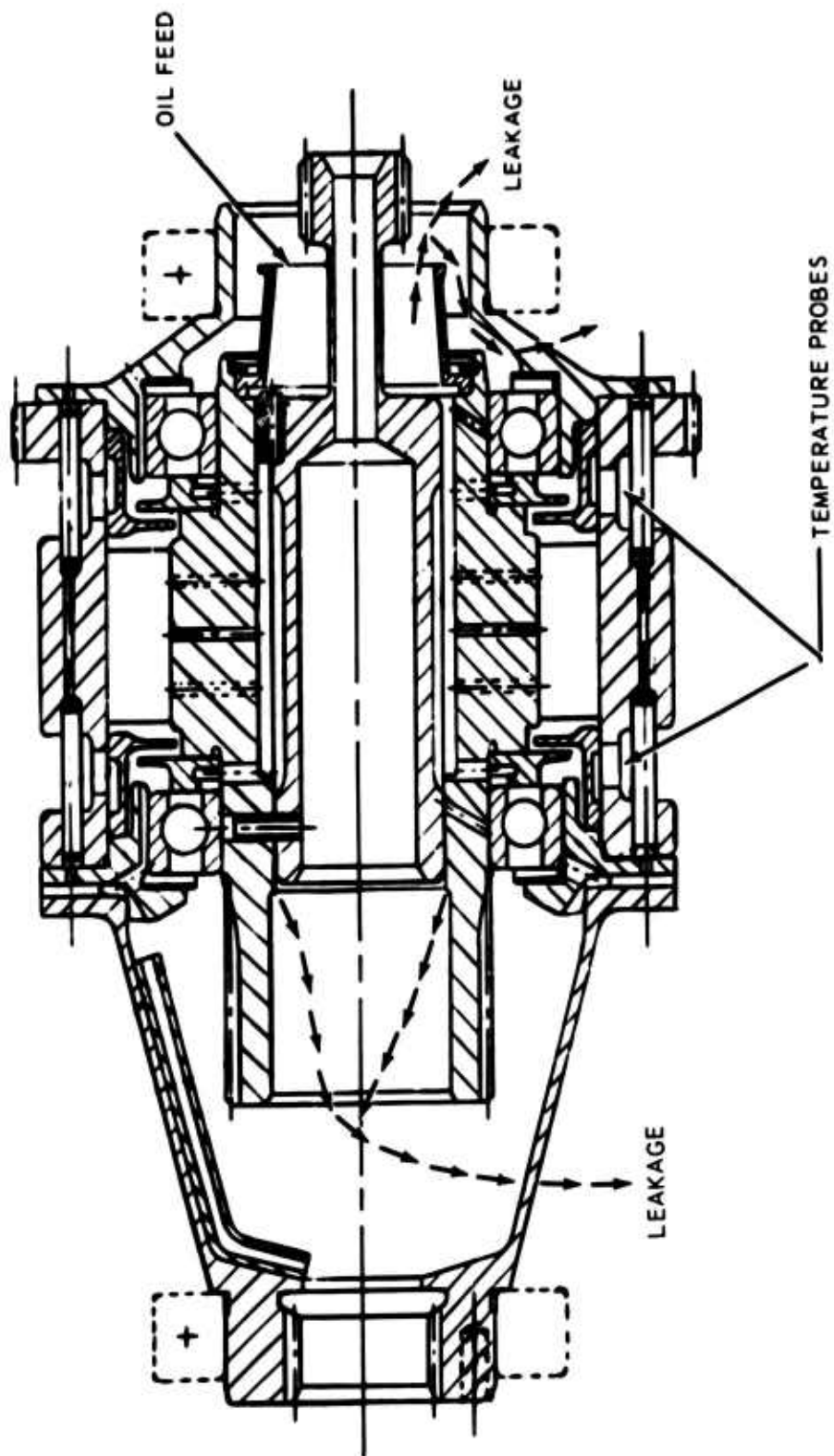


Figure 30. Oil Leakage Paths.

The raw data for shaft torque, reaction torque, and oil temperature are shown in Appendix III.

Oil temperature changes versus oil flow at 26,500 rpm for designs A and B are shown in Figures 31 and 32. Clutch and bearing race metal temperatures are shown in Figures 33 through 36.

On the basis of the condition of the sprags, the torque measurements, and the metal temperatures, it was decided to designate 200 percent design flow, 1.6 gpm, as the optimum flow for design A and 67 percent design flow, 0.54 gpm, for design B. These flows were to be used in the differential speed and dynamic engagement tests. Design A flow was chosen mainly on the basis of the sprag wear experienced. Design B performed well at all oil flows down to 33 percent; however, it was decided to use 67 percent, since metal temperatures were approaching 300° F and nearing the range where tempering of the case-carburized inner and outer races might occur.

Clutch design A sprag wear could be eliminated by incorporating design changes that would force the sprags further into the release position and away from inner race contact during periods of override. The mechanism by which this function can be accomplished is a force exerted on the sprags by the inner retainer (Figure 37).

The addition of a drag band between the inner retainer and the inner race would create a frictional force on the retainer that, when transmitted to the sprags, would tend to reduce the energizing moment. The drag band approach would result in the transferral of sliding from the sprags to the band and might result in band wear as noted on the outer cage drag band in the test program. This problem could be resolved by proper choice of band material and sufficient drag band area.

Another method of obtaining drag between the inner cage and race is to interrupt the inner cage flanges with a series of cutouts that are directly in line with the oil holes in the inner race (Figure 37). This method would be applicable only to a centrifugally lubricated clutch design.

Drag torques measured in the override test were on the order of 4 to 10 inch-pounds or 2 to 4 horsepower at 26,500 rpm. Drag torques and temperature data were measured at speeds from 26,500 rpm down to 10,000 rpm to provide more useful design data. These data are presented in Appendix III. Operation at speeds lower than 26,500 will be less severe in terms of heat generation and wear.

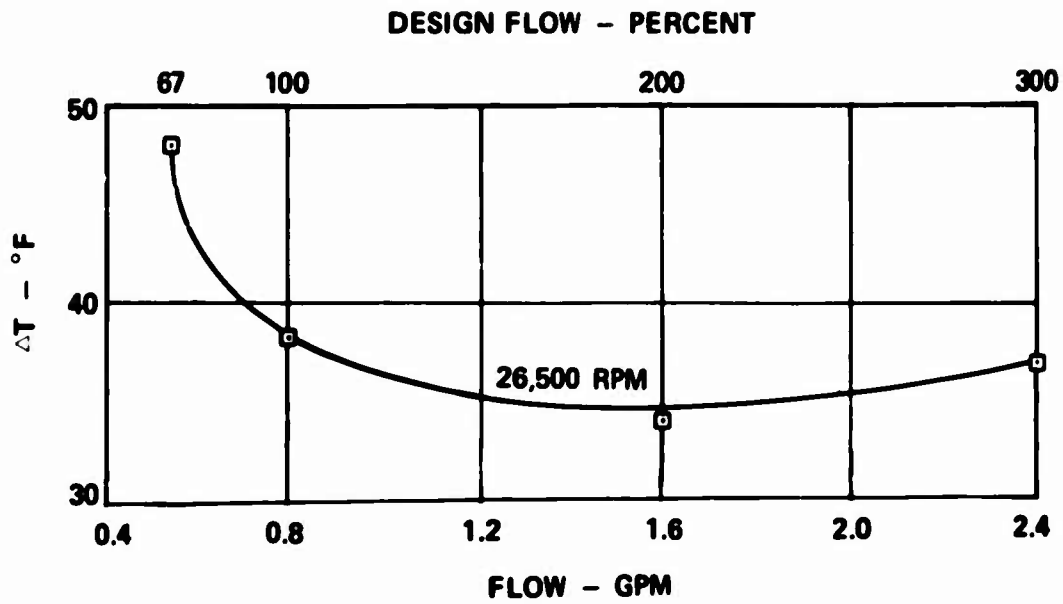


Figure 31. Oil ΔT Versus Flow, Design A Full-Speed Override (Input Stationary).

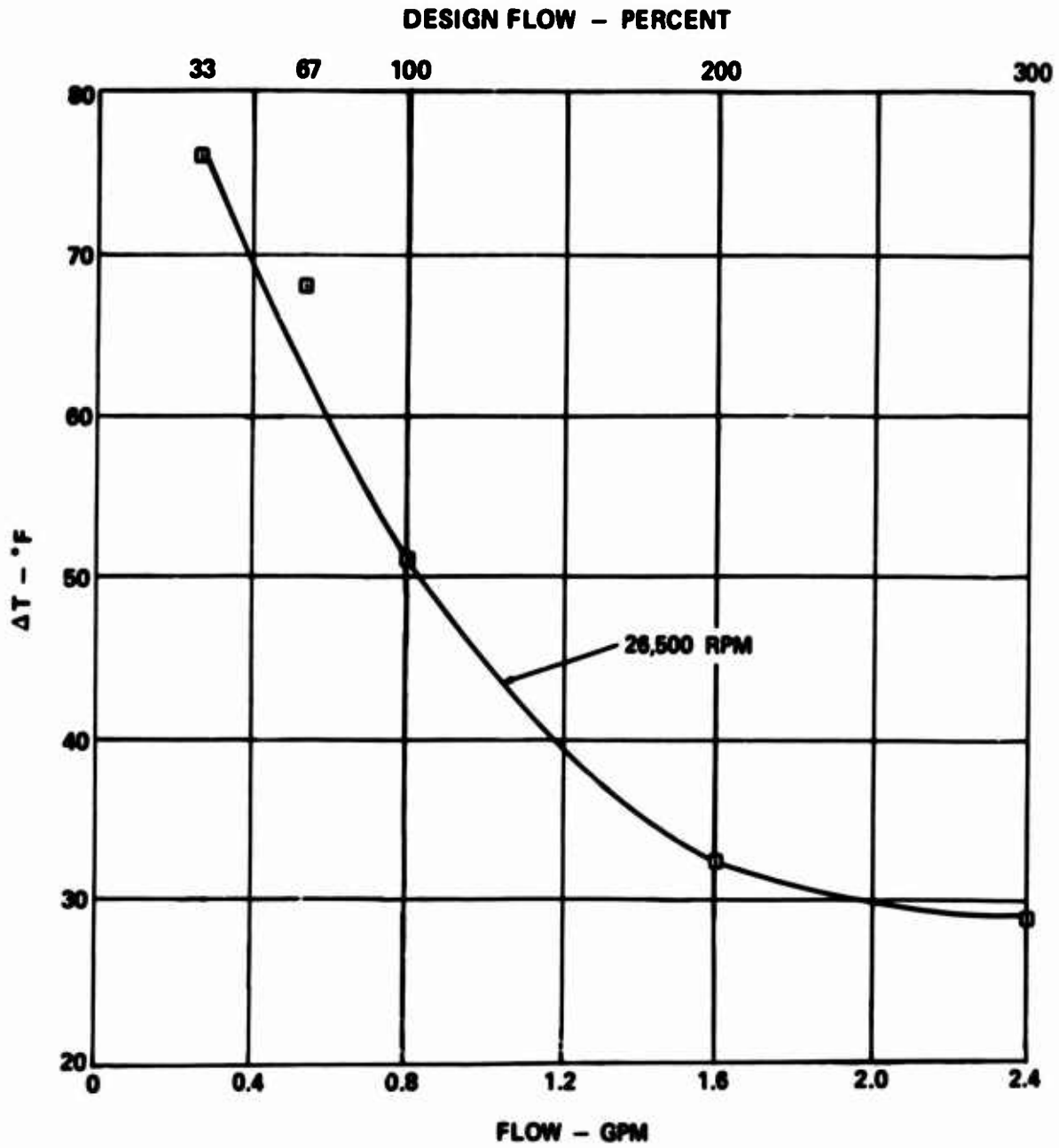


Figure 32. Oil ΔT Versus Flow, Design B Full-Speed Override (Input Stationary).

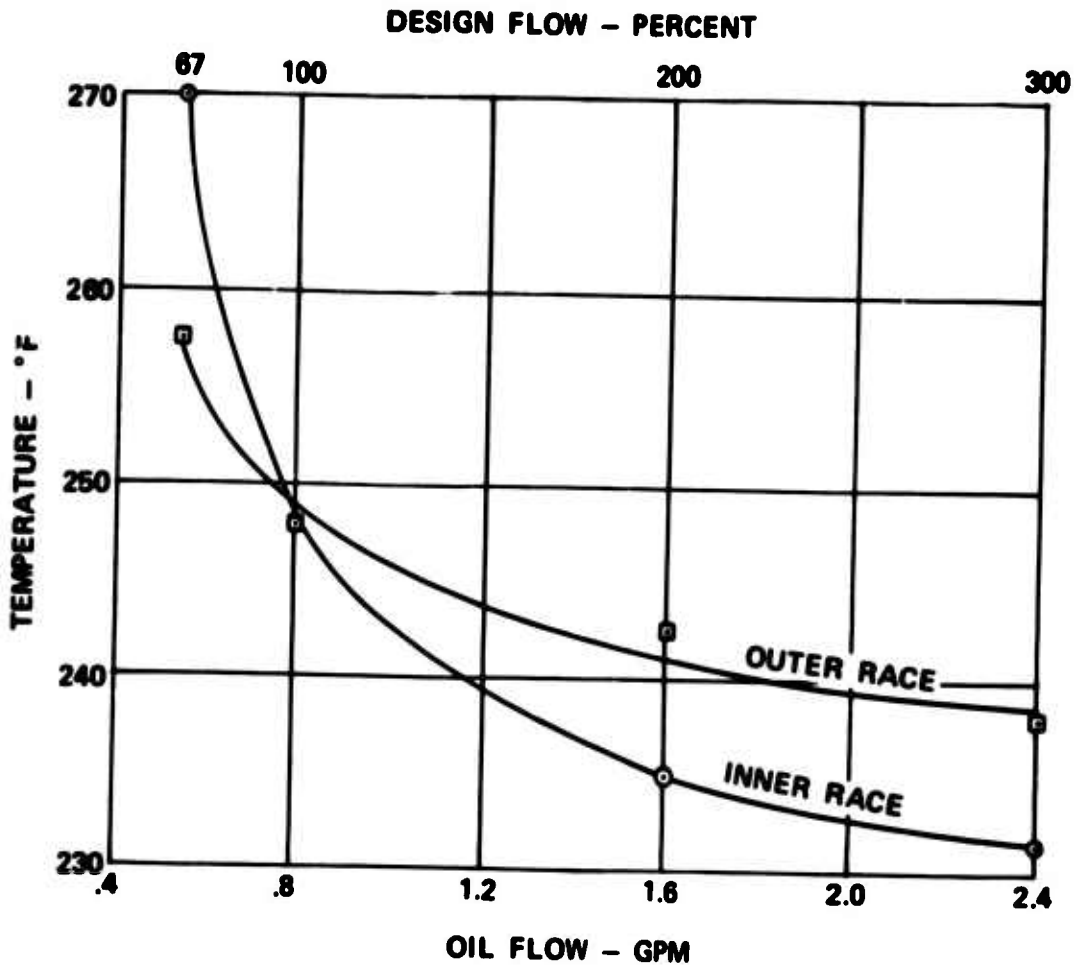


Figure 33. Clutch Race Temperature Versus Oil Flow, Override Test, Design A.

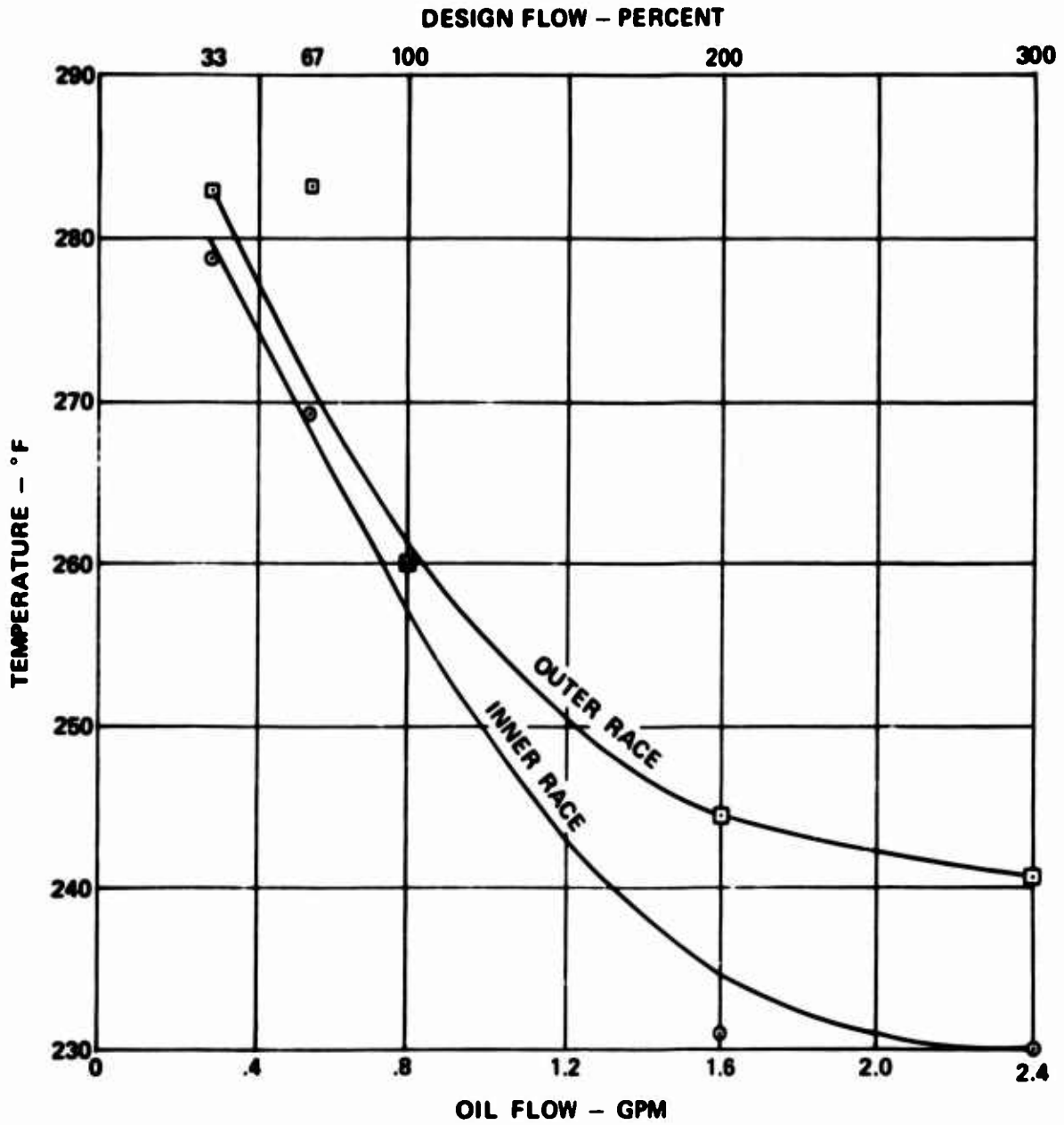


Figure 34. Clutch Race Temperature Versus Oil Flow, Override Test, Design B.

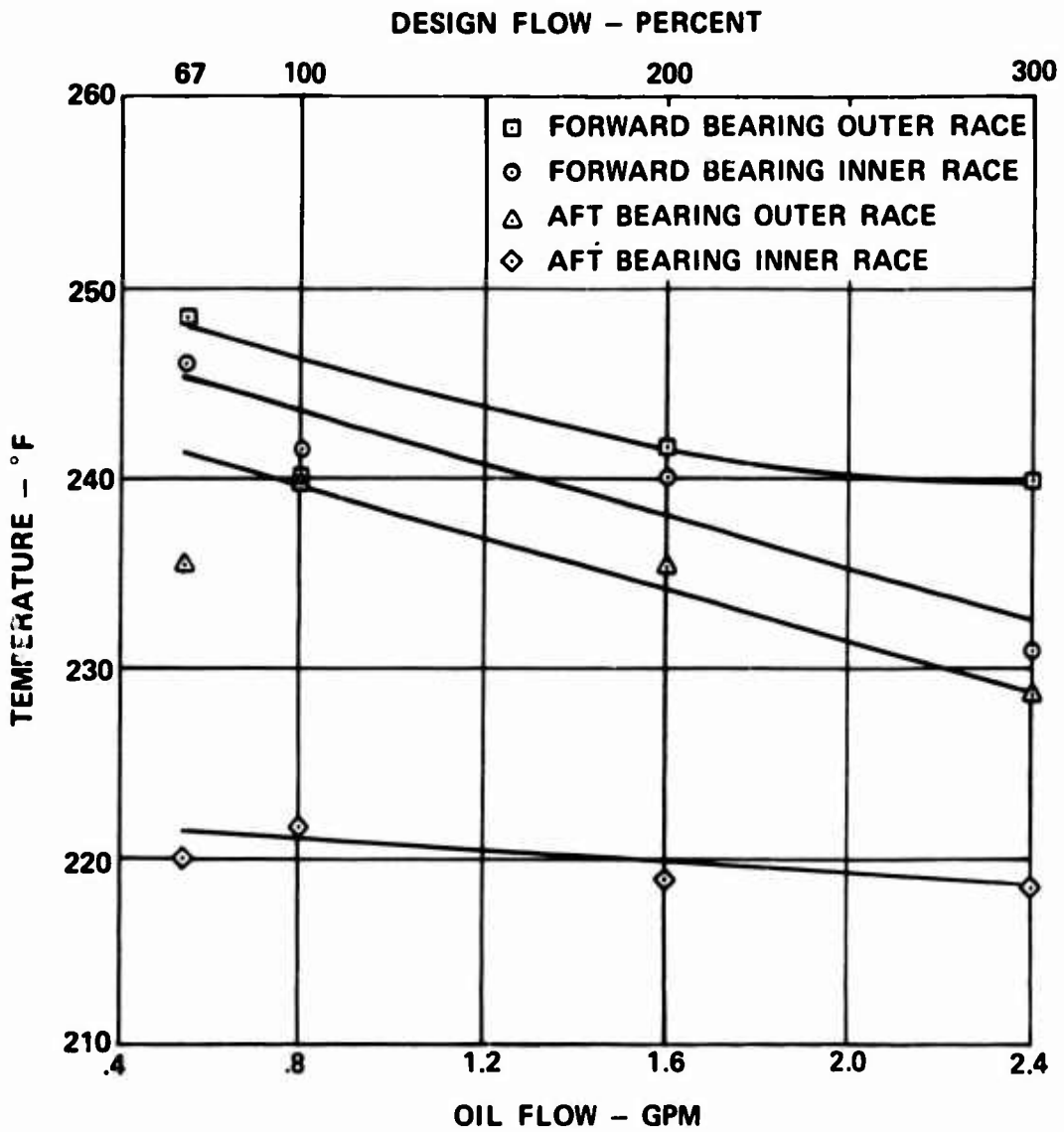


Figure 35. Bearing Race Temperature Versus Oil Flow, Override Test, Design A.

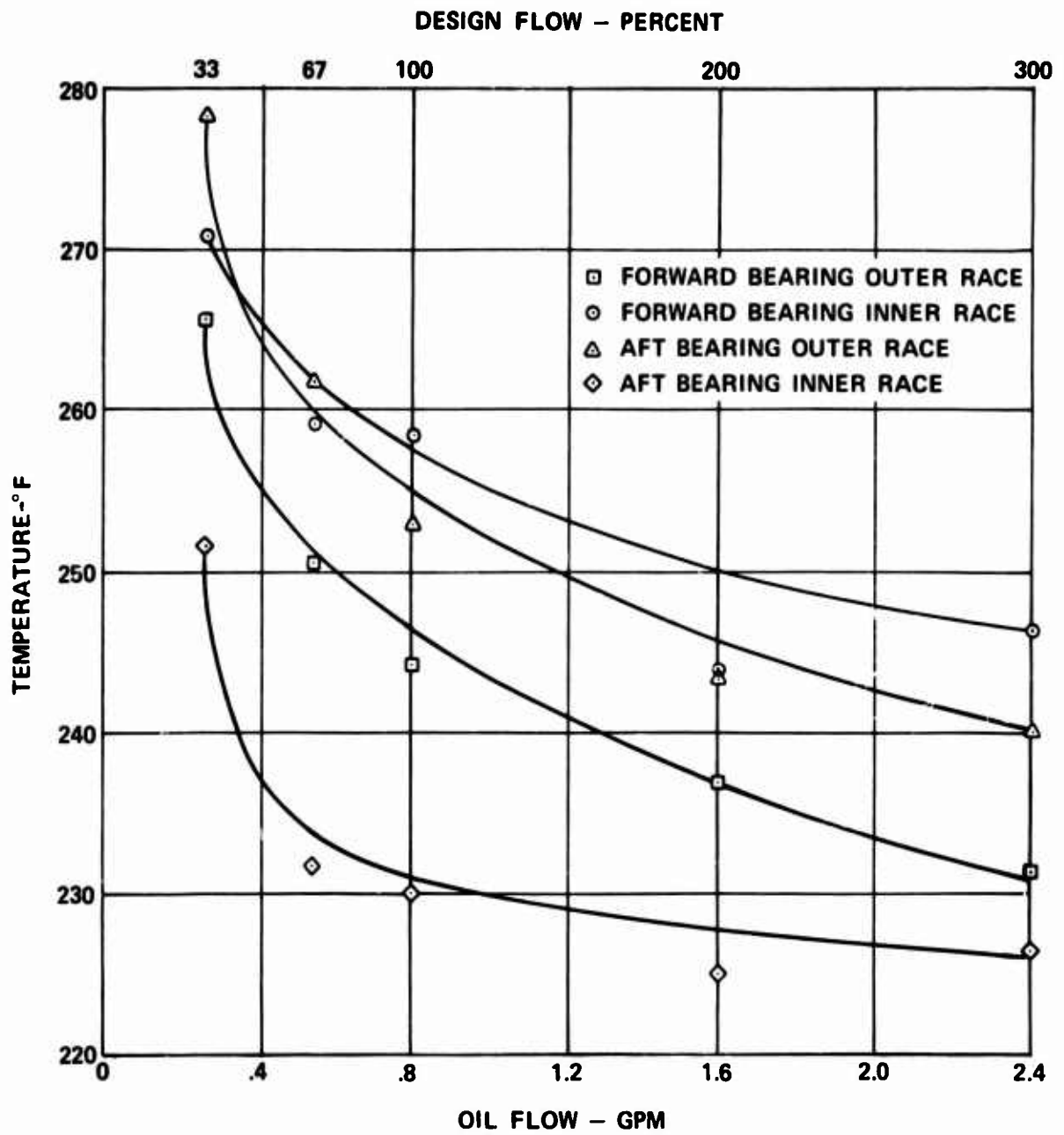


Figure 36. Bearing Race Temperature Versus Oil Flow, Override Test, Design B.

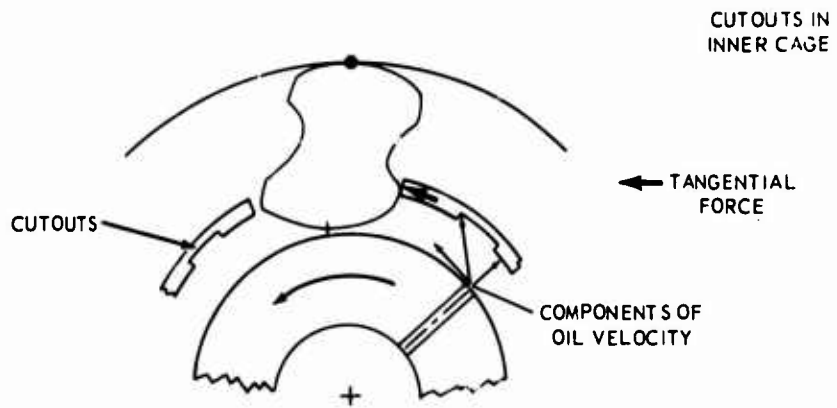
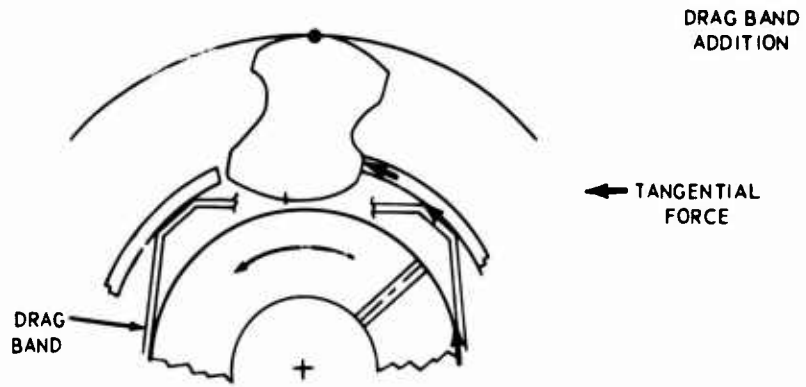
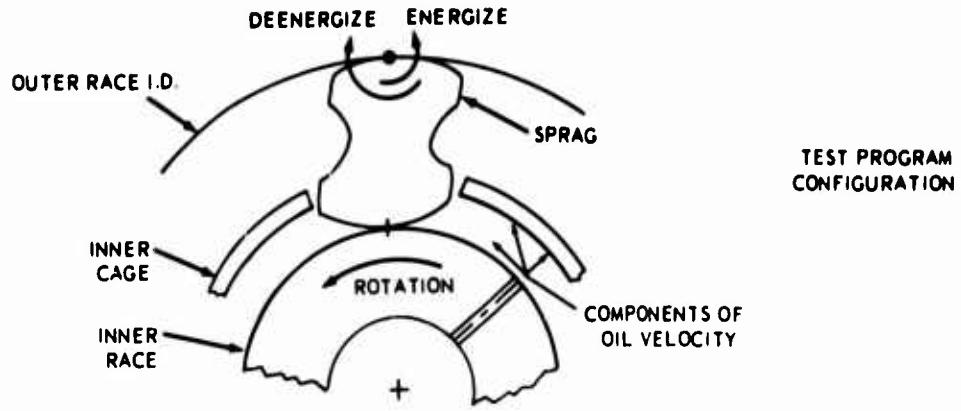


Figure 37. Design Modifications.

DIFFERENTIAL SPEED DYNAMIC CLUTCH OVERRIDE TEST

The design A clutch oil flow was 1.6 gpm. This clutch exhibited its highest drag torque at a differential speed of 50 percent, and a 5-hour test was conducted at this condition. The sprags exhibited a wear band 0.047 inch wide and 0.002 inch deep on the inner cam surface following the test. Slight scuffing was noted on the inner race; however, no wear was measured on either the inner or outer races. Clutch component condition is shown in Figures 38 through 40.

Drag torque and oil temperature results are listed in Table VI. Note that the torque calculated with oil-in and oil-out temperatures compares well with the shaft torque, especially for the 50 and 67 percent speed points. The torques presented are average values. Actual readings varied ± 5 percent from the average. The oil leakage encountered in the override test was not noted here because with the outer race rotating, centrifugal force assists in scavenging the sprag area. Therefore, a greater percentage of the feed oil was able to flow through the clutch.

It is interesting to note that the 'PRS-V' factor, interface pressure (psi) times sliding velocity (fps), is a maximum at 50 percent differential speed. The 'P-V' factor, load/inch times sliding velocity (fpm), commonly used in the clutch industry, becomes a maximum at approximately 67 percent differential speed. These factors come to a maximum because as the speed differential between the races decreases, the sliding velocity decreases. As the outer race speed increases, however, the sprag load due to centrifugal force increases; therefore, the product of the two comes to a maximum within the speed range.

The design B clutch exhibited strong centrifugal engaging characteristics and could not be made to operate at the test points. An explanation follows.

With the inner race rotating at 26,500 rpm, the outer race was held stationary by applying reverse steam to the turbine prime mover. As the outer race was brought up to speeds of 6000 to 9000 rpm, by reducing reverse steam, the clutch commenced to engage. The inner race speed decreased, the outer race speed increased, and full engagement was accomplished at approximately 17,000 rpm. This relationship occurred because the steam turbines could not exert sufficient torque to hold the races at the required differential speeds. The test results are further illustrated in Figure 41. The plot is accomplished by reading the inner and outer race speeds on an X-Y plotter.

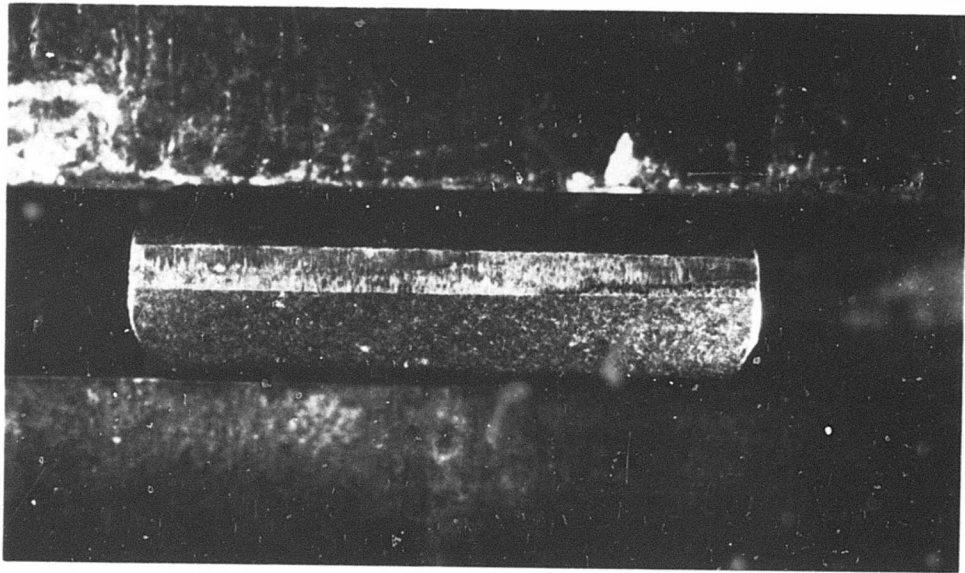


Figure 38. Sprag Wear Following Differential Speed Test, Design A.



Figure 39. Inner Race Following Differential Speed Test, Design A.

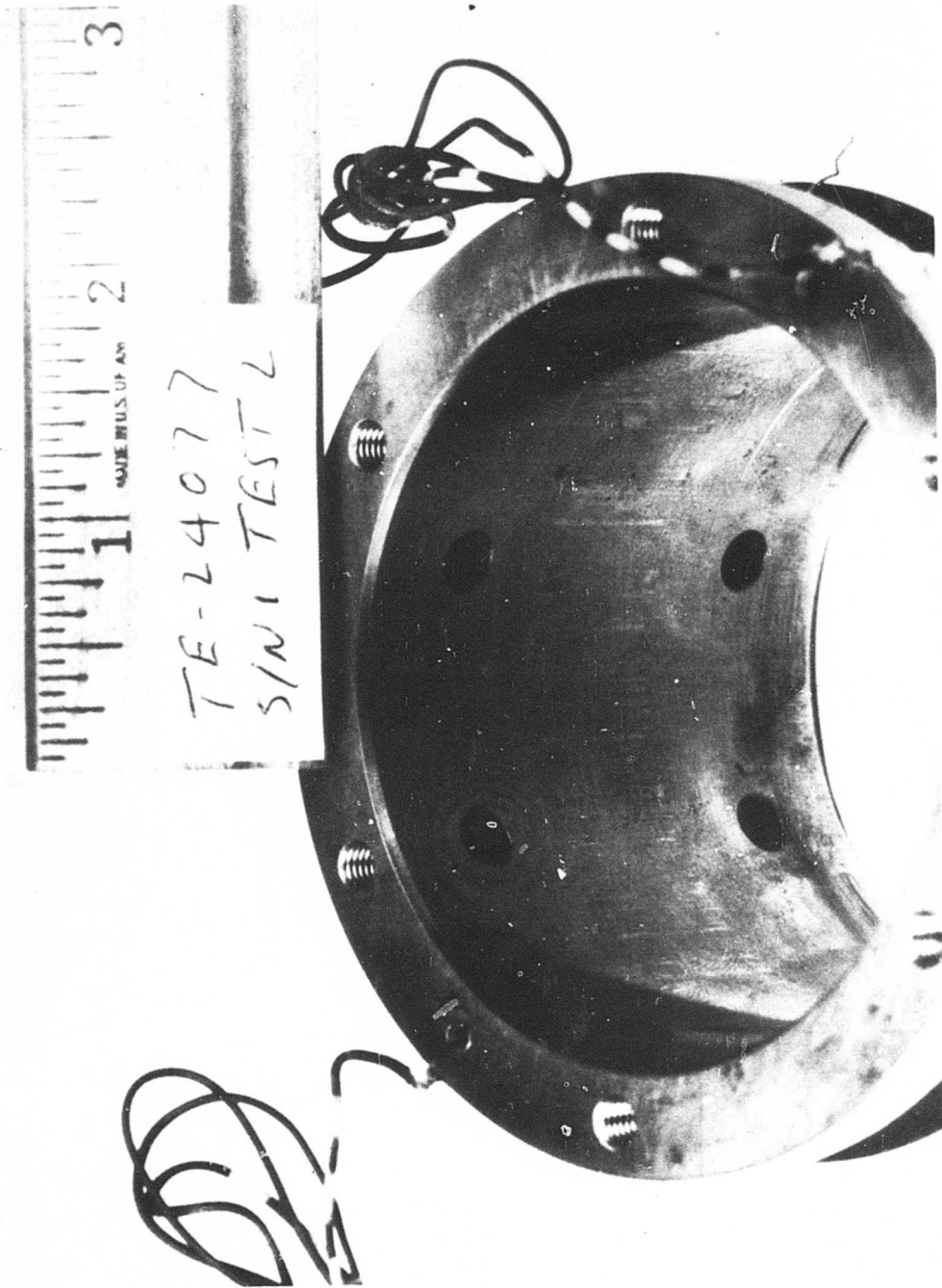


Figure 40. Outer Race Following Differential Speed Test, Design B.

TABLE VI. DIFFERENTIAL SPEED TEST RESULTS, DESIGN A

Speed Point (pct)	Inner Race (rpm)	Outer Race (rpm)	Shaft Torque (in. -lb)	Oil Temp. ΔT °F	Drag Torque		PRS-V Factor $\frac{(\text{psi} \times \text{fps})}{\text{Design A}}$
					Calculated (in. -lb)	Using Temp. Design B	
50	26,500	13,250	12.9	18.9	12.3	6.8x10 ⁶	4.2x10 ⁶
67	26,500	17,755	7.7	7.2	7.1	6.0x10 ⁶	3.7x10 ⁶
75	26,500	19,875	8.0	9.0	11.7	5.0x10 ⁶	3.0x10 ⁶

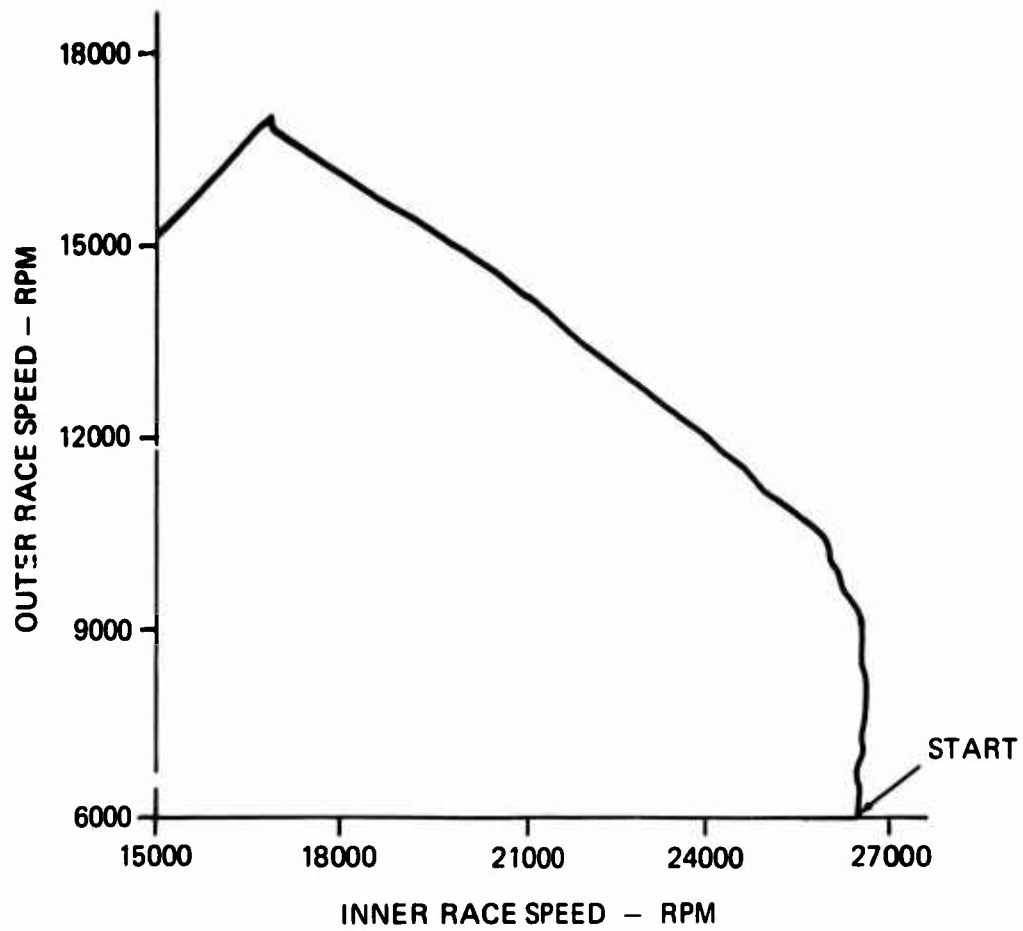


Figure 41. Plot of Clutch Engagement, Design B.

The scale ratio is 1:1, so that if both races are accelerating or decelerating at the same rate, the resulting plot is a 45-degree line. The Figure 41 curve starts with the inner race at 26,500 rpm and the outer race at 6,000 rpm. As outer race speed is increased to 9,000 rpm, by reducing reverse steam, engagement commences. Although no adjustment is made to the prime movers, the inner race speed decreases as the outer race speed increases. Full engagement occurs with both races at 17,000 rpm. The engagement time was approximately 2 seconds. If more torque were available in the prime movers, the design B clutch could have been made to operate at the test differential speed points; however, this is academic, since heat generation and wear would have been excessive.

Initial design B clutch differential testing was with 0.54 gpm oil flow, the optimum determined from the override test. Because the design A clutch had been able to operate with 1.6 gpm flow at the test points, it was decided to test the design B clutch at this flow. Again the clutch engaged at outer race speeds of over 6,000 rpm. A 5-hour run was then conducted with the inner race at 26,500 rpm and the outer race varying between 3,400 and 5,400 rpm. Sprag and race condition following this test are shown in Figures 42 through 44. The sprag wear band width was 0.039 inch, and the depth was 0.001 inch. The inner race was scored. Drag torque measured during the 5-hour run was 5.3 inch-pounds, and the oil temperature differential was 26° F.

There was some question as to whether the wear occurred during the period of operation at 0.54 gpm oil flow, and whether this operation affected the ability of clutch B to operate successfully at the higher oil flow. To investigate this possibility, another unworn clutch of design B was operated at 2.4 gpm oil flow. Attempts were made to operate at the test points, and again the clutch engaged at over 6,000 rpm. Sprag wear was again noted at disassembly equivalent to the wear noted in the previous test.

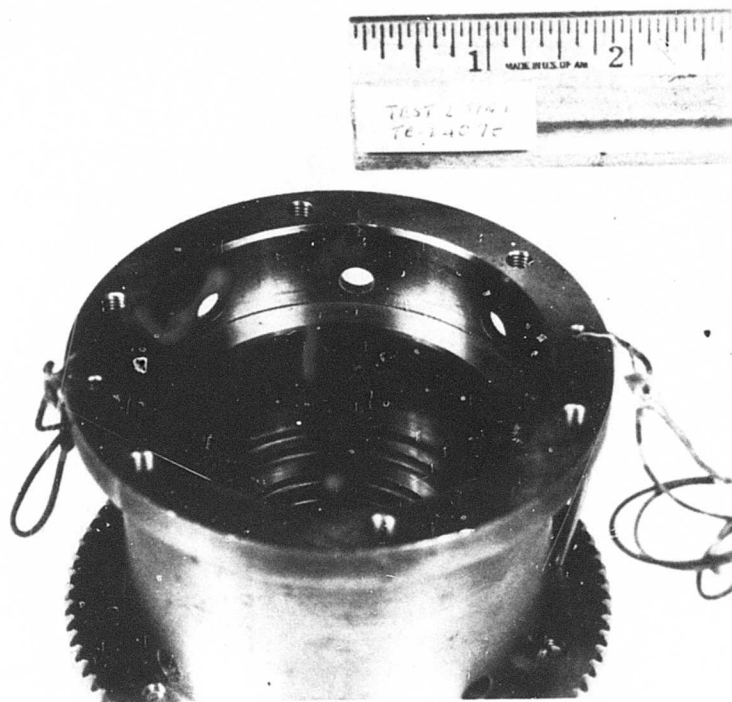


Figure 42. Sprag Wear Following Differential Speed Test, Design B.

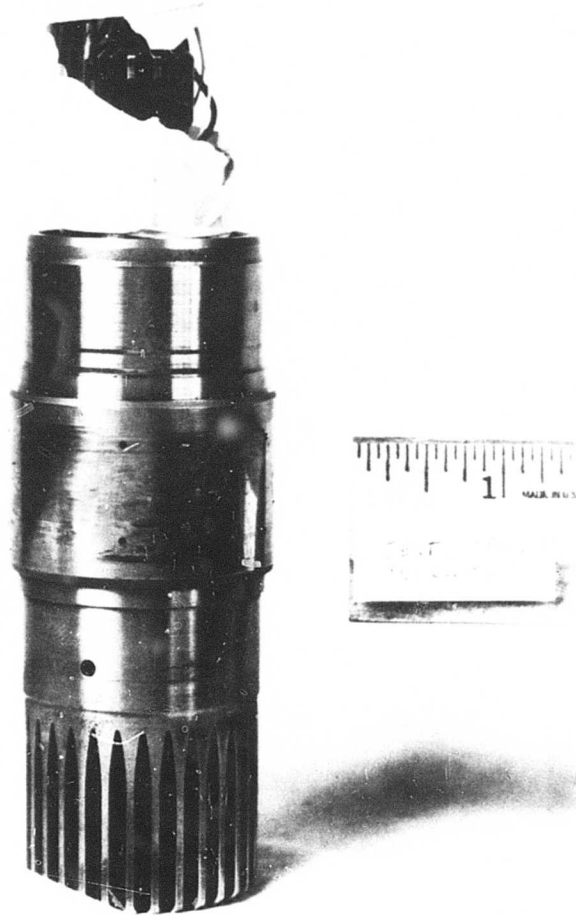


Figure 43. Inner Race Following Differential Speed Test, Design B.

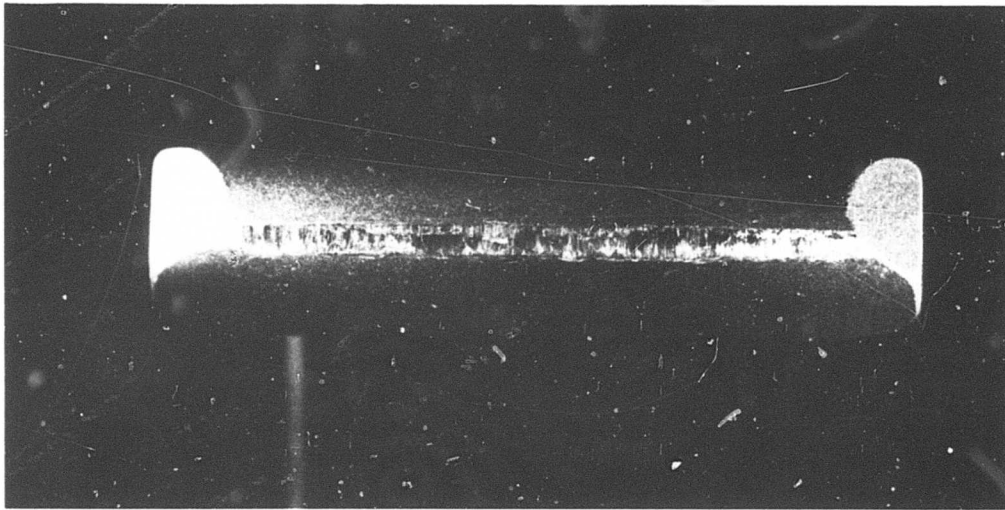


Figure 44. Outer Race Following Differential Speed Test, Design B.

The differential speed condition is clearly the most severe in terms of clutch component wear and drag torque. Further high-speed clutch development should concentrate on this mode of operation. High-speed sprag clutches can operate successfully in the differential speed mode if close attention is paid to the following areas:

1. Precise definition of sprag geometry; location of center of gravity and points of spring contact at speed
2. Development of lubrication method; amount of flow, location, and pattern of oil inlet jets and scavenge ports
3. Close attention to clutch component surface texture and hardness, including surface treatment to reduce wear

The design A clutch exhibited excessive wear at the sprag inner cam surface. To overcome this wear characteristic, the same design recommendation as for the overriding test is made; namely, to reduce the energizing moment on the sprags. (See Figure 37.)

The design B clutch was unable to fulfill the differential speed test requirements because of excessive positive centrifugal engaging action by the sprags. The action also resulted in wear of sprag inner race cams and metal flow of the inner race sprag contact surface. Positive centrifugal engaging can be reduced in two ways (Figure 45):

1. Reduction of sprag energizing moment by profile modification; i. e., move sprag center of gravity closer to the radial line from the center of the clutch to the outer race contact point.
2. Reduction in the energizing moment due to spring mass by modifying the sprag profile to move the spring energizing contact toward the center of the sprag.

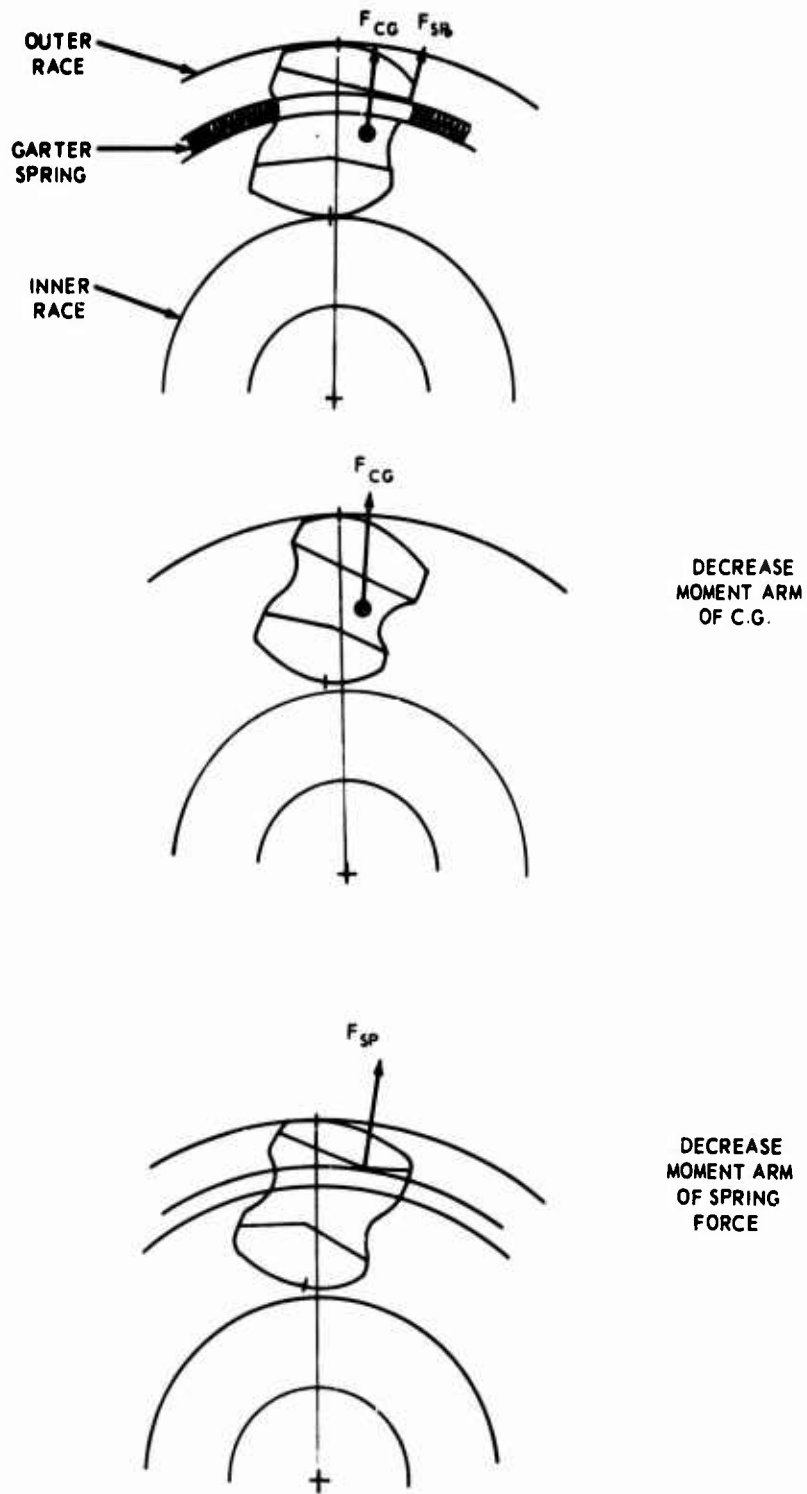


Figure 45. Methods of Decreasing Centrifugal Energizing Moment.

DYNAMIC ENGAGEMENT TEST

The design A and B clutches that underwent the 5-hour differential speed tests were used in the dynamic engagement test to determine if the wear experienced in the differential speed test would affect the clutch's ability to engage or disengage. No difficulty was experienced with either design at any of the engaging speeds:

13,250 rpm - 2 engagements and disengagements

19,875 rpm - 2 engagements and disengagements

26,500 rpm - 5 engagements and disengagements

Measurements following the test indicated no change in clutch component condition. Oil flows of 1.6 gpm for design A and 0.54 gpm for design B were used.

No attempt was made in this test to exactly simulate acceleration rates or inertias that would be experienced in an aircraft installation.

Figure 46 illustrates a typical engagement of a design A clutch using an XY plotter hooked up to the inner and outer race speed signals. Initially, the inner race is rotating at 25,200 rpm and the outer at 12,000 rpm. As the outer race speed is increased, engagement commences at point A with the outer race accelerating and the inner race decelerating. Complete engagement is at point B with both races at 17,700 rpm. Engagement time was approximately 3 seconds.

STATIC CYCLIC TORQUE FATIGUE TEST

Two design A and two design B clutches were subjected to this test. All four specimens survived $7,140 \pm 900$ inch-pounds for 10^7 cycles with no failures. Neither the angular displacement of the input shaft with respect to the output nor the outer shaft radial deflection varied over the 10^7 cycles. Although there were visible traces on the inner and outer races where the sprags had contacted (Figure 47), there was no measurable wear. Magnaflux inspection showed no crack indications. Angular displacement, outer race diametral growth, and calculated clutch stresses at 8,040 inch-pounds torque are listed in Table VII.

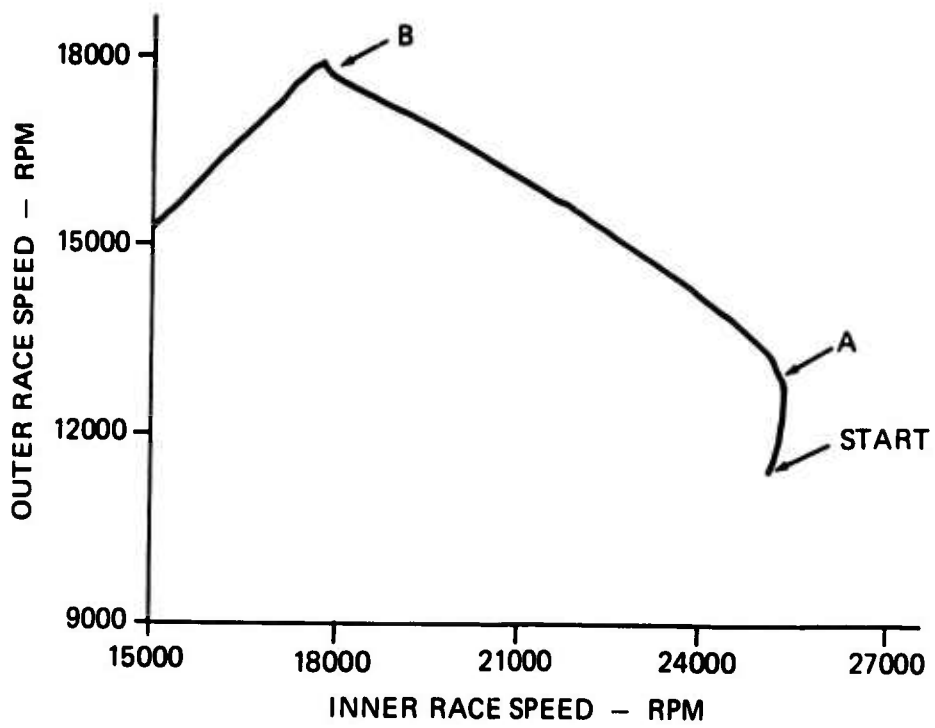
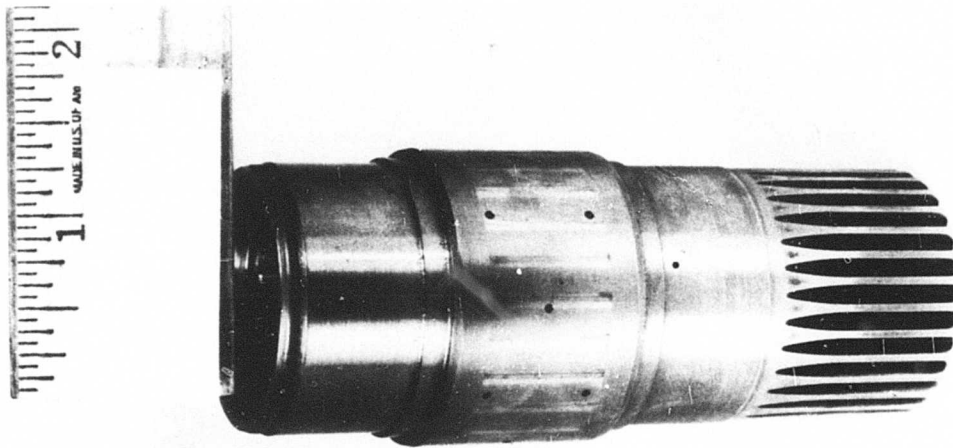
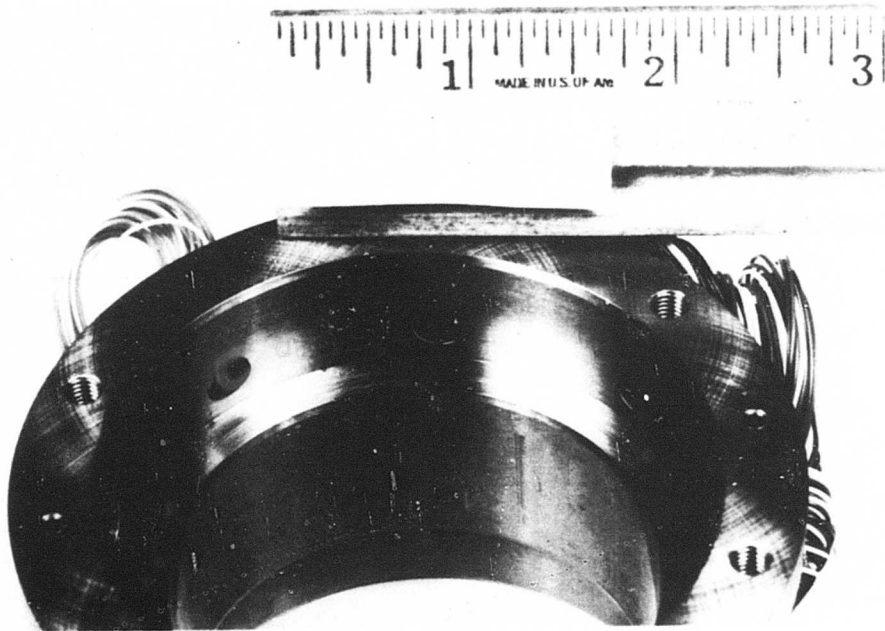


Figure 46. Plot of Dynamic Engagement Test, Design A.



Inner Race



Outer Race

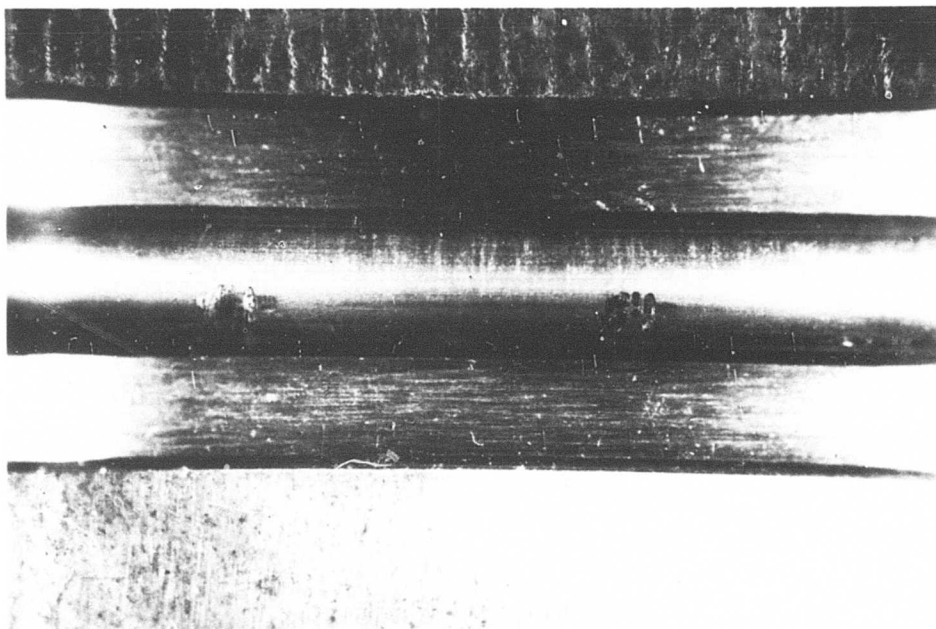
Figure 47. Typical Clutch Race Condition Following Cyclic Fatigue Test.

TABLE VII. CONDITIONS AT MAXIMUM CYCLIC FATIGUE TORQUE, 8,040 INCH-POUNDS				
Design	Angular Displacement (deg)	Outer Race Diametral Growth (in.)	Compressive Stress, Inner Race OD (psi)	Hcop Stress, * Outer Race ID (psi)
A	4.9	.0038	497,900	73,700
A	4.9	.0038		
B	7.2	.0049	500,500	94,400
B	5.7	.0049		

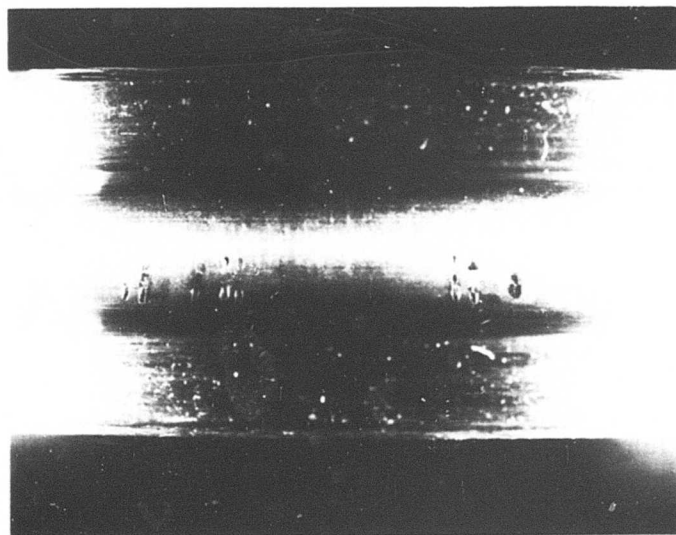
* This stress does not include rotational effects.

A problem noted following the cyclic torque fatigue tests was fretting of the bearing balls and races. Figure 48 illustrates fretting on an inner and outer race, which was measured to be approximately 0.0001 inch in depth. Several patterns are visible on the races, since there were shutdowns during the test and the bearing angular positions changed several times during the 10^7 cycles. Also, this bearing was used in two cyclic fatigue tests.

The fretting experienced may not be representative of an actual application, since lubrication conditions would be better in a rotating installation. Also, the application of load would be different. The degree of fretting, however, if experienced in an application, would be detrimental to bearing performance and could cause vibration and/or initiation of bearing fatigue.



Bearing Outer Race



Bearing Inner Race

Figure 48. Bearing Fretting in Cyclic Fatigue Test.
Mag: 5X

Bearing fretting in an application could be forestalled by investigating four areas of improvement:

1. Coating of the bearing races with a dry lubricant
2. Use of dissimilar materials in the bearing balls and races
3. Surface hardening of the balls or races using such processes as nitriding or chromizing
4. Use of roller or journal bearings

STATIC OVERLOAD TEST

Two design A and two design B clutches were subjected to this test. Torque was applied in 500 inch-pound increments until failure.

The mode of failure of the design A clutch was sprag rollover, which occurred at 22,500 inch-pounds. This failure is a catastrophic type, which renders the clutch inoperable.

Design B clutch failures, because of the sprag lockup feature (Figure 3), resulted in slippage of the outer race with respect to the inner race. One sample slipped at 15,500 inch-pounds, and the other at 18,000 inch-pounds. This mode of failure is preferable to sprag rollover since the clutch is still functional when the overload is relieved. In fact, no deterioration in clutch condition was noted due to the overload test.

The first overload test, using a design A clutch, resulted in a sprag rollover failure at 5,000 inch-pounds. This rollover was attributed to a rig assembly problem whereby the outer race was assembled eccentrically to the inner. Eccentricity of the races results in unequal load sharing among the sprags, which causes premature rollover of the overloaded sprags. Evidence of this occurrence was that five of twenty sprags were heavily edge loaded. This failure is shown in Figure 49, which illustrates the quadrant of heavily pitted sprags. When the overloaded sprags rolled over, the remaining sprags tried to pick up the load and also rolled over. Further evidence that an unbalanced radial load had occurred was that the bearings were heavily Brinelled.

The assembly procedure was modified to ensure concentricity of the races, and three overload tests (one design A, two design B) were conducted without difficulty.

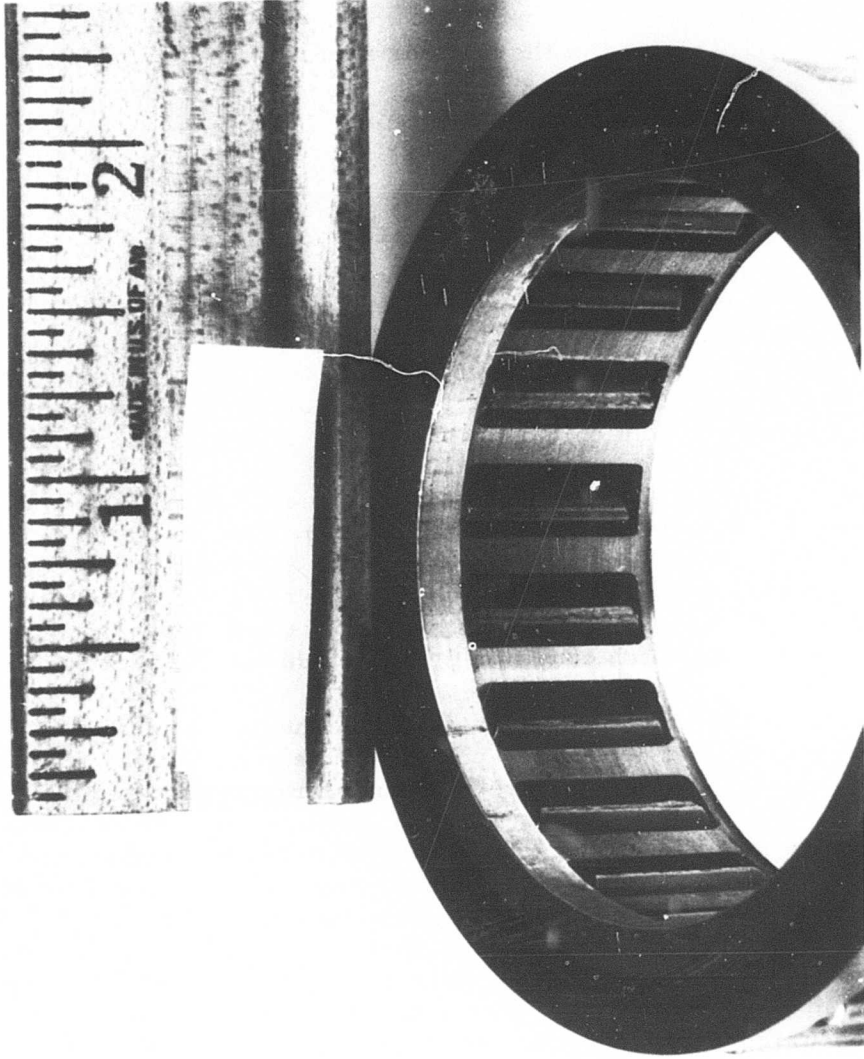


Figure 49. Sprag Rollover Failure.

The diametral growth of the outside of the outer race measured during the overload test is shown in Figure 50. The angular displacement of the outer race versus the inner race during the overload test is shown in Figure 51. The angular displacement plotted includes windup of the inner and outer race shafts.

Sprag rollover and/or slippage due to overload occurs when the tangent of the strut angle (α'_i) at the inner race contact approaches the value of the coefficient of friction. Using the computer analysis and inputting torques of 22,500 inch-pounds for design A and 18,000 inch-pounds for design B, strut angles of 4.69 and 4.26 degrees were calculated. Therefore, the computer results agree well with the test results.

METALLURGICAL STUDY

Sprags and races of designs A and B were sectioned and analyzed to determine metallurgical characteristics. Laboratory measurements for the case carburized races are listed in Table VIII.

TABLE VIII. METALLURGICAL RESULTS, CASE-CARBURIZED RACES				
	Case Depth (in.)	Case Hard- ness (R _C)	Core Hard- ness (R _C)	Remarks
<u>Design A</u>				
Inner Race	.051	62.5	36	
Outer Race	.042	62.5	37	
<u>Design B</u>				
Inner Race	.047	60.0	37	Retained austenite in case, approxi- mately 10%
Outer Race	.048	62.5	37	Traces of retained austenite in case

The design A sprag is of M50 steel that was through hardened and gas nitrided for an especially hard outer case. Sprag microstructure is shown in Figure 52. The case consisted of tempered martensite, carbides, and nitrides. The core consisted of tempered martensite and carbides.

The design B sprag uses 52100 steel, through hardened and surface treated by a pink phase chromizing process. Sprag microstructure is shown in Figure 52. The compound layer due to chromizing was found to be 0.00025 inch thick, and the actual surface hardness could not be determined.

Sprag case hardness versus depth for designs A and B is shown in Figure 53.

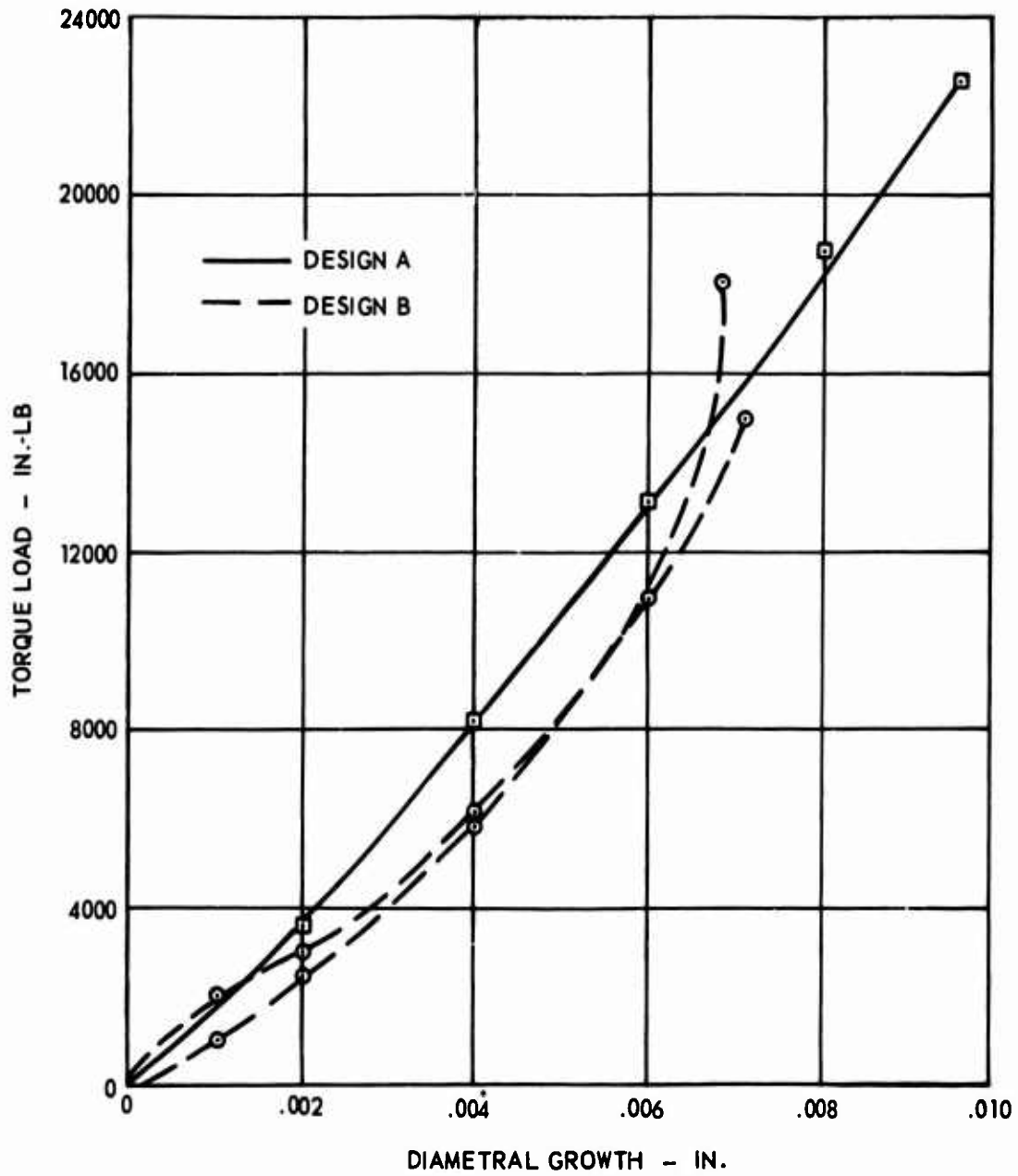


Figure 50. Diametral Growth of Outer Race.

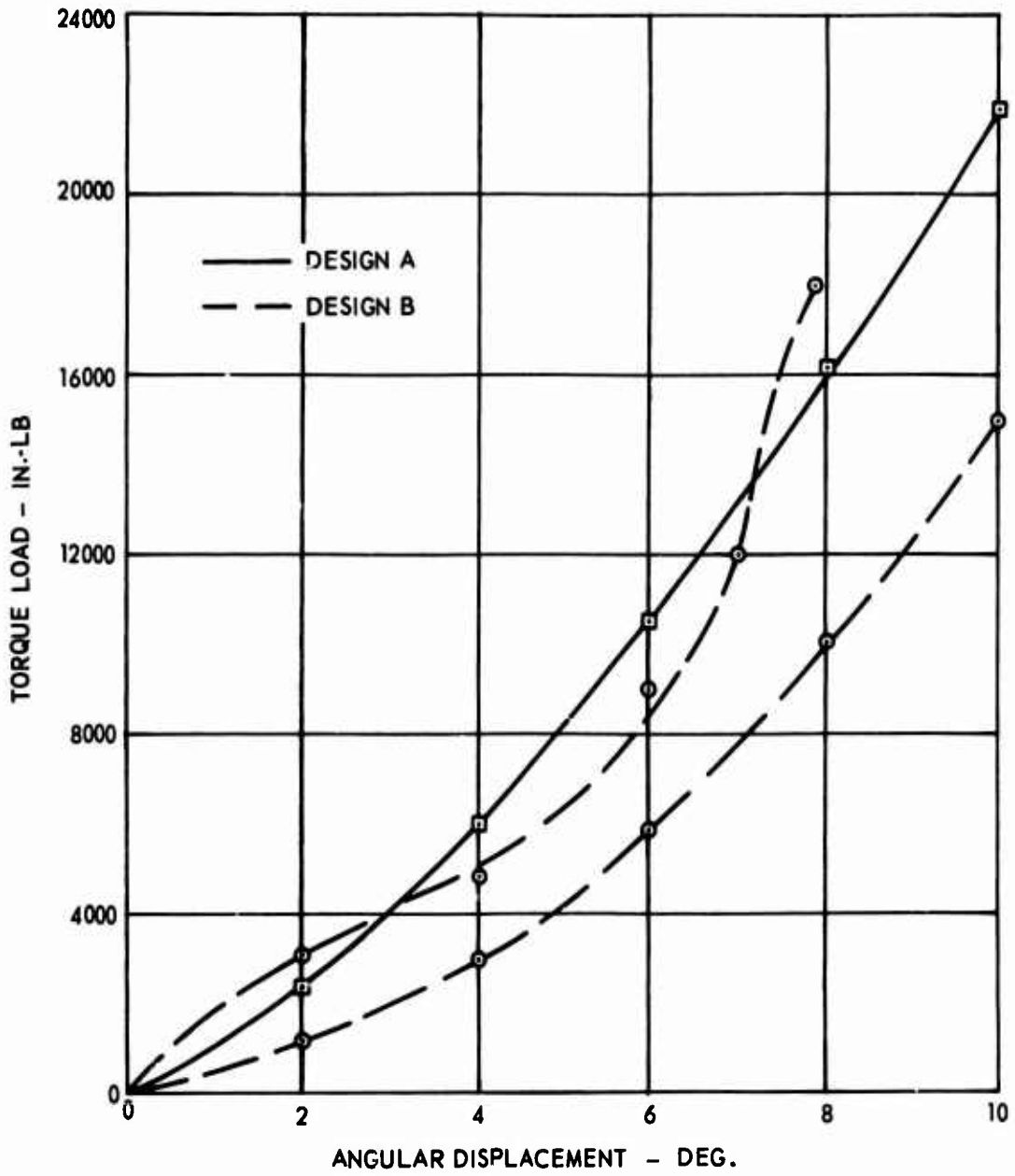
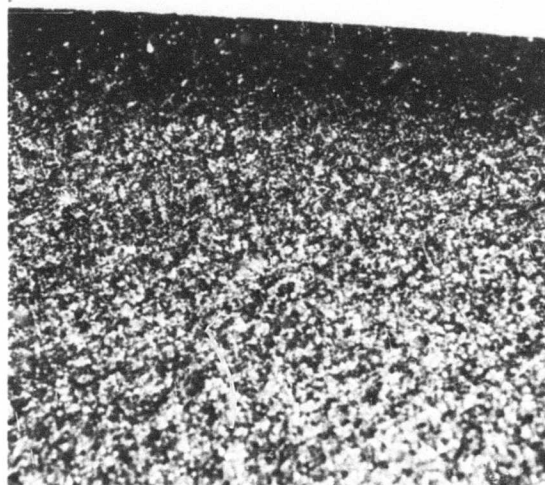


Figure 51. Angular Displacement of Outer Race.

Case →

Core →

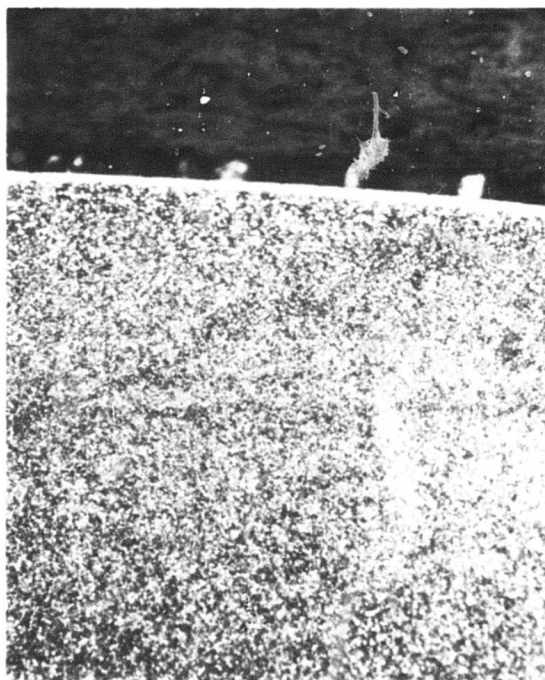


Design A

Compound Layer →

Diffusion Zone →

Core →



Design B

Figure 52. Sprag Microstructure.
Mag: 200X

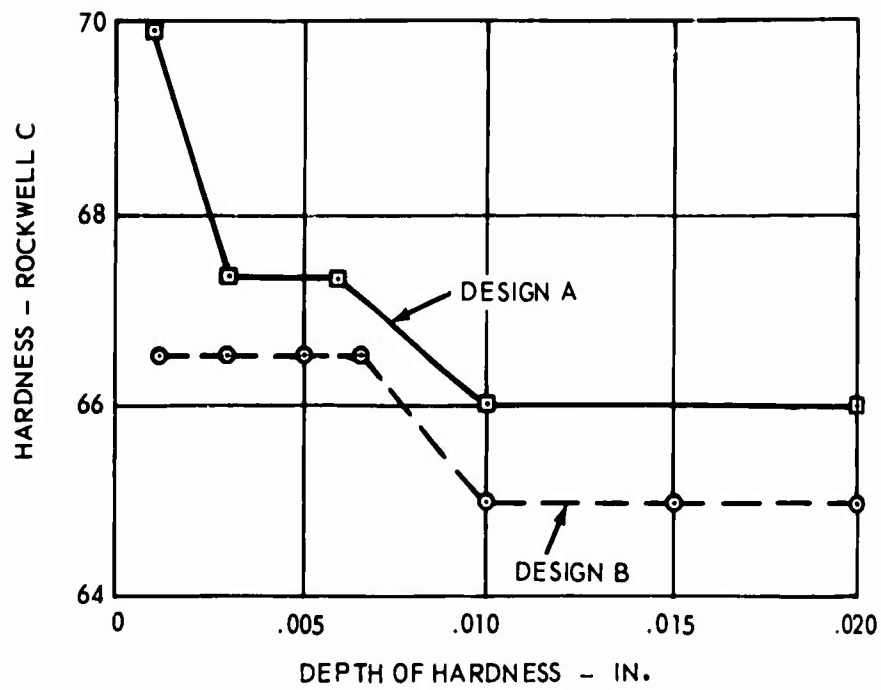


Figure 53. Sprag Case Hardness Versus Depth.

CONCLUSIONS

1. Full-speed dynamic clutch override testing showed that:
 - a. Design A clutch sprags wore at the inner cam surface.
 - b. Design B clutch operation was successful at all oil flows tested.
 - c. Oil flow requirements in the override mode are relatively low.
2. Differential speed dynamic clutch override testing showed that:
 - a. The design A clutch completed the test, but sprag wear occurred at the inner cam surface.
 - b. The design B clutch did not meet the test requirements because of excessive positive centrifugal engaging action by the sprags.
 - c. Differential speed operation is the most severe mode in terms of clutch component wear, heat generation, and drag torque. Future testing to develop high-speed overriding clutches and determine operating characteristics such as optimum oil flow, drag torque, etc., should concentrate on the differential speed mode of operation.
3. Dynamic engagement testing was successfully completed by the design A and B clutches.
4. Static cyclic torque fatigue testing showed that:
 - a. Two clutches each of designs A and B successfully completed the test at rated torque for 10^7 cycles. Clutch industry standards which generally work to an allowable Hertz stress of 450,000 psi for 10^6 cycles of torque application may be conservative for aircraft quality clutches.
 - b. A potential clutch bearing fretting problem exists.
5. Static overload testing showed that:
 - a. The design A clutch failed in the sprag rollover mode at 22,500 inch-pounds (six times design point) torque.

- b. The design B failures resulted in slippage at the inner race at torques of 18,000 and 15,500 inch-pounds.
 - c. The design B clutch sprag lockup feature, which prevents sprag rollover due to overtorque, was found to be very effective.
6. The mathematical mode of clutch operation and the computer program that was developed can provide a valuable tool for clutch analysis and design trade-off studies.

APPENDIX I ANALYSIS OF CLUTCH OPERATION

Presented in this appendix is the mathematical model upon which the computer program is based.

In order to analyze the various operating conditions, an iteration procedure involving the sprag position with respect to the outer race is performed. A sprag position is assumed which sets the outer and inner race contact points. For the overriding condition, the inner and outer race contact points are at radii corresponding to the engineering drawing dimensions. For the load condition, the outer race contact point radius will exceed the specified dimension. The outer race deflection due to speed and load is then calculated and compared with the assumed outer race radius. At some sprag position, the assumed and calculated outer race radii will be equal, and this is the position used to calculate stresses and deflections.

The following assumptions were used in the analysis:

1. The radial growth of the outer race was calculated using thick wall cylinder theory with the length of the cylinder assumed equal to the effective sprag length.
2. Deflection of the outer race inside diameter was calculated with consideration given to rotation and pressure loading of the outer race only. Hertzian deformation at the contact points was neglected.
3. Loading of the outer race due to centrifugal force on the sprags is negligible compared with the normal load due to the transmitted torque.
4. In overriding, the sprags are assumed to slip only at the inner race. A coefficient of friction of 0.05 is used.

This analysis represents an initial step toward establishing a mathematical model for high-speed clutch analysis. As more experience is gained and test data become available, the analysis will be refined and expanded.

MATHEMATICAL PROCEDURE

Evaluation of a clutch design is begun by determining the relationship between an angle of rotation θ and the distance between inner and outer races J , Figure 54, for positions of the sprag from overrun, Figure 54 (1), to overload, Figure 54 (4). Once this relationship has been established,

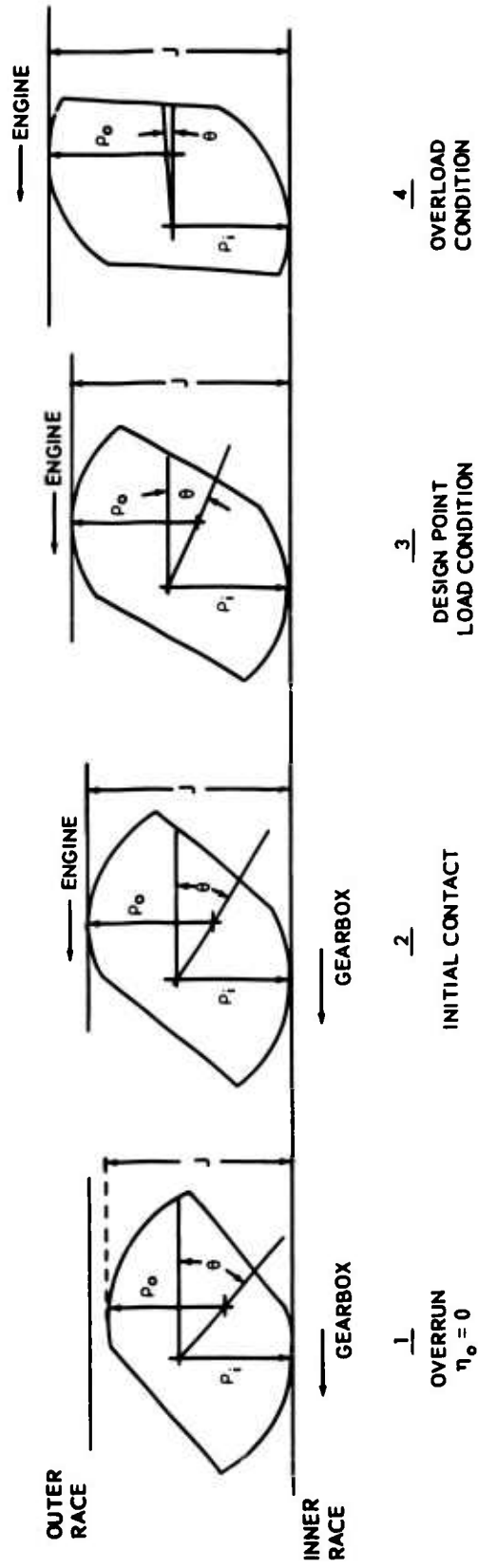


Figure 54. Sprag Cam Positions for Various Operating Conditions.

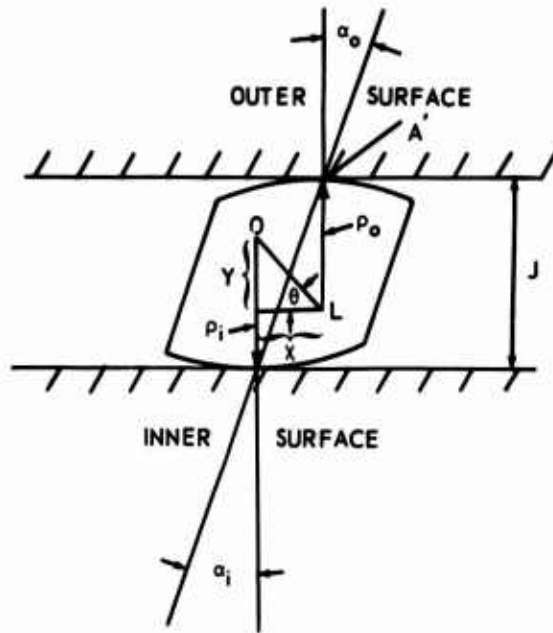
the various operating conditions such as override and load transmittal can be analyzed. Parallel flat plates have been used to represent the inner and outer races because clutch companies employ an inspection instrument for checking actual sprags in this manner; the curved raceways will be substituted later on.

Rotational angle θ is bounded by a line passing through the centers of the sprag radii of curvature and a line passing through the center of the inner race sprag radius ρ_i that is parallel to the flat plates. In Figure 54 (1), the distance between the flat plates is greater than the sprag height J , which indicates that contact between sprag and raceways has not yet taken place. In actual operation a spring force is acting to energize the clutch so that this condition cannot occur. The gap as shown between the sprag and the outer race is used in the computer program. When the rotational angle is such that the gap equals zero, initial contact has occurred. In Figure 54 (2), the sprag height just equals the distance between the flat plates. In the computer program this condition applies to override, differential speeds (inner race speed greater than outer race speed), and up to the point where the engine begins driving and transmitting torque (inner and outer race speeds are equal). Different engine driving conditions are represented in Figures 54 (3) and 54 (4). The sprag height continues to increase and tends to expand the outer race (J increases).

The relationship between rotation angle and sprag height is developed in Figure 55. Since the strut or gripping angles (α'_i, α'_o) are more commonly used terms in clutch analysis, their values have been used instead of the rotation angle in the final form of the equation:

$$(1 + \tan^2 \alpha) J^2 - 2 (\rho_o + \rho_i) J + \left(\rho_o + \rho_i \right)^2 - \overline{OL}^2 = 0$$

This equation in quadratic form relates sprag height to strut angle given the sprag inner and outer race radii of curvature and the distance between their centers. The inspection equipment used by sprag clutch manufacturers to check out sprag radii of curvature can now be more fully described. Reference to Figure 54 shows that the inner race flat plate is fixed while the outer race flat plate is made to contact the sprag surface and is kept parallel to the inner race. As the outer race plate is moved axially to the left, the sprag height J increases. The axial motion can be related to the strut angle α . The outer race plate is connected electronically to a pen recorder, and a continuous plot of J versus α is made.



- α_i = inner strut angle
- α_o = outer strut angle
- J = sprag height
- ρ_i = sprag cam inner radius of curvature
- ρ_o = sprag cam outer radius of curvature

NOTE: Outer and inner surfaces are parallel; therefore $\alpha_o = \alpha_i = \alpha$

GIVEN: $\rho_o, \rho_i, \overline{OL}$

Find: $J = f(\alpha)$

Development

$$\cos \theta = \frac{X}{\overline{OL}}, \quad \tan \alpha = \frac{X}{J}$$

$$\cos \theta = \frac{J \tan \alpha}{\overline{OL}}$$

$$\sin \theta = \frac{Y}{\overline{OL}} = \frac{\rho_o + \rho_i - J}{\overline{OL}}$$

since

$$\cos^2 \theta + \sin^2 \theta = 1$$

$$\frac{J^2 \tan^2 \alpha}{\overline{OL}^2} + \frac{(\rho_o + \rho_i - J)^2}{\overline{OL}^2} = 1$$

reduces to

$$(1 + \tan^2 \alpha) J^2 - 2(\rho_o + \rho_i) J + (\rho_o + \rho_i)^2 - \overline{OL}^2 = 0$$

Figure 55. Relationship Between Sprag Rotation Angle and Sprag Height for Parallel Flat Plates.

The flat plates have been replaced by actual curved raceways in Figure 56, and the contact point at the outer race has shifted from $\underline{A'}$ to \underline{A} . The inner and outer strut angles α_i' , α_o' respectively are no longer equal. The important parameters to be determined are D_o , α_i' , and α_o' . The inner race radius of curvature is R_i . $D_o/2$ represents the radius of curvature that the outer race would need in order for the sprag to have strut angles α_i' and α_o' . R_i , therefore, remains constant while $D_o/2$ varies as a function of α_i' .

These relationships will now be used to evaluate the various operating conditions.

DESIGN LOAD POINT STRESS AND DEFLECTION ANALYSIS

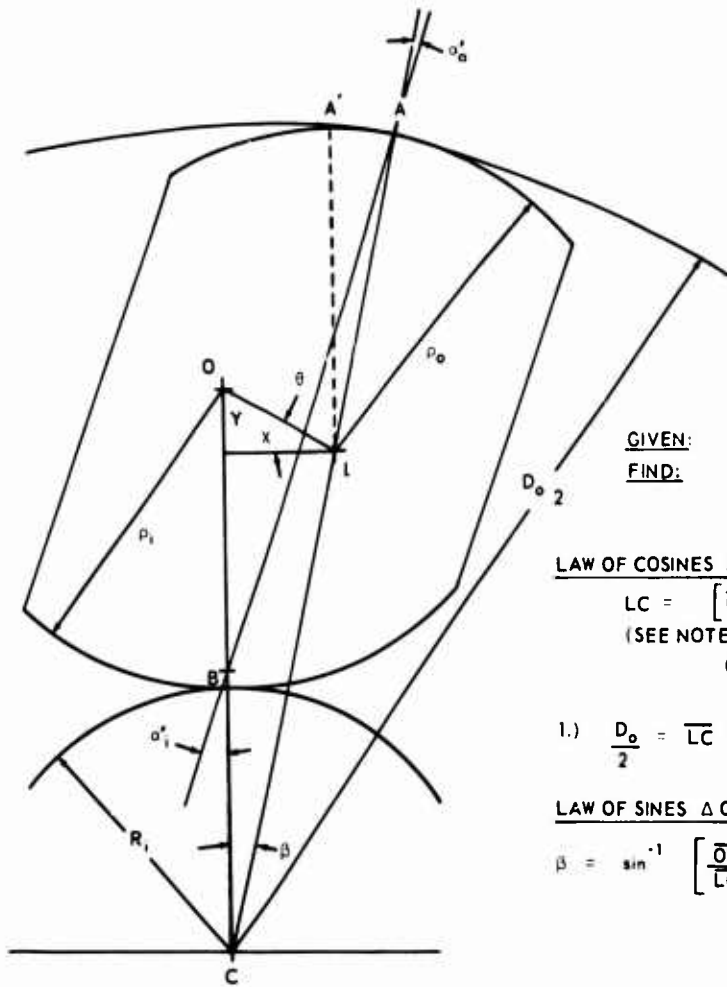
A load point condition with the engine transmitting torque through the outer race is represented in Figure 57. Sprag inertia and spring force have been neglected in this analysis because their magnitude is small compared with the force being transmitted.

Before the stresses in the various elements can be calculated, the deflections due to the transmitted loads and rotation of the elements must be correlated with the assumed strut angle of the sprag. This analysis is performed at the outer race contact point only, since the deflections are far greater than those at the inner race contact point. The method of superposition is used to determine the total growth at the outer race. The following iteration procedure is used:

1. From Figure 56, assume θ , R_i , \overline{OL} , ρ_i and ρ_o at the start of load transmission (initial contact) and calculate D_o , α_i' , and α_o' .
2. From Figure 57, calculate $RTOL$, RNO_L , and R_{NIL} using design point horsepower and speed.
3. Calculate the radial growth of the outer race inside and outside diameters due to rotation.

$$S_{rR} = \frac{3 + \nu}{8} \frac{\delta}{g} \left(\frac{\pi \eta}{30} \right)^2 \left[r_1^2 + r_2^2 - \frac{r_1^2 r_2^2}{r^2} - r^2 \right]$$

$$S_{tR} = \frac{3 + \nu}{8} \frac{\delta}{g} \left(\frac{\pi \eta}{30} \right)^2 \left[r_1^2 + r_2^2 + \frac{r_1^2 r_2^2}{r^2} - \frac{1 + 3\nu}{3 + \nu} r^2 \right]$$



GIVEN: $R_1, \overline{OL}, \rho_1, \rho_0$

FIND: $\frac{D_o}{2}, \alpha'_i, \alpha'_o$

LAW OF COSINES ΔOLC

$$LC = \left[\overline{OL}^2 + \overline{OC}^2 - 2 (\overline{OL}) (\overline{OC}) \cos (90-\theta) \right]^{1/2}$$

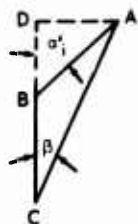
(SEE NOTE BELOW)

$$\overline{OC} = \rho_1 + R_1$$

$$1.) \frac{D_o}{2} = \overline{LC} + \rho_0$$

LAW OF SINES ΔOLC

$$\beta = \sin^{-1} \left[\frac{\overline{OL}}{\overline{LC}} \sin (90-\theta) \right]$$



$$\tan \alpha'_i = \frac{\overline{AD}}{\overline{DB}}$$

$$\overline{AD} = \overline{AC} \sin \beta = \frac{D_o}{2} \sin \beta$$

$$\overline{DB} = \overline{DC} - \overline{BC} = \frac{D_o}{2} \cos \beta - R_1$$

$$2.) \alpha'_i = \tan^{-1} \left[\frac{\frac{D_o}{2} \sin \beta}{\frac{D_o}{2} \cos \beta - R_1} \right]$$

$$3.) \alpha'_o = \alpha'_i - \beta$$

NOTE: USE θ FROM PARALLEL PLATE THEORY SO THAT $\alpha'_o, \alpha'_i, D_o$ (CURVED SURFACES) AND J, α (PARALLEL PLATES) CAN ALL BE RELATED TO THE SAME ANGLE θ .

Figure 56. Relationship Between Sprag Rotation Angle and Strut Angles for Curved Surface Raceways.

- where S_{rR} = radial stress due to rotation (psi)
 S_{tR} = tangential stress due to rotation (psi)
 η = design point speed (rpm)
 r_1 = outer race inside radius (in.) – engineering drawing
 r_2 = outer race outside radius (in.) – engineering drawing
 r = radius to any point (in.)
 δ = density (lb mass/in³)

The radial growth is

$$\Delta r_R = \frac{r}{E} (S_{tR} - \nu S_{rR})$$

NOTE: $S_{rR} = 0$ at outer race inside and outside diameter

where $\Delta r_R = \Delta r_{R1}$ for $r = r_1$

$\Delta r_R = \Delta r_{R2}$ for $r = r_2$

4. Calculate new outer race inside and outside radii due to rotation.

$$r_{11} = r_1 + \Delta r_{R1}$$

$$r_{22} = r_2 + \Delta r_{R2}$$

5. Calculate the radial growth of the outer race inside diameter due to the transmitted load while assuming the normal forces to be acting as a pressure distribution on the outer race. For the outer race inside diameter,

$$S_{r_p} = -P_o$$

$$S_{t_p} = P_o \frac{r_{22}^2 + r_{11}^2}{r_{22}^2 - r_{11}^2}$$

$$P_o = \frac{N R_{NO_L}}{\pi D_o L}$$

where S_{r_p} = radial stress due to transmitted load (psi)
 S_{t_p} = tangential stress due to transmitted load (psi)

Note: Sign is chosen so that (+) represents tension and (-) represents compression

P_o = internal pressure at outer race inside diameter due to loading (psi)
 R_{NO_L} = normal force from step 2
 D_o = outer race inside diameter from step 1

The superimposed radial growth due to pressure is

$$\Delta r_p = \frac{r_{11}}{E} (S_{t_p} - \nu S_{r_p})$$

6. Calculate the final outer race inside diameter from the superimposed radial growth due to pressure:

$$D_{o_f} = 2r_{11} + 2\Delta r_p$$

7. Compare this final diameter with D_o from Step 1. If they are equal, the correct sprag strut angles have been assumed; if not, the process is repeated by incrementing on θ .

- a. When the correct condition of loading has been found, the maximum hoop stress for the outer race inside diameter may be determined:

$$S_h = S_{t_R} + S_{t_p}$$

b. The maximum compressive stress and deflection are determined as follows:

1) For the outer race

$$s_{CO} = \frac{2 R_{NO_L}}{\pi b_{OL} L}$$

$$b_{OL} = \sqrt{\frac{8 R_{NO_L}}{\pi L} \frac{\rho_o D_o 2}{\frac{D_o}{2} - \rho_o} \left(\frac{1 - \nu^2}{E} \right)} \quad (*)$$

$$\Delta r_o = \frac{2(1 - \nu^2)}{E} \frac{R_{NO_L}}{L \pi} \left[i'_n \left(\frac{2 \rho_o L}{b_{OL}^2} \right) + 1.6002 \right] \quad (*)$$

where s_{CO} = compressive stress of outer race contact point

b_{OL} = half width of outer race contact area

Δr_o = deflection of outer race contact point

2) For the inner race

$$s_{CI} = \frac{2 R_{NI_L}}{\pi b_{IL} L}$$

$$b_{IL} = \sqrt{\frac{8 R_{NI_L}}{\pi L} \frac{\rho_i R_i}{\rho_i + R_i} \left(\frac{1 - \nu^2}{E} \right)} \quad (*)$$

$$\Delta r_i = \frac{2(1 - \nu^2)}{E} \frac{R_{NI_L}}{L \pi} \left[i'_n \left(\frac{2 \rho_i L}{b_{IL}^2} \right) + 1.6002 \right] \quad (*)$$

(*) H. Rothbart, MECHANICAL DESIGN AND SYSTEMS HANDBOOK, New York, McGraw-Hill, 1964.

where S_{C_1} = compressive stress of inner race contact point
 b_{1L} = half width of inner race contact area
 Δr_1 = deflection of inner race contact point

VERRIDE AND DIFFERENTIAL SPEED ANALYSIS

Refer again to Figure 54, where item 2 represents initial contact. For the clutches analyzed in this program, the spring force acts to keep the sprag cams always in contact with the inner and outer races; and since no torque is being transmitted as in Figures 54 (3) and 54 (4), Figure 54 (2) represents the override and differential speed modes of operation. The forces acting on a sprag during these modes of operation are shown in Figure 58. D_o , α'_i , and α'_o can be calculated for various positions of the sprag angle θ as explained above. When the value of D_o equals that of the outer race inside diameter given by the engineering drawing, the correct position of the sprag for override and differential speed analysis has been found. The forces acting on the sprag are as follows:

F_{CG} = centrifugal force of the sprag (lb)

$F_{SP'}$ = spring deflection force (lb)

$F_{SP''}$ = centrifugal force of the spring (lb)

Since the clutch is not transmitting any torque during these modes of operation, the reaction forces on the sprag at the inner and outer races are due solely to the spring and centrifugal forces just described (Figure 58). The reaction forces are:

R_{T_i} = tangential force at inner race (lb)

R_{N_i} = normal force at inner race (lb)

R_{T_o} = tangential force at outer race (lb)

R_{N_o} = normal force at outer race (lb)

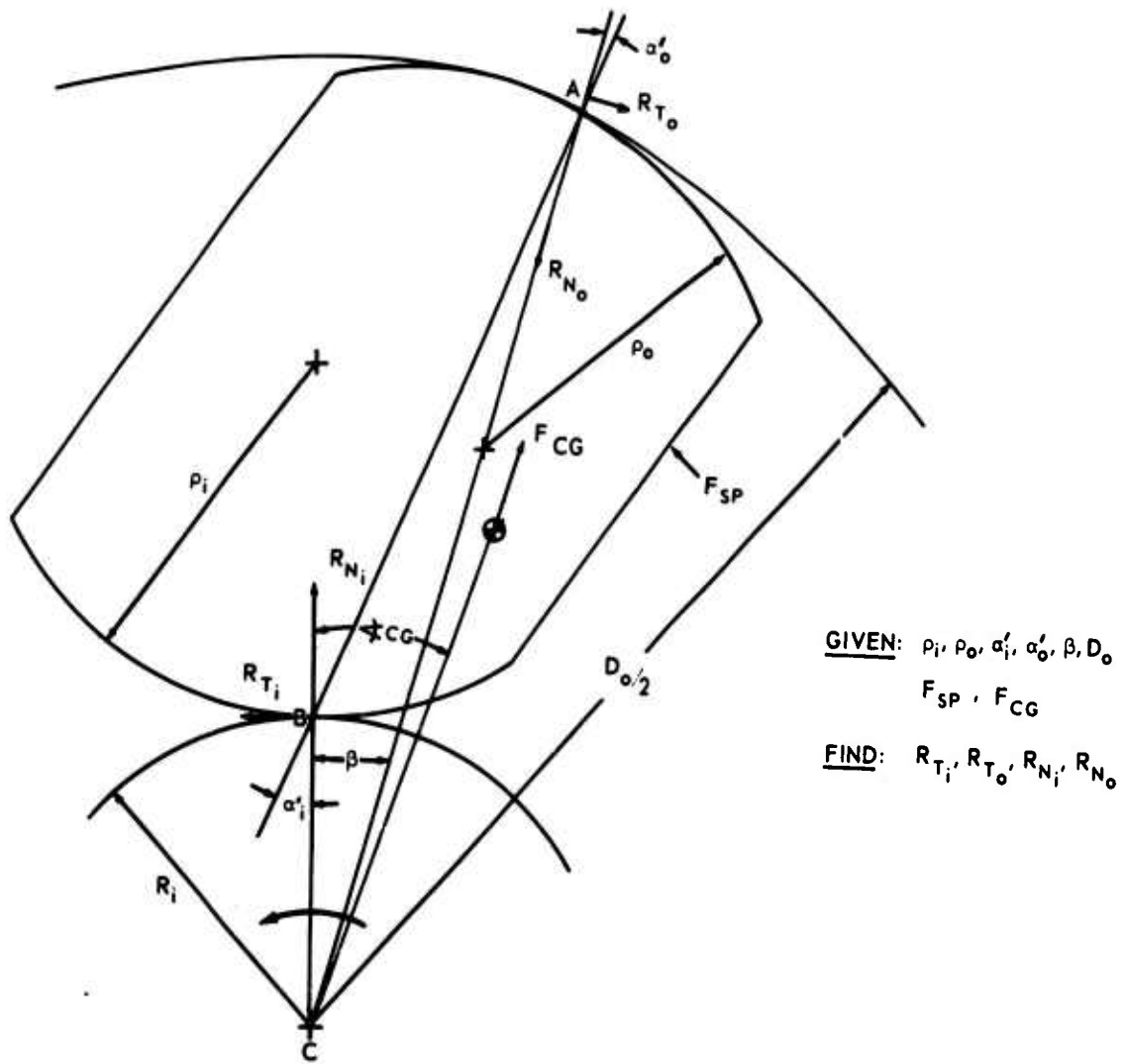


Figure 58. Sprag Forces for the Override or Differential Speed Modes of Operation.

The spring and centrifugal forces are determined as follows:

Clutch design B employs two garter springs (one at each end of the sprag). The total spring force F_{SP} acts radially outward at the corner of the slot, Figure 59 (1).

$$F_{SP} = F_{SP'} + F_{SP''}$$

$$F_{SP'} = \frac{2 \pi K_S (D_f - D)}{N} N_S$$

where N = number of sprags
 N_S = number of springs
 K_S = spring constant (lb/in.) - measured
 D_f = free spring diameter (in.) - measured
 D = as-assembled spring diameter at point of contact (in.)

Note: $D_f > D$ so that spring always acts at outer slot surface rather than at inner slot surface.

$$F_{SP''} = m_S \frac{D}{2} \omega^2 \frac{N_S}{N}, \quad m_S = \frac{W_S}{g} K_{Wt}, \quad \omega = \frac{2 \pi \eta_o}{60}$$

$$F_{SP''} = \frac{W_S K_{Wt} D}{2g} \left(\frac{2 \pi \eta_o}{60} \right)^2 \frac{N_S}{N}$$

W_S = weight of one spring (gm) - measured
 K_{Wt} = 2.205×10^{-3} (lb/gm)
 η_o = speed of the outer race (rpm)

Clutch design A employs a ribbon-type spring with a center tang. When the sprag is inserted in the slot, the tang is deflected, and the spring is assumed to apply a normal force to both the front and back faces of the sprag (friction forces are neglected). The radial force required to deflect the spring to its assembled position is F_{SRF} .

$$F_{SRF} = K_S Y$$

where Y = difference between free and deflected position of tang (in.)

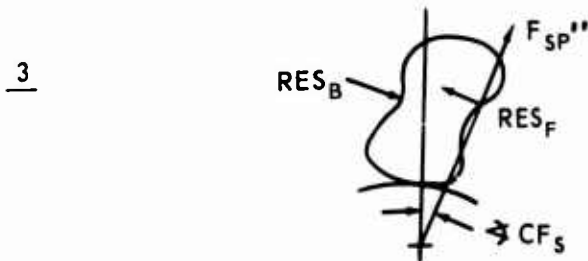
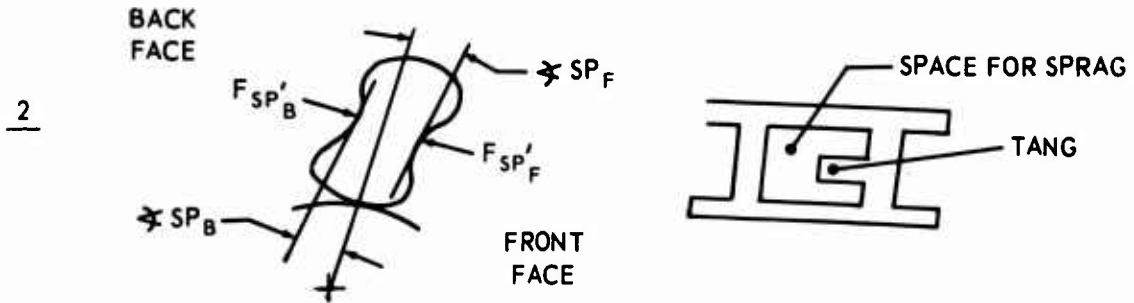
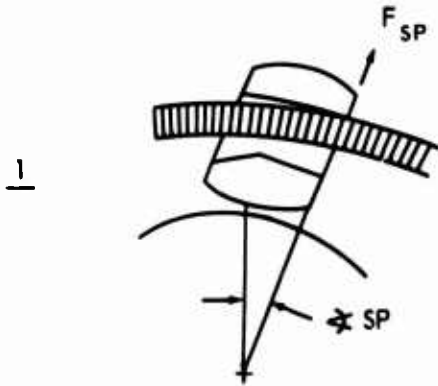


Figure 59. Spring Forces Acting on Sprag for Override or Differential Speed Modes of Operation.

The resulting spring force acting normal to the front face of the sprag is $F_{SP'_F}$, Figure 59 (2)

$$F_{SP'_F} = \frac{F_{SRF}}{\cos (90 - \angle SP_F + \angle CF_S)}$$

where $\angle SP_F =$ angle between a line that is tangent to the spring contact point at the sprag front face and a line passing through the inner race contact point and the center of the clutch (deg) – measured

$\angle CF_S =$ angle between a radial line to the spring contact point at the sprag front face and a line passing through the inner race contact point and the center of the clutch (deg)

The spring load acting on the back face of the sprag is found from a free body diagram of the spring. The tangential components of the spring acting at the front and back faces of the sprag must be equal in order for the spring to be in torsional equilibrium. Therefore, the tangential component of the spring at the front face equals F_{STF} :

$$F_{STF} = F_{SRF} \tan (90 - \angle SP_F + \angle CF_S)$$

For torsional equilibrium,

$$F_{STB} = F_{STF}$$

The spring force acting normal to the back face of the sprag is $F_{SP'_B}$, Figure 59 (2):

$$F_{SP'_B} = \frac{F_{STB}}{\cos (\angle SP_B + \angle CB_S)}$$

where $\angle SP_B =$ angle between a line that is tangent to the spring contact point at the sprag back face and a line passing through the inner race contact point and the center of the clutch (deg) – measured

$\angle CB_S =$ angle between a radial line to the spring contact point at the sprag back face and a line passing through the inner race contact point and the center of the clutch (deg)

For purposes of this analysis, the centrifugal force of the spring has been applied to the front face of the sprag, and the contact points at the front and back faces are the same for differential and overriding modes of operation. Therefore, the effect of the spring's centrifugal force is to increase the load on the sprag without changing its position. The centrifugal force of the spring is $F_{SP''}$, Figure 59 (3):

$$F_{SP''} = m_S \frac{D}{2} \frac{\omega^2}{N}, \quad m_S = \frac{W_S K_{Wt}}{g}, \quad \omega = \frac{2\pi \eta_o}{60}$$

$$F_{SP''} = \frac{W_S K_{Wt} D}{2g} \left(\frac{2\pi \eta_o}{60} \right)^2 \frac{1}{N}$$

where $D =$ as-assembled spring diameter at point of contact (in.)

The total spring forces acting on the front and back faces of the sprag are RES_F and RES_B , respectively. These resultant forces are found by combining the effects of the spring force and centrifugal force as follows:

$$RES_F = F_{SP'_F} + \frac{F_{SP''}}{\sin(\angle SP_F - \angle CF_S)}$$

The tangential component of the spring acting at the sprag front face is RES_{TF} :

$$RES_{TF} = RES_F \sin(90 - \angle SP_F + \angle CF_S)$$

For torsional equilibrium of the spring, $RES_{TB} = RES_{TF}$.

The resulting total spring force acting normal to the back face of the sprag is RES_B :

$$RES_B = \frac{RES_{TB}}{\cos(\angle SP_B + \angle CB_S)}$$

The sprag centrifugal force for either clutch is determined as follows:

$$F_{CG} = m_G r_{CG} \omega^2, \quad m_G = \frac{K_{Wt}}{g} W_G, \quad \omega = \frac{2 \pi n_o}{60}$$

$$F_{CG} = \frac{K_{Wt} W_G}{g} r_{CG} \left(\frac{2 \pi n_o}{60} \right)^2$$

$$W_G = \text{weight of one sprag (gm)}$$

$$r_{CG} = \text{radius to the center of gravity of the sprag (in.)}$$

In all of the preceding equations, the sprags, and therefore the springs, are assumed to stay with the outer race (no slipping occurs between the outer race cam and the inside diameter point of contact). It is evident therefore, that for the overriding condition of operation, the sprags remain stationary with slippage occurring at the inner race, and the centrifugal components of both the sprag and spring equal zero.

Now that the spring and centrifugal force equations have been determined, the normal and tangential forces at the sprag cam points of contact may be calculated.

Assume: 

For clutch design A,

$$\Sigma F_X = 0 = RES_B \cos \angle SP_B - RES_F \cos \angle SP_F + R_{T_o} \cos \beta - R_{N_o} \sin \beta - R_{T_i} + F_{CG} \sin \angle CG$$

$$\Sigma F_Y = 0 = -RES_B \sin \angle SP_B + RES_F \sin \angle SP_F - R_{T_o} \sin \beta - R_{N_o} \cos \beta + R_{N_i} + F_{CG} \cos \angle CG$$

$$\Sigma M_C = 0, \quad RES_B (M_B) - RES_F (M_F) - R_{T_i} (R_i) + R_{T_o} (r_1)$$

where M_B = moment arm to back face spring contact point (in.)
 M_F = moment arm to front face spring contact point (in.)
 R_i = inner race outside radius (in.) - engineering drawing
 r_1 = outer race inside radius (in.) - engineering drawing

For clutch design B,

$$\sum F_X = 0 = F_{SP} \sin \angle SP + F_{CG} \sin \angle CG + R_{T_o} \cos \beta - R_{N_o} \sin \beta - R_{T_i}$$

$$\sum F_Y = 0 = F_{SP} \cos \angle SP + F_{CG} \cos \angle CG - R_{T_o} \sin \beta - R_{N_o} \cos \beta + R_{N_i}$$

$$\sum M_C = 0, R_{T_i} (R_i) = R_{T_o} (r_1)$$

where

$\angle SP$ = angle between a line connecting the inner race contact point and center of the clutch and a line connecting the spring contact point and center of the clutch.

For both clutches, a fourth equation is needed for a solution. This equation is obtained by assuming a coefficient of friction for sliding at the inner race point of contact:

$$R_{T_i} = \mu_k R_{N_i}$$

where μ_k = sliding coefficient of friction.

The above four equations can now be solved simultaneously for R_{N_i} , R_{T_i} , R_{N_o} and R_{T_o} .

Now that all of the forces acting on a sprag have been determined, the following parameters may be evaluated:

1. Inner race drag torque - This parameter is calculated with the following equation:

$$\tau_d = N R_{T_i} R_i \text{ (in.-lb)}$$

2. Pressure-velocity factor (psi-fps) - This factor is useful as a wear correlating parameter in high-speed mechanical components. A value of 2×10^6 is considered to be within good design practice.
 Pressure = P_i .

$$P_i = \frac{R_{N_i}}{b_i L} \quad (\text{psi})$$

where R_{N_i} = normal force at the inner race (lb)

$$b_i = \sqrt{\frac{8 R_{N_i}}{\pi L} \frac{R_i \rho_i}{R_i + \rho_i} \left(\frac{1-\nu^2}{E} \right)}$$

Velocity = V.

$$V = \frac{\pi R_i}{360} (\eta_i - \eta_o) \quad (\text{fps})$$

where η_i = inner race speed (rpm)

η_o = outer race or sprag cam speed (rpm)

3. Load per inch-velocity factor (lb/in. - fpm) - This factor is used by some clutch companies as a wear-correlating parameter. A value of 14,000 is considered to be within good design practice. (*)

$$\text{Load per inch} = \frac{R_{N_i}}{L} \quad (\text{lb in.})$$

$$\text{Velocity} = V = \frac{\pi R_i}{30} (\eta_i - \eta_o) \quad (\text{fpm})$$

(*) Formsprag Company, SPRAG-TYPE OVER-RUNNING CLUTCHES, Power Transmission and Bearing Handbook, 1969-1970 Edition, Cleveland, Industrial Publishing Company, pp. A/196-A/202.

4. Hydrodynamic and elastohydrodynamic oil film thickness - The following equations are used to calculate the elastohydrodynamic and hydrodynamic oil film thickness: (*)

$$h_{\text{EHD}} = \frac{1.6 (G)^{.6} (U)^{.7} R}{W^{.13}}$$

$$h_{\text{HYD}} = \frac{4.9 U R}{W}$$

where h_{EHD} = elastohydrodynamic film thickness (in.)

h_{HYD} = hydrodynamic film thickness (in.)

R = equivalent radius = $R_i \rho_i / (R_i + \rho_i)$

G = materials parameter = $\alpha_L E'$

where α_L = pressure viscosity coefficient (in.²/lb)

E' = materials parameter = $E / (1-\nu^2)$ (lb/in.²)

W = load parameter = $R_{N_i} / E' R_L$

U = velocity parameter =
$$\frac{1}{2} \frac{(V_R + V_G) \mu_o}{E' R}$$

where μ_o = absolute viscosity (reyns)

V_R = tangential velocity of the inner race at the contact point = $R_i \eta_i \pi / 30$ (fps)

V_G = tangential velocity of the sprag at the inner race contact point = $\rho_i \eta_o \pi / 30$ (fps)

(*) D. Dowson, and G. Higginson, ELASTOHYDRODYNAMIC LUBRICATION - THE FUNDAMENTALS OF ROLLER AND GEAR LUBRICATION, London, Pergamon Press, 1966.

APPENDIX II

COMPUTER PROGRAM

This computer program was written specifically for one-way, sprag-type overriding clutches. The program calculates pertinent sprag geometry data in double precision for each incremented rotation angle from minimum to maximum sprag cam travel. Override and design point data are stored, so that after incrementing is completed, these data can be used to calculate the design point stresses and radial deflections as well as the override and differential speed point wear and film thickness parameters.

The clutch is assumed to drive through the outer race and override through the inner race, the sprag cams remaining stationary with the outer race. In addition, the clutches contain single ribbon or double garter type springs, and the inertia and spring forces act to energize the clutch during the overriding mode of operation.

The program evaluates drag torque, load per inch-velocity, and pressure-velocity (wear correlating parameters), as well as hydrodynamic and elastohydrodynamic oil film thicknesses for the override and differential speed modes of operation. Pressure loads are superimposed onto rotational loads to determine compressive stresses, hoop stresses, and their deflections for the driving mode of operation.

Other specific features of the computer program are as follows:

1. Cyclic testing stresses and deflections can be determined by inputting the load point torque and zero speed.
2. The slip or rollover point for the overload test can be determined because the inner strut or gripping angle is calculated and printed out for the load point condition.

If $\alpha_i > 4$ degrees, slip or rollover should occur.

3. Sprag height J' , parallel plate strut angle α , and curved surface inner strut angle α_i' have been subscripted for future addition of a plotting subroutine.

4. The program can accommodate a maximum of six radii of curvature, three for the inner race and three for the outer race, for each input case.
5. There is no limitation on the number of cases that may be run.

The subject program is written in FORTRAN IV language and was developed on an IBM 370 system, model 155 computer. Computer running time is 19 seconds for compile and link edit and 2 seconds per executable case.

INPUT DATA

Note: All angles must be in degrees and decimal fractions.

Card One - Format (1X, 79H)

Identification

Card Two - Format (6F12.5)

Word 1: Horsepower

Word 2: Torque (in. -lb)

Word 3: Speed (rpm)

Word 4: Coefficient of sliding friction at inner race for override mode of operation

Word 5: Number of springs

Note: Words 1 and 2 - One value must be given and the other value must be 0.0.

Word 3 - design point speed

Word 5 - use 1.0 for one ribbon type spring, use 2.0 for two garter type spring

Card Three - Format (6F12.5)

- Word 1: Inner race inside diameter (in.)
Word 2: Inner race outside diameter (in.)
Word 3: Number of increments on rotation angle
Word 4: Minimum rotation angle
Word 5: Maximum rotation angle

Note: Word 3: Maximum number of increments = 190

Words 3, 4, 5: The rotation angle referred to is Σ

See Figure 60 for definition and relationship to θ .

Card Four - Format (6F12.5)

- Word 1: Outer race inside diameter (in.)
Word 2: Outer race outside diameter (in.)

Card Five - Format (3(F6.5, F6.2, 2F6.5)) (See Figure 61)

- Word 1: Inner race radius of curvature for override position (in.)
Word 2: Rotation angle for Word 1. This value must be at the junction point with the next value of inner race radius of curvature.
Word 3: 'X' coordinate for Word 1 (in.)
Word 4: 'Y' coordinate for Word 1 (in.)

Note: A total of three values of inner race radius of curvature may be read in as input so that words 5 through 8 correspond to the second value and words 9 through 12 correspond to the third value.

Words 3, 4, 7, 8, 11, and 12 note proper sign convention used in Figure 61.

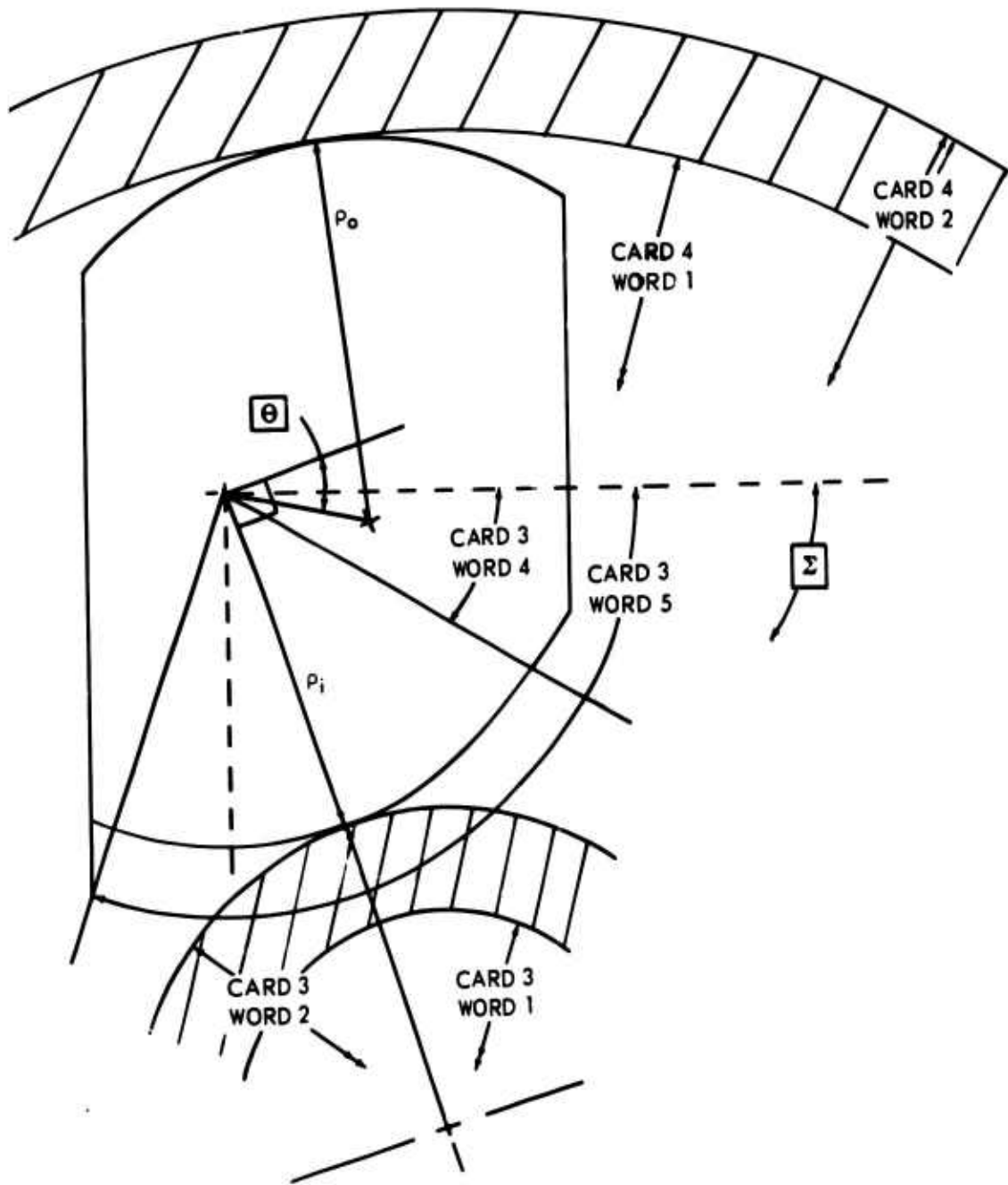
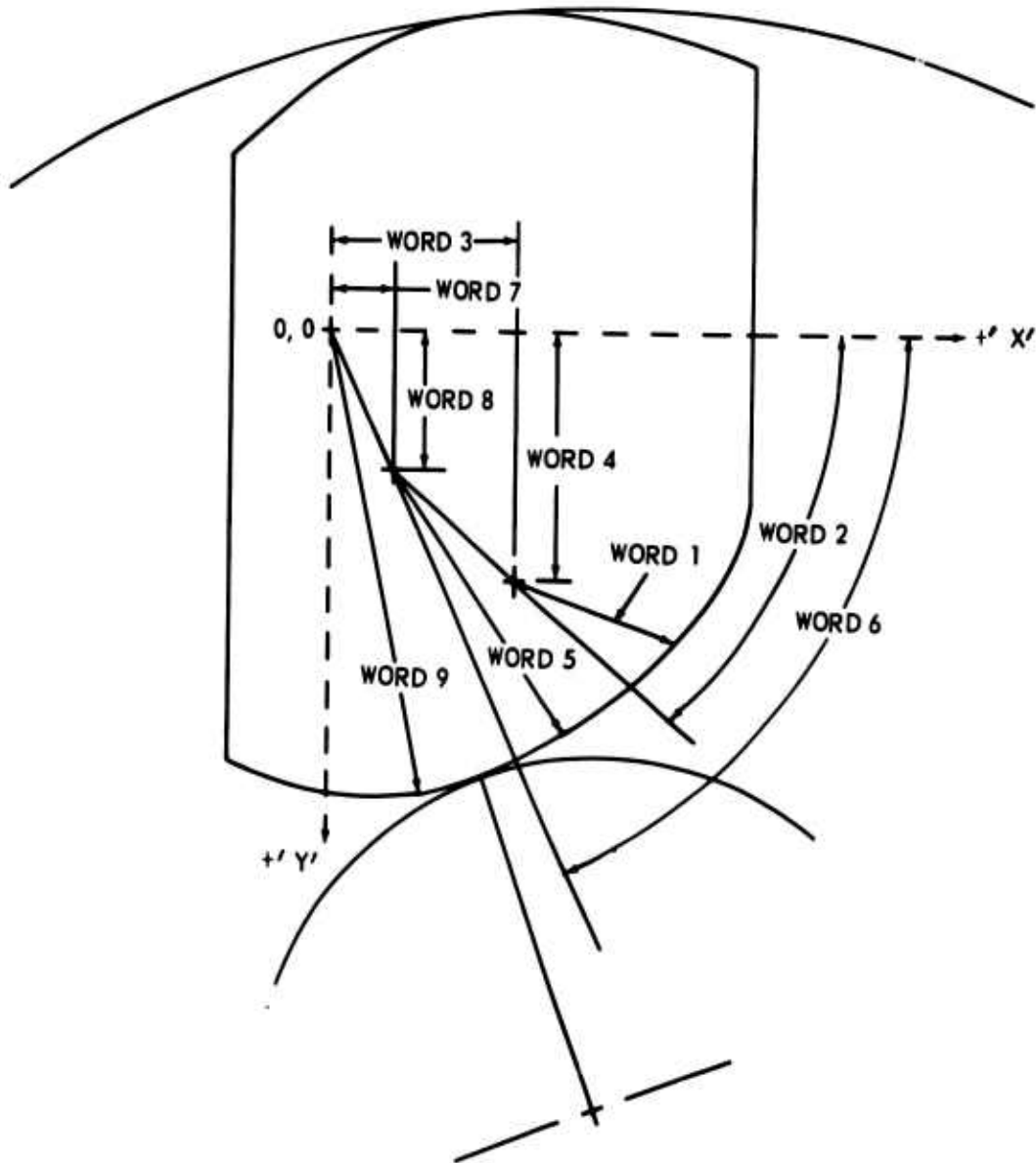


Figure 60. Computer Program Input Cards 3 and 4.



NOTE: WORD 10 = WORD 5, CARD 3 (Σ MAX)
 WORD 11 = 0.0
 WORD 12 = 0.0

Figure 61. Computer Program Input Card 5.

Card Six - Format (3(F6.5, F6.2, 2F6.5)) (See Figure 62)

- Word 1: Outer race radius of curvature for override position (in.)
- Word 2: Rotation angle for Word 1. This value must be at the junction point with the next value of outer race radius of curvature.
- Word 3: 'X' coordinate for Word 1 (in.)
- Word 4: 'Y' coordinate for Word 1 (in.)

Note: A total of three values of inner race radius of curvature may be read in as input so that words 5 through 8 correspond to the second value and words 9 through 12 correspond to the third value.

Words 3, 4, 7, 8, 11, and 12 note proper sign convention used in Figure 61.

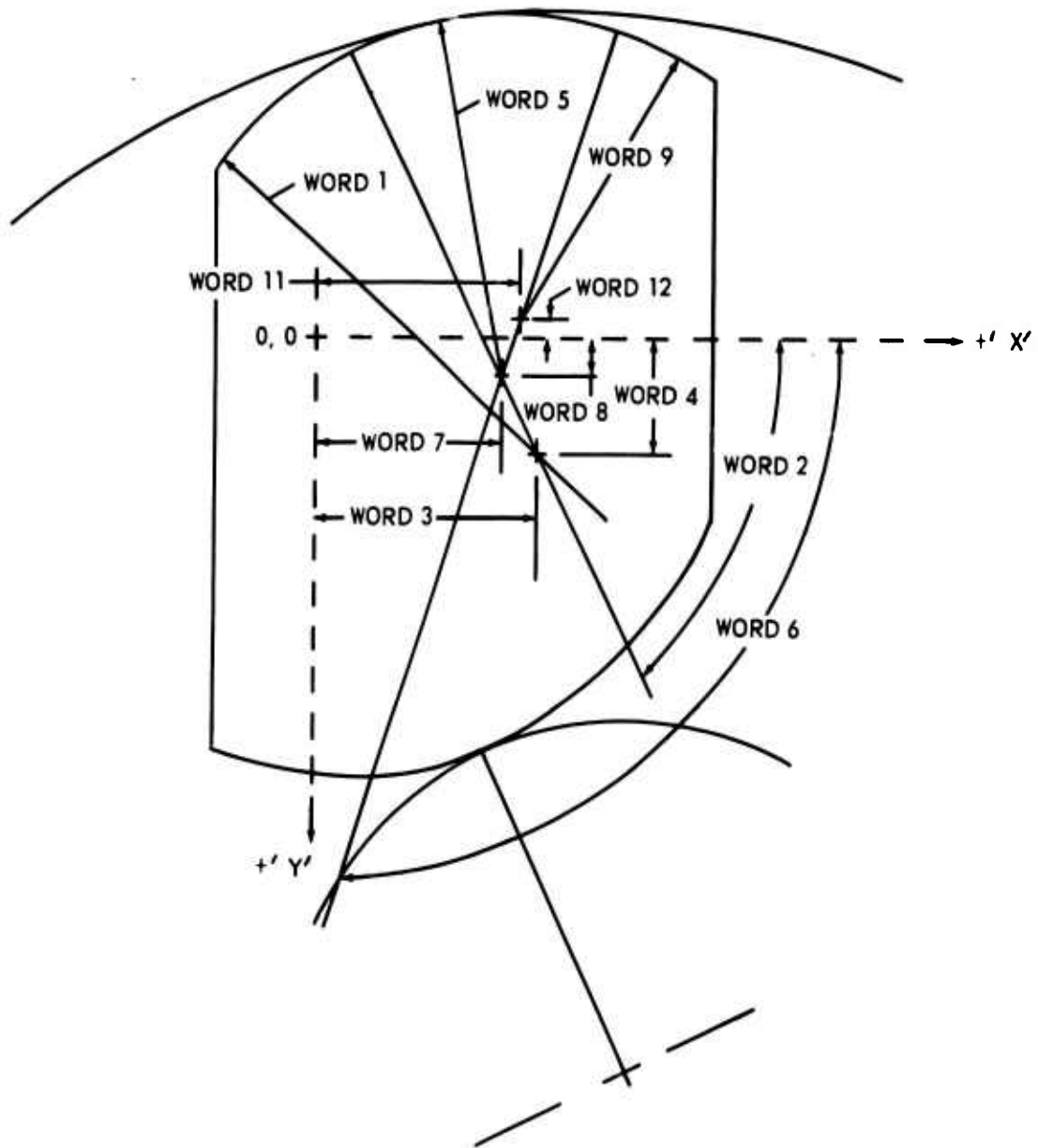
Card Seven - Format (6F12.5) (See Figure 63)

- Word 1: 'X' coordinate of center of gravity (in.)
- Word 2: 'Y' coordinate of center of gravity (in.)
- Word 3: Weight of one sprag (gm)
- Word 4: Number of sprags
- Word 5: Effective sprag length (in.)
- Word 6: Code word for type of output desired

Note: Words -- as used in this program neglects chamfering of the edges.

Word 6: Use 1.0 for minimum output - includes input data, overriding data, and maximum stresses and deflections for load point.

Use 2.0 for all of 1.0 plus stress and deflection distribution in inner and outer races.



NOTE: WORD 10 = WORD 5, CARD 3 (Σ MAX)

Figure 62. Computer Program Input Card 6.

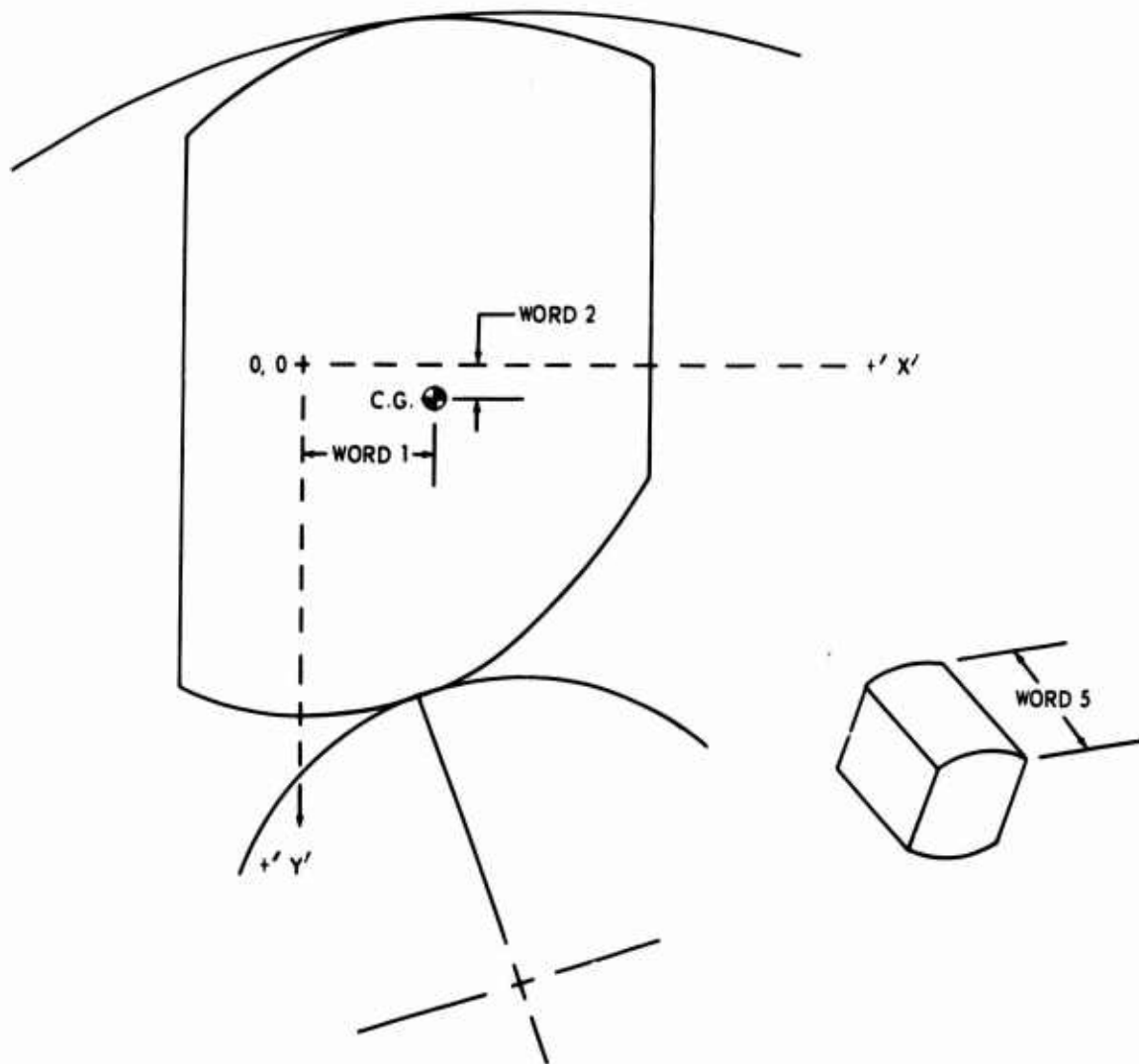


Figure 63. Computer Program Input Card 7.

Use 3.0 for maximum output - includes all of 2.0 and computer table of sprag height versus strut angle and other sprag cam geometry.

Card Eight A - Format (3(F6.5, F6.2, 2F6.5) (See Figure 64)

(For use with garter type spring; Card Two - Word 5 = 2.0)

Word 1: 'X' coordinate of spring contact point on sprag (in.)

Word 2: 'Y' coordinate of spring contact point on sprag (in.)

Word 3: Spring weight (gm)

Word 4: Free spring diameter (in.)

Word 5: Spring constant (lb/in.)

Note: Word 4: Spring is designed to be compressed radially before insertion into cam slots.

Card Eight B - Format (3(F6.5, F6.2, 2F6.5)) (See Figure 65)

(For use with ribbon type spring; Card Two - Word 5 = 1.0)

Word 1: 'X' coordinate of spring contact point with front face of sprag (in.)

Word 2: 'Y' coordinate of spring contact point with front face of sprag (in.)

Word 3: 'X' coordinate of spring contact point with back face of sprag (in.)

Word 4: 'Y' coordinate of spring contact point with back face of sprag (in.)

Word 5: Spring weight (gm)

Word 6: Spring deflected height (in.)

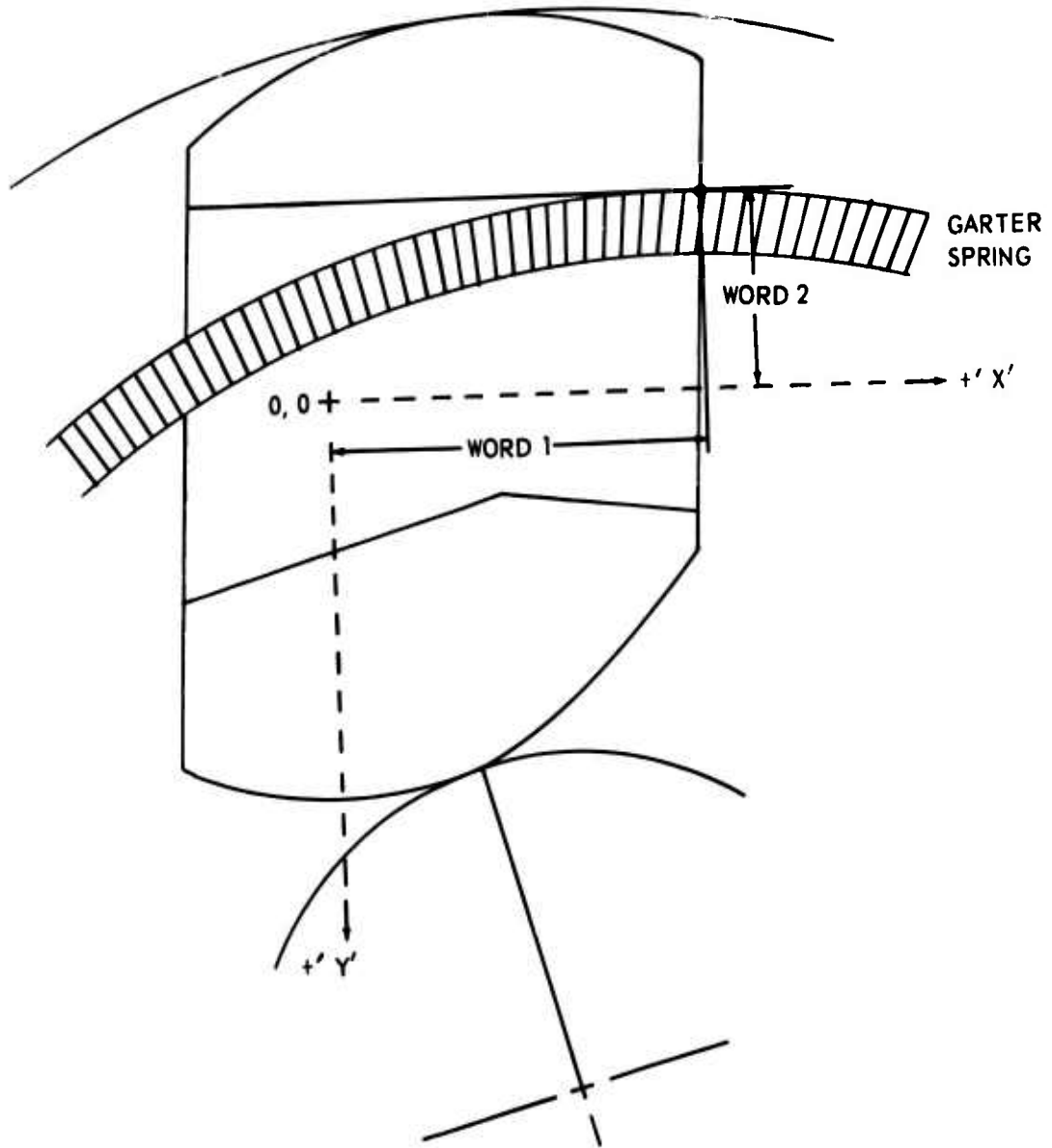


Figure 64. Computer Program Input Card 8A.

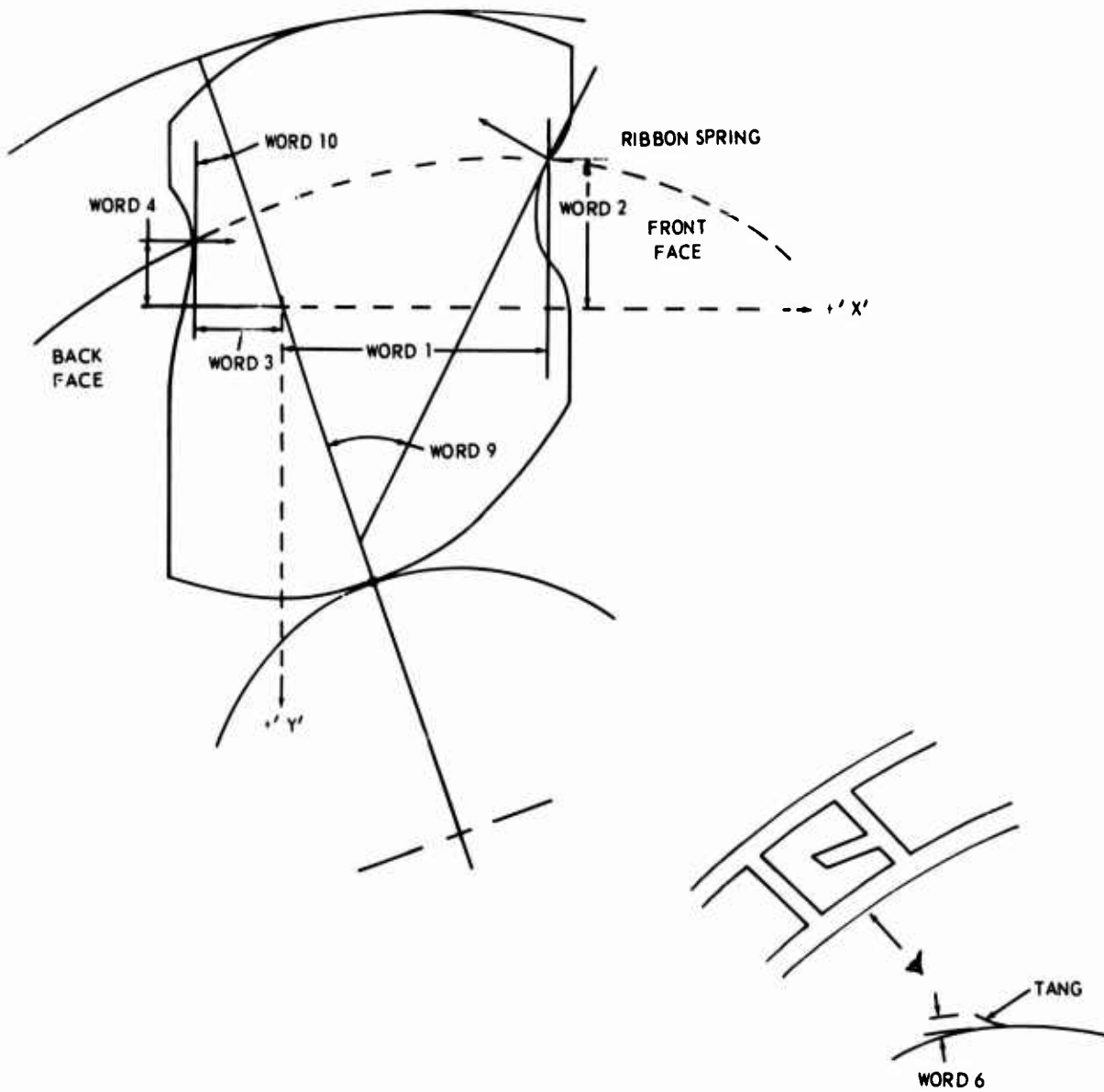


Figure 65. Computer Program Input Card 8B.

- Word 7: Spring constant (lb/in.)
- Word 8: Angle between front face contact point of spring and inner race contact points
- Word 9: Angle between back face contact point of spring and inner race contact points

Note: Only one card, either 8A or 8B, is to be used in each case.

OUTPUT DATA

The short form (input Card 7, Word 6 = 1.0) of computer program output for both clutch designs A and B is shown in Figures 66 and 67. The first 11 or 13 lines following the heading represent input data.

The next section of output relates to sprag cam geometry and is only obtained with extensive printout (input Card 7, Word 6 = 3.0). Two sample rows of values beginning with 'SIGMA ANGLE' are listed. For 105 increments there would be 105 rows of data, and each row would represent a 1/2-degree increment on 'SIGMA ANGLE'. The significance of each term is explained as follows:

SIGMA ANGLE - Angle of rotation of sprag cam as explained in the input section of the computer program discussion.

J PRIME - Flat plate dimension, sprag height as measured between flat plates.

INNER STRUT OR GRIPPING ANGLE - Flat plate dimension, angle between strut and inner race contact point correspond to J PRIME.

Note: The two preceding values are used by sprag clutch manufacturing companies as a means of sprag cam inspection (see Figures 68 and 69).

STRUT ANGLE INNER AND STRUT ANGLE OUTER - Curved surface dimension, angle between strut and inner and outer radii contact points respectively for an actual clutch. These values relate to the ones previously discussed except that now the flat plates have been replaced by the curved surfaces of an actual clutch. All computer program stress calculations are based on the curved surface strut angles.

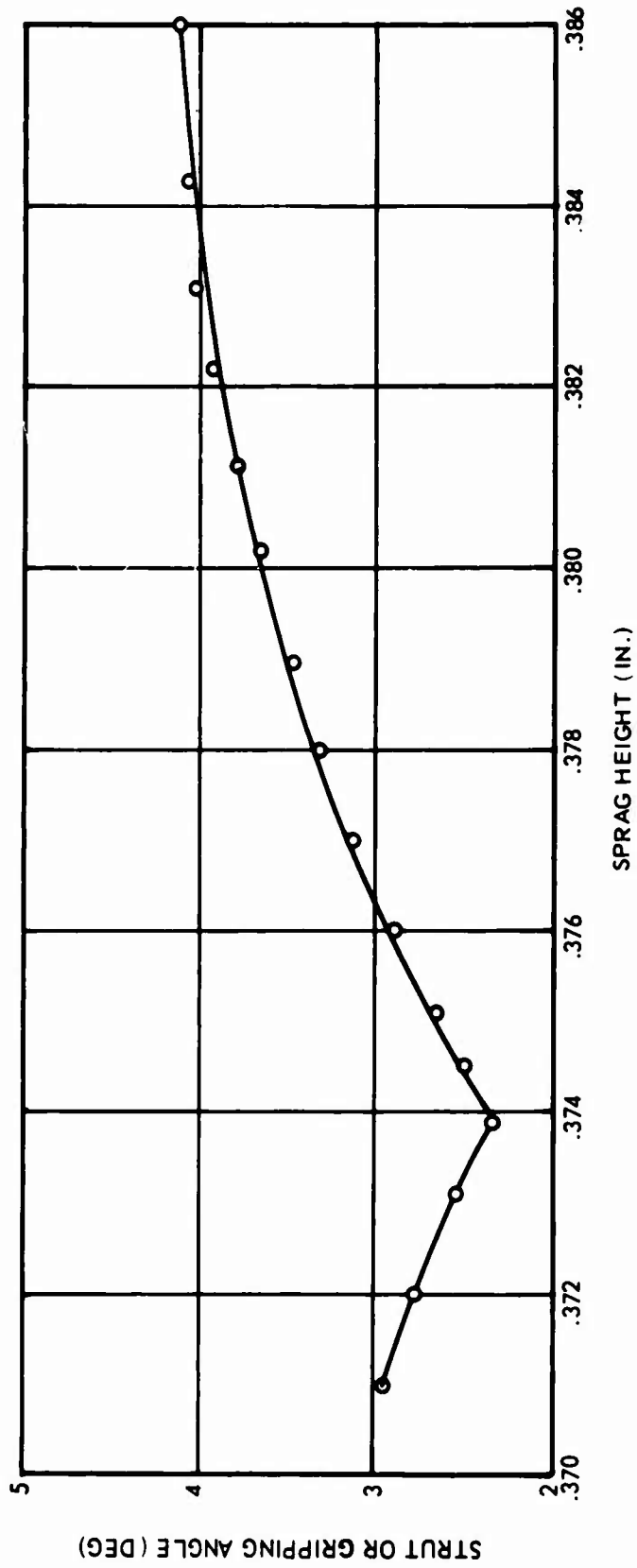


Figure 68. Strut Angle Versus Sprag Height for Clutch Design A.

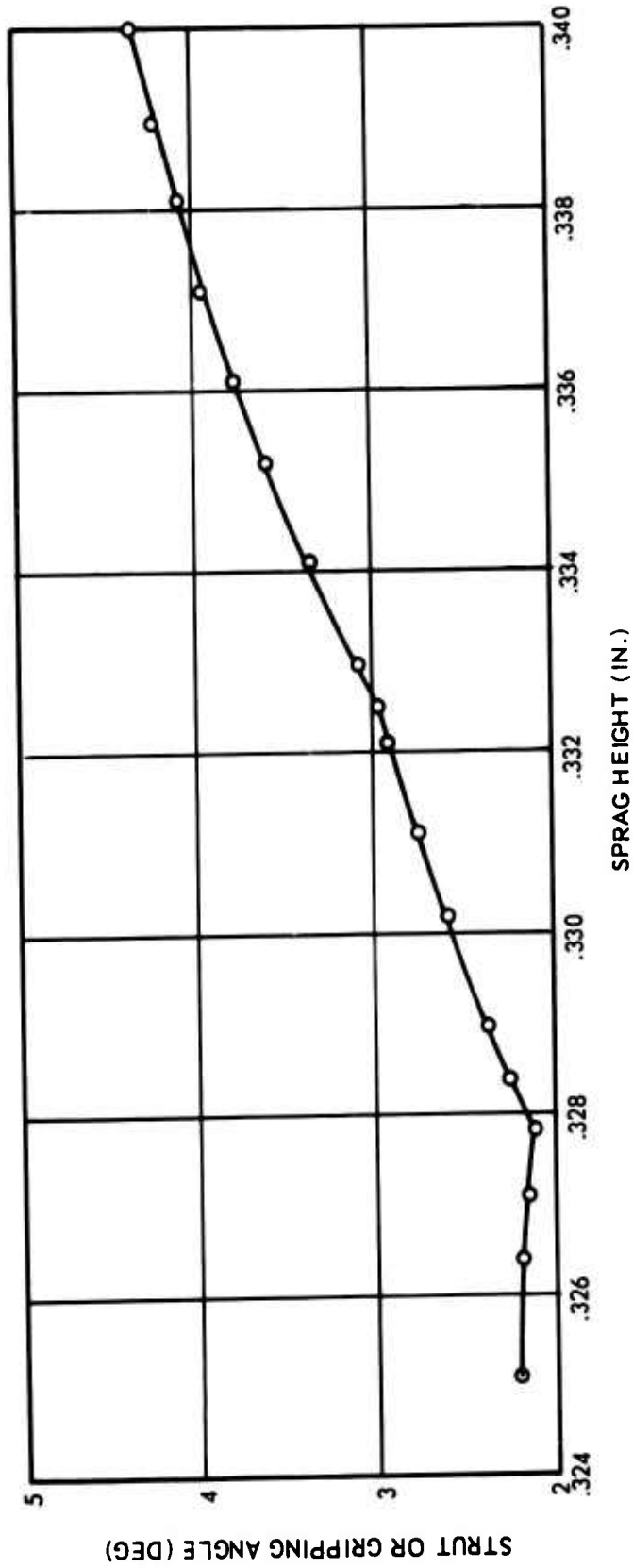


Figure 69. Strut Angle Versus Sprag Height for Clutch Design B.

OUTER RACE I. D. - Value that the outer race inside diameter would need in order to correspond with the curved surface inner and outer strut angles.

C. G. ANGLE - Angle between the center of gravity force component and the inner race contact point. See Figure 58.

DIFF. ANGLE - ($\angle CG - \angle \beta$) See Figure 58. As long as this angle remains positive, the sprag centrifugal force will act to energize the clutch.

The next section of output data is entitled 'OVERRUN + DIFFERENTIAL SPEED POINT VALUES'.

The first two rows of data define the actual contact points of the sprag on the inner and outer races as explained in Appendix I and as shown in Figure 54(2). At this point, the calculated value of 'DEFLECTED OUTER RACE I. D.' is equal to the nominal input value (Card 4, Word 1). It is assumed that all override and differential speed modes take place at these points of contact.

The override mode occurs at zero rpm outer race speed and 26,500 rpm inner race speed (design point). As the outer race increases in speed (differential mode), the sprags will rotate also (sprags assumed to remain with outer race). The effect of sprag and spring centrifugal force will now be felt as increased 'DRAG TORQUE' at the inner race contact point. The same four points of differential speed mode of operation are calculated for every case. These points are listed under the 'PERCENT SPEED' column as 25, 50, 75, and 100. The race speeds are listed under the columns entitled 'INNER' and 'OUTER RACE SPEED'. A fifth point, representing the maximum 'P-V' value, is also listed. The 'P-V' factor in (lb/in. - ft/min.) is a wear correlating parameter used by some sprag clutch manufacturers. 'P' is the normal load per inch of effective sprag length and 'V' is the relative tangential (sliding) velocity; both values are determined at the inner race contact point. If the spring effect is neglected, the maximum 'P-V' value occurs mathematically at $\eta_0 = (2/3) \eta_i$. This value is shown in data headed 'WITHOUT SPRING'.

When the spring effects are accounted for, the maximum value occurs at a slightly different percent speed (65.15 percent for design B, and 64.38 percent for design A).

The 'PRS-V' factor in (lb/in.² - ft/sec) is also a wear correlating parameter used by industry in the design of other mechanical components. 'PRS' is the normal load per square inch of contact area as defined by Hertzian equations. 'V' is again the sliding velocity. Both values are determined at the inner race contact point. Values in the other columns listed in this section are calculated at each percent speed point according to the formulas presented in Appendix I.

The next section of output is entitled 'LOAD POINT VALUES.' As the outer race comes up to the design point speed and then starts to transmit torque, the outer race expands. When the radial growth of the outer race inside diameter due to loading and centrifugal force effects matches the value calculated from sprag geometry, the correct position of sprag contact on the raceways has been found. The first two lines of data, i. e., 'SIGMA ANGLE' and 'INNER STRUT ANGLE,' represent this geometry.

The next line of output represents the tangential stress at the outer race inside diameter and the corresponding radial deflection. Both values are a maximum at this point, and they are arrived at by superimposing the pressure loads onto the rotational loads. The next two lines of output represent the compressive stress and deflection at the inner and outer race contact points, respectively. A FORTRAN listing of the computer program follows.

FORTRAN LISTING OF COMPUTER PROGRAM

```
C SPRAG CLUTCH DESIGN - BY AL MEYER
  IMPLICIT REAL*8 (A-H,O-Z)
  KRD=5
  KPR=6
  DIMENSION XJPR(200),ALFP(200),ALFI(200),RHJI(3),SIGMI(3),XI(3),YI
  I(3),RHJU(3),SIGMU(3),XD(3),YD(3),SIGMA(200)
  PI=3.14159263
  Z=PI/180.0
  GRAVITY=386.4
  GRAMLB=.002205
  ELSMOD=29.0*10.0**6.0
  PUISSN=0.25
  WIDENS=.282
  COPRVI=.000095
  REYNS=.00000073
1  READ(KRD,1000)
  READ(KRD,1002)HORPOW,TORQ,SPEED,FRCOSL,SPRNGS
  READ(KRD,1002)XIRID,XIROD,SINC,SIGMIN,SIGMAX
  READ(KRD,1002)XORID,XOROC
  READ(KRD,1003)RHOI(1),SIGMI(1),XI(1),YI(1),RHOI(2),SIGMI(2),XI(2),
  YI(2),RHOI(3),SIGMI(3),XI(3),YI(3)
  READ(KRD,1003)RHOU(1),SIGMO(1),XU(1),YU(1),RHOU(2),SIGMO(2),XU(2),
  YU(2),RHOU(3),SIGMO(3),XU(3),YU(3)
  READ(KRD,1002)XCG,YCG,WTSPAG,SPRAGS,WIDTH,CODE1
  IF(SPRNGS.EQ.1.0) GO TO 490
  READ(KRD,1003)XSP,YSP,WTSPNG,DSPRNG,SPRNGK
  GO TO 491
490 READ(KRD,1003) XSF,YSF,XSB,YSB,WTSPNG,SPNGHT,SPRNGK,ANGSPF,ANGSPB
491 WRITE(KPR,1100)
  WRITE(KPR,1000)
  WRITE(KPR,1001)
  IF(HORPOW)2,3,2
2  TJK=63025.0*HORPOW/SPEED
  GO TO 4
3  HORPOW=TORQ*SPEED/63025.0
4  WRITE(KPR,1004)HORPOW,TORQ
  WRITE(KPR,1005)SPEED,FRCOSL
  IF(SPRNGS.EQ.1.0) GO TO 495
  WRITE(KPR,1006)XSP,XCG
  WRITE(KPR,1007)YSP,YCG
  WRITE(KPR,1008)WTSPNG,WTSPAG
  WRITE(KPR,1009)SPRNGS,SPRAGS
  WRITE(KPR,1012)DSPRNG,WIDTH
  WRITE(KPR,1013)SPRNGK
  GO TO 496
495 WRITE(KPR,1023)XSF,XSB
  WRITE(KPR,1024)YSF,YSB
  WRITE(KPR,1025)ANGSPF,XCG
  WRITE(KPR,1026)ANGSPB,YCG
  WRITE(KPR,1008)WTSPNG,WTSPAG
  WRITE(KPR,1009)SPRNGS,SPRAGS
  WRITE(KPR,1027)SPNGHT,WIDTH
  WRITE(KPR,1013)SPRNGK
496 WRITE(KPR,1010)XIROD,XORID
  WRITE(KPR,1022)XIRID,XOROC
```

```

WRITE(KPR,1011)S INC, SIGMIN, SIGMAX
IF(CCDE1.LT.3.0) GO TO 500
WRITE(KPR,1014)
WRITE(KPR,1015)
I=1
J=1
M=1
WRITE(KPR,1016)XI(I),YI(J),RHOI(I),SIGMI(M)
SIGMI(M)=SIGMI(M)*Z
I=2
J=2
M=2
WRITE(KPR,1017)XI(I),YI(J),RHOI(I),SIGMI(M)
SIGMI(M)=SIGMI(M)*Z
I=3
J=3
M=3
WRITE(KPR,1018)XI(I),YI(J),RHOI(I),SIGMI(M)
SIGMI(M)=SIGMI(M)*Z
II=1
JJ=1
MM=1
WRITE(KPR,1019)XO(II),YO(JJ),RHO(II),SIGMO(MM)
SIGMO(MM)=SIGMO(MM)*Z
II=2
JJ=2
MM=2
WRITE(KPR,1020)XO(II),YO(JJ),RHO(II),SIGMO(MM)
SIGMO(MM)=SIGMO(MM)*Z
II=3
JJ=3
MM=3
WRITE(KPR,1021)XO(II),YO(JJ),RHO(II),SIGMO(MM)
SIGMO(MM)=SIGMO(MM)*Z
WRITE(KPR,1033)
WRITE(KPR,1034)
WRITE(KPR,1035)
WRITE(KPR,1036)
WRITE(KPR,1039)
GO TO 503
500 DD 501 M=1,3
SIGMI(M)=SIGMI(M)*Z
501 CONTINUE
DD 502 MM=1,3
SIGMO(MM)=SIGMO(MM)*Z
502 CONTINUE
503 N=1
SIGMA(N)=SIGMIN*Z
SIGINC=(SIGMAX-SIGMIN)*Z/(S INC)
I=1
II=1
J=1
JJ=1
K=1
KK=1
M=1
MM=1
L=1
LL=1
ISINC=S INC

```

FORTRAN LISTING OF COMPUTER PROGRAM

```

C   SPRAG CLUTCH DESIGN - BY AL MEYER
      IMPLICIT REAL*8 (A-H,O-Z)
      KRD=5
      KPR=6
      DIMENSION XJPRI(200),ALFP(200),ALFI(200),RHDI(3),SIGMI(3),XI(3),YI
      L(3),RHJU(3),SIGMU(3),XD(3),YD(3),SIGMA(200)
      PI=3.14159263
      Z=PI/180.0
      GRAVITY=386.4
      GRAML8=.002205
      ELSMOD=29.0*10.0**6.0
      PUISSV=0.25
      WTDENS=.282
      COPRVI=.000095
      MEYNS=.00000073
      1 READ(KRD,1000)
      READ(KRD,1002) HOKPOW,TORQ,SPEED,FRCSL,SPRNGS
      READ(KRD,1002) XIRID,XIRDD,SINC,SIGMIN,SIGMAX
      READ(KRD,1002) XORID,XORCD
      READ(KRD,1003)RHOI(1),SIGMI(1),XI(1),YI(1),RHOI(2),SIGMI(2),XI(2),
      LYI(2),RHOI(3),SIGMI(3),XI(3),YI(3)
      READ(KRD,1003)RHOD(1),SIGMO(1),XD(1),YD(1),RHOD(2),SIGMO(2),XD(2),
      LYD(2),RHOD(3),SIGMO(3),XD(3),YD(3)
      READ(KRD,1002)XCG,YCG,WTSPAG,SPRAGS,WIDTH,CODE1
      IF(SPRNGS.EQ.1.0) GO TO 490
      READ(KRD,1003)XSP,YSP,WTSPNG,DSPRNG,SPRNGK
      GO TO 491
      490 READ(KRD,1003) XSF,YSF,XSB,YSB,WTSPNG,SPNGHT,SPRNGK,ANGSPF,ANGSPB
      491 WRITE(KPR,1100)
      WRITE(KPR,1000)
      WRITE(KPR,1001)
      IF(HOKPOW)2,3,2
      2 TJR)=63025.0*HOKPOW/SPEED
      GO TO 4
      3 HOKPOW=TORQ*SPEED/63025.0
      4 WRITE(KPR,1004)HOKPOW,TORQ
      WRITE(KPR,1005)SPEED,FRCSL
      IF(SPRNGS.EQ.1.0) GO TO 495
      WRITE(KPR,1006)XSP,XCG
      WRITE(KPR,1007)YSP,YCG
      WRITE(KPR,1008)WTSPNG,WTSPAG
      WRITE(KPR,1009)SPRNGS,SPRAGS
      WRITE(KPR,1012)DSPRNG,WIDTH
      WRITE(KPR,1013)SPRNGK
      GO TO 496
      495 WRITE(KPR,1023)XSF,XSB
      WRITE(KPR,1024)YSF,YSB
      WRITE(KPR,1025)ANGSPF,XCG
      WRITE(KPR,1026)ANGSPB,YCG
      WRITE(KPR,1008)WTSPNG,WTSPAG
      WRITE(KPR,1009)SPRNGS,SPRAGS
      WRITE(KPR,1027)SPNGHT,WIDTH
      WRITE(KPR,1013)SPRNGK
      496 WRITE(KPR,1010)XIRDD,XORID
      WRITE(KPR,1022)XIRID,XORCD

```

```

ISINC=ISINC+1
C RADIAL GROWTH OF OUTER RACE DUE TO ROTATION
B2=((3.0+POISSN)/8.0)*(WTDENS/GRAVY)*(PI*SPEED/30.0)*(PI*SPEED/30
1.0)
B3=(1.0+3.0*POISSN)/(3.0+POISSN)
STROT2=B2*((0.5*XOROD*XOROD)+(XOROD*.25*XOROD)*(1.0-B3))
URROT2=0.5*XOROD*STROT2/ELSMOD
XUROR=XOROD+2.0*URROT2
STROT3=B2*((0.5*XOROD*XOROD)+(XOROD*.25*XOROD)*(1.0-B3))
URROT3=0.5*XOROD*STROT3/ELSMOD
XURORR=XOROD+2.0*URROT3
C END OF RADIAL GROWTH CALCULATION
5 DO 50 N=1,ISINC
6 CENDIS=DSQRT((XO(I)-XI(I))**2+(YI(J)-YC(JJ))**2)
IF(YI(J).GT.YO(JJ)) GO TO 7
XLAMB=DARSIN((YO(JJ)-YI(J))/CENDIS)
THETA=(90.0*Z)-SIGMA(N)+XLAMB
ANG=(9.0*Z)-THETA
GO TO 8
7 XLAMB=DATAN((YI(J)-YO(JJ))/(XO(I)-XI(I)))
THETA=SIGMA(N)-(90.0*Z)+XLAMB
ANG=(9.0*Z)+THETA
8 XX=CENDIS*DCOS(THETA)
YY=CENDIS*DSIN(THETA)
XJPRI(N)=YY+RHOD(I)+RHO(I)
IF(YO(JJ).GT.YI(J))XJPRI(N)=RHOD(I)+RHO(I)-YY
ALFP(N)=DATAN(XX/XJPRI(N))
XKPRIC=RHOD(I)+(.5*XIROD)
XKC=DSQRT(CENDIS*CENDIS+XKPRIC*XKPRIC-2.0*CENDIS*XKPRIC*DCOS(ANG))
RU=XKC+RHOD(I)
UUU=2.0*RU
BETA=DARSIN(CENDIS*DSIN(ANG)/XKC)
ALFI(N)=DATAN(RU*(CSIN(BETA))/(RU*(CCOS(BETA))-(.5*XIROD)))
ALFO=ALFI(N)-BETA
C CENTER OF GRAVITY CALCULATION
CJCG=DSQRT((XCG-XI(I))**2+(YI(J)-YCG)**2)
XOMEGA=DATAN(DABS((YI(J)-YCG)/(XCG-XI(I))))
SUMANG=SIGMA(N)-XOMEGA
IF(YI(J).GT.YCG) SUMANG=SIGMA(N)+XOMEGA
CGC=DSQRT(XKPRIC*XKPRIC+CDCG*CDCG-2.0*XKPRIC*CDCG*DCOS(SUMANG))
ANGCG=DARSIN(CDCG*DSIN(SUMANG)/CGC)
DELANG=ANGCG-BETA
C END OF CENTER OF GRAVITY CALCULATION
SIGMA(N)=SIGMA(N)/Z
THETA=THETA/Z
BETA=BETA/Z
ALFP(N)=ALFP(N)/Z
ALFI(N)=ALFI(N)/Z
ALFO=ALFO/Z
ANGCG=ANGCG/Z
DELANG=DELANG/Z
IF(K.GT.1.0R.KK.GI.1) GO TO 9
IF(CONE1.LT.3.0) GO TO 5C5
WRITE(KPR,1037) SIGMA(N),XJPRI(N),ALFP(N),ALFI(N),ALFO,UUU,ANGCG,DE
LANG
505 CONTINUE
SIGMA(N)=SIGMA(N)*Z
THETA=THETA*Z
BETA=BETA*Z
ALFP(N)=ALFP(N)*Z

```

```

ALFI(N)=ALFI(N)*Z
ALFO=ALFO*Z
SIGMA(N)=SIGMA(N)+SIGINC
GO TO 11
9 IF(CODEL.LT.3.0) GO TO 510
WKI TE(KPR,1039) SIGMA(N),XJPRI(N),ALFP(N),ALFI(N),A.FD,DJO,ANGCG,DE
ILANG
510 CCNTINUE
SIGMA(N)=SIGMA(N)*Z
THETA=THETA*Z
BETA=BETA*Z
ALFP(N)=ALFP(N)*Z
ALFI(N)=ALFI(N)*Z
ALFO=ALFO*Z
11 IF(DCO.LT.XORID) GO TO 19
IF(LL.EQ.2) GO TO 12
C SAVE DATA FOR PV AND CRAG TORQUE CALCULATION
U1=CDCG
-----
U2=XOMEGA
U3=SUMANG
U4=CGC
U5=XKPRIC
U6=ANGCG*Z
-----
U7=XI(I)
U8=YI(J)
U9=SIGMA(N)
IF(K.EQ.1)U9=U9-SIGINC
U10=DOO
U11=BETA
U12=RHOI(I)
-----
U13=ALFI(N)/Z
U14=ALFO/Z
U15=U9/Z
L=2
C END OF SAVE DATA FOR PV
C CALC. AND SAVE DEFLECTION DATA FOR LOAD POINT STRESS COMPUTATIONS
C CALC.
12 RTOL=(TORQ*2.0)/(SPRAGS*DOO)
RNUL=RTOL/DTAN(ALFO)
RTIL=(TORQ*2.0)/(SPRAGS*XIROD)
RNIL=RTIL/DTAN(ALFI(N))
PRESSJ=SPRAGS*RNUL/(PI*DOO*WIDTH)
-----
SRPRS2=-PRESSJ
RISQ=XORIDR*.25*XURODR
RISQ=XORIDR*.25*XORICR
STPRS2=PRESSJ*(RISQ+RISQ)/(KOSQ-RISQ)
URPRS2=0.5*XORIDR*(STPRS2-POISSN*SRPRS2)/ELSMOD
CALCID=XORIDR+2.0*URPRS2
-----
C SAVE
IF(CALCID.GT.1000) GO TO 19
IF(LL.EQ.2) GO TO 19
UU1=SIGMA(N)-SIGINC
UU2=ALFI(N)
UU3=ALFO
-----
UU4=DJJ
UU5=RHOI(I)
UU6=RHOJ(II)
UU7=RTOL
UU8=RNIL
UU9=RTIL
-----

```

```

UU10=RVIL
UU11=CALCID
SHPMAX=STPRS2 +STROT2
UK-PMX=URPRS2+URROT2
LL=2

```

C END OF SAVE DATA FOR LCAC POINT

```

19 IF(SIGMI(M).EQ.0.0) GO TO 20
   IF(SIGMA(N).GE.SIGMI(M).AND.K.EQ.1) GO TO 30
   IF(K.EQ.2) GO TO 31
   IF(K.EQ.3) GO TO 32
20 IF(SIGMO(MM).EQ.0.0) GO TO 50
   IF(SIGMA(N).GE.SIGMO(MM).AND.KK.EQ.1) GO TO 35
   IF(KK.EQ.2) GO TO 36
   IF(KK.EQ.3) GO TO 37
   GO TO 50
30 TEMP=SIGMA(N)
   SIGMA(N)=SIGMI(M)
   K=2
   GO TO 6
31 SIGMA(N)=SIGMI(M)
   I=I+1
   J=J+1
   K=3
   GO TO 5
32 SIGMA(N)=TEMP
   K=1
   M=M+1
   GO TO 50
35 TEMP=SIGMA(N)
   SIGMA(N)=SIGMI(MM)
   KK=2
   GO TO 6
36 SIGMA(N)=SIGMO(MM)
   II=II+1
   JJ=JJ+1
   KK=3
   GO TO 6
37 SIGMA(N)=TEMP
   KK=1
   MM=M+1
50 SIGMA(N+1)=SIGMA(N)

```

C PV AND DRAG TORQUE CALCULATIONS

```

WRITE(KPR,1045)
WRITE(KPR,1046)
WRITE(KPR,1047) U15,U10
WRITE(KPR,1048) U13,U14
WRITE(KPR,1051)
WRITE(KPR,1052)
WRITE(KPR,1053)
WRITE(KPR,1054)
WRITE(KPR,1057)
WRITE(KPR,1062)
ANGSPF=ANGSPF*Z

```

```

ANGSPB=ANGSPB*Z
NNN=1
DO 86 NNN=1,2
IF (NNN.EQ.1) GO TO 62
SPRNGK=0.0
WTSPNG=0.0
62 IF (SPRNGS.EQ.1.0) GO TO 63
CJSP=DSQRT((XSP-U7)*(XSP-U7)+(U8-YSP)*(U8-YSP))
TAU=DATAN((U8-YSP)/(XSP-U7))
SPC=DSQRT(U5*U5+COSP*CCSP-2.0*U5*COSP*DCOS(TAU+J9))
ANGSP=DARSIN(COSP*DSIN(TAU+U9)/SPC)
S4=(2.0*PI*SPRNGK*(DSPRNG-2.0*SPC))/SPRAGS
A1=DSIN(ANGSP)
A2=DCOS(ANGSP)
GO TO 64
63 CUSPF=DSQRT((XSF-U7)*(XSF-U7)+(U8-YSF)*(U8-YSF))
CUSPB=DSQRT((U7-XSB)*(U7-XSB)+(U8-YSB)*(U8-YSB))
TAUF=DATAN((U8-YSF)/(XSF-U7))
TAUH=DATAN((U8-YSB)/(U7-XSB))
SFC=DSQRT(U5*U5+CUSPF*CCSPF-2.0*U5*CCSPF*DCOS(TAU+U9))
SBC=DSQRT(U5*U5+CUSPB*CCSPB-2.0*U5*CUSPB*DCOS(TAU+PI-U9))
SFC=0.5*(SFC+SBC)
ANGCFS=DARSIN(CUSPF*DSIN(TAUF+U9)/SFC)
ANGCBS=DARSIN(CUSPB*DSIN(TAUH+PI-U9)/SBC)
S4=SPRNGK*SPNGHT
64 S4=SPRNGS*S5
S5=(PI*PI*GRAMLB*WTSPNG*SPC)/(900.0*SPRAGS*GRAVTY)
S5=SPRNGS*S5
S6=(PI*PI*GRAMLB*WTSPAG*U4)/(900.0*GRAVTY)
A3=DSIN(U6)
A4=DCOS(U6)
A5=DSIN(U11)
A6=DCOS(U11)
IF (SPRNGS.EQ.1.0) GO TO 640
S1=A2-(A1*A6/A5)
S2=A4-(A3*A6/A5)
S3=((XIROD*FRCOSL)/(U10*A5))-((FRCOSL*A6)/(A5))-1.0
S7=(S1*S4)/(WIDTH*S3)
S8=(S1*S5)/(WIDTH*S3)
S9=(S2*S6)/(WIDTH*S3)
GO TO 641
640 A30=CSIN(ANGSPB)
A31=DCOS(ANGSPB)
A32=DSIN(ANGSPF)
A33=DCOS(ANGSPF)
XMB=SPC*DSIN(0.5*PI-ANGCBS-ANGSPB)
XMF=SPC*DCOS(ANGSPF-ANGCFS)
SS0=A5+FRCOSL*A6
SS1=A6*A31+A30*A5
SS2=A6*A33+A32*A5
SS3=A6*A3-A4*A5
SSS1=SS1-((2.0*XMB)/U10)
SSS2=((2.0*XMF)/U10)-SS2
SSS3=SS0-((FRCOSL*XIROD)/U10)
SSS5=DSIN(ANGSPF-ANGCFS)

```

```

SS7=S4/(DCOS(0.5*PI-ANGSPF+ANGCBS))
SS8=DSIN(0.5*PI-ANGSPF+ANGCBS)/DCOS(ANGSPF+ANGCBS)
SS7=(SS7*(SS1+SS8+SS2))/(WIDTH*SS3)
SS8=(SS7*(SS1+SS8+SS2))/(WIDTH*SS3+SS5)
SS9=(SS3*S6)/(WIDTH*SS3)
S7=S7
S8=S8
S9=S9
641 S10=PI*XIR0D/12.0
S11=S7*S10
S12=(S8+S9)*S10
FSPEED1=4.0*SPEED*SPEED/9.0
FSPEED2=(4.0*S11)/(3.0*S12)
FSPEED=FSPEED1-FSPEED2
IF(FSPEED.LT.0.0)GO TO 642
MXSPEED=0.5*(2.0*SPEED/3.0)+DSQRT(FSPEED)
642 BB=DSQRT((A.0/(PI*WIDTH))*(U12*0.5*XIR0D/(U12+0.5*XIR0D))*(1.0-POI
ISSN*POISSN)/ELSMOD)
65 NN=1
DO 85 NN=1,6
GO TO (66,67,69,69,70,71),NN
66 PERCNT=0.0
SPEED0=PERCNT*SPEED/100.0
GO TO 72
67 PERCNT=25.0
SPEED0=PERCNT*SPEED/100.0
GO TO 72
68 PERCNT=50.0
SPEED0=PERCNT*SPEED/100.0
GO TO 72
69 IF(SPEED.GT.0.0)GO TO 511
SPEED0=0.0
MXSPEED=0.0
PERCNT=0.0
GO TO 72
511 IF(FSPEED.LT.0.0)GO TO 75
SPEED0=MXSPEED
PERCNT=100.0*SPEED0/SPEED
GO TO 72
512 PERCNT=100.0*SPEED0/SPEED
GO TO 72
70 PERCNT=75.0
SPEED0=PERCNT*SPEED/100.0
GO TO 72
71 PERCNT=100.0
SPEED0=SPEED
72 FSP=S4
FSPPP=S5*SPEED0*SPEED0
FCG=S6*SPEED0*SPEED0
IF(SPRNGS.EQ.1.0)GO TO 721
FSP=FSP+FSPPP
NNI=(FSP*S1+FCG*S2)/S3
GO TO 722
721 FSRACF=S4
FSPPF=FSRACF/DCOS(0.5*PI-ANGSPF+ANGCBS)
FSTANF=FSRACF*CTAN(0.5*PI-ANGSPF+ANGCBS)
FSTANB=FSTANF
FSPPH=FSPPF/DCOS(ANGSPF+ANGCBS)
RESF=FSPPF+FSPPP/SS5
RESTNF=RESF*DSIN(0.5*PI-ANGSPF+ANGCBS)
KLSNB=RESTNF
KLSB=RESTNF/DCOS(ANGSPF+ANGCBS)

```

```

RNI=(RESB*SSS1+RESF*SSS2+FCG*SS3)/SSS3
722 RTI=FRCDL/RNI
TURQDG=0.5*SPRAGS*RTI*XIROD
V=SIO*(SPEED-SPEEDC)
P=RNI/WIDTH
PV=P*V
B=B*DSQRT(RNI)
IF(RNI.EQ.0.0) GO TO 73
PKS=RNI/(B*WIDTH)
GO TO 74
73 PKS=0.0
C FILM THICKNESS CALCULATIONS
74 PKSV=(PRS*VI)/60.0
WPRI=RNI/WIDTH
CMRACE=SPEED*PI/30.0
OMSPRG=SPEEDO*PI/30.0
JVELRA=XIROD*OMRACE*.5
JVELSP=XIROD*OMSPRG*.5
EQUIVR=UI2*XIROD*.57/(UI2+XIROD*.5)
EPRI=ELSMOD/(1.0-POISSN*POISSN)
WFILM=WPRI/(EPRI*EQUIVR)
JFILM=(JVELRA-JVELSP)*.5*REYNS/(EPRI*EQUIVR)
GFILM=COPRVI*EPRI
IF(WFILM.EQ.0.0) GO TO 76
HFILM=1.6*GFILM**.5*JFILM**.7/WFILM**.13
FILEHD=HFILM*EQUIVR*100000.0
FILMYD=(4.9*JFILM*EQUIVR/WFILM)*1000000.0
75 IF(FSPED.LT.0.0.AND.NN.EQ.4) GO TO 77
WRITE(KPR,1055) PERCNT,P,V,PV,SPEED,SPEEDO,TORQDG,PRS,PRSV,FCG,FSPP
1,FSPPP,FILMYD,FILEHD
GO TO 85
76 WRITE(KPR,1058) PERCNT,P,V,PV,SPEED,SPEEDO,TORQDG,PRS,PRSV,FCG,FSPP
1,FSPPP
GO TO 85
77 WRITE(KPR,1060)
78 CONTINUE
IF(NN.EQ.2) GO TO 86
WRITE(KPR,1063)
79 CONTINUE
C STRESS AND DEFLECTION CALCULATIONS
UU1=UU1/Z
UU2=UU2/Z
UU3=UU3/Z
WRITE(KPR,1075)
WRITE(KPR,1076)
WRITE(KPR,1077) UU1,UU4
WRITE(KPR,1078) UU2,UU3
IF(CCDE1.LT.2.0) GO TO 515
WRITE(KPR,1079)
WRITE(KPR,1080)
WRITE(KPR,1081)
WRITE(KPR,1082)
WRITE(KPR,1083)
WRITE(KPR,1084)
515 CONTINUE
DIVIC2=10.0
RINC1=(XIKOU-XIRID)/DIVIC2
RINC2=(XOROD-XORID)/DIVIC2
RUTCOV=((3.0*POISSN)/8.0)*(PI*PI*SPEED*SPEED*WTDENS)/(900.*GRAVITY)
DIARTI=DSQRT(XIRID*XIROC)

```

```

DIARTJ=DISORT(XORID*XOROD)
DIAINN=XIRID
DIAOUT=XORID
ILI=1
INNER=1
DO 100 INNER=1,11
92 IF(DIAINN.LT.DIARTJ) GO TO 95
IF(ILI.GT.1) GO TO 93
TEMPI=DIAINN
DIAINN=DIARTJ
ILI=2
GO TO 95
93 IF(ILI.GT.2) GO TO 95
DIAINN=TEMPI
ILI=3
95 AA1=XIRID*.25*XIRID
AA2=XIROD*.25*XIROD
AA3=DIAINN*.25*DIAINN
AA4=(1.0+3.0*POISSN)/(3.0+POISSN)
SKROTJ=ROTCON*(AA1+AA2-AA1*AA2/AA3-AA3)
STROTJ=ROTCON*(AA1+AA2+AA1*AA2/AA3-AA4*AA3)
URROTJ=(0.5*DIAINN/ELSMOD)*(STROTJ-PCISSN*SRROTJ)
PRSI=(SPRAGS*UJ10)/(PI*XIRID*WIDTH)
SKPRSI=(-PRSI)*AA2*(AA3-AA1)/(AA3*(AA2-AA1))
STPRSI=(-PRSI)*AA2*(AA3+AA1)/(AA3*(AA2-AA1))
UKPRSI=(0.5*DIAINN/ELSMOD)*(STPRSI-POISSN*SRPRSI)
SRROTJ=SRROTJ+SKPRSI
STROTJ=STROTJ+STPRSI
URROTJ=URROTJ+URPRSI
IF(CODE1.LT.2.0) GO TO 520
WRITE(KPR,1085) DIAINN, SRROTJ, STROTJ, URROTJ, SRPRSI, STPRSI, JRPRSI, SR
LTOTJ, STTOTJ, URTOTJ
520 CONTINUE
IF(ILI-2) 100,92,100
100 DIAINN=DIAINN+RINCI
IF(CODE1.LT.2.0) GO TO 525
WRITE(KPR,1086)
525 CONTINUE
ILO=1
I OUTER=1
DO 110 I OUTER=1,11
102 IF(DIAOUT.LT.DIARTC) GO TO 105
IF(ILO.GT.1) GO TO 103
TEMPO=DIAOUT
DIAOUT=DIARTC
ILO=2
GO TO 105
103 IF(ILO.GT.2) GO TO 105
DIAOUT=TEMPO
ILO=3
105 AA5=XORID*.25*XORID
AA6=XOROD*.25*XOROD
AA7=DIAOUT*.25*DIAOUT
SKROTJ=ROTCON*(AA6+AA5-AA5*AA6/AA7-AA7)
STROTJ=ROTCON*(AA6+AA5+AA5*AA6/AA7-AA4*AA7)
URROTJ=(0.5*DIAOUT/ELSMOD)*(STROTJ-PCISSN*SRROTJ)
PKSO=(SPRAGS*UUB)/(PI*XORID*WIDTH)
SKPRSO=(-PKSO)*AA5*(AA6-AA7)/(AA7*(AA6-AA5))
STPRSO=(-PKSO)*AA5*(AA6+AA7)/(AA7*(AA6-AA5))
UKPRSO=(0.5*DIAOUT/ELSMOD)*(STPRSO-PCISSN*SRPRSO)

```

```

SRTOTO=SRROT+SRPRS0
STTOTO=STRTOT+STPRS0
URTOTO=URROT+URPRS0
IF(I OUTER.GT.1) GO TO 530
530 IF(CCDE1.LT.2.0) GO TO 535
WRITE(KPR,1085)DIAOUT,SRRO TO,STKOTO,URRO TO,SRPRS0,STPRS0,URPRS0,SR
LTOFO,STTOTC,URTOTO
535 CONTINUE
IF(ILO-2)110,102,110
110 DIAOUT=DIAOUT+RINCO
WRITE(KPR,1092)UUA
WRITE(KPR,1089)S+FMAX,URHPMX
C
DX=DSQRT(8.0*(1.0-POISSN*POISSN)/(PI*WIDTH*ELSMOD))
DI=BX*DSQRT(UU10*0.5*(RCD*UU5/(0.5*(IROD+JJ5)))
DU=DX*DSQRT(UU8*0.5*(UU11*UU6/(0.5*(UU11-UU6)))
SCOMP1=2.0*UU10/(PI*BI*WIDTH)
SCOMP2=2.0*UU8/(PI*BO*WIDTH)
UX=2.0*(1.0-POISSN*POISSN)/ELSMOD
URHTZ1=(UX*UU10/(PI*WIDTH))*(DLOG((2.0*UU5*WIDTH)/(BI*BI))+1.6002)
URHTZ0=((UX*UU8)/(PI*WIDTH))*(DLOG((2.0*UU6*WIDTH)/(BO*BO))+1.6002)
1)
WRITE(KPR,1090)SCOMP1,URHTZ1
WRITE(KPR,1091)SCOMP2,URHTZ0
WRITE(KPR,1100)
GO TO 1
1000 FORMAT(1X,79+
1
1001 FORMAT(116X,' G117-1.7- 3/72d)
1002 FORMAT(6F12.5)
1003 FORMAT(3(F6.5,F6.2,2F6.5))
1004 FORMAT(3X,' HORSEPOWER ..... @,F10.4,5X, 'T
TORQUE (IN-LBS) .....@,F10.4)
1005 FORMAT(3X,' SPEC (RFM) .....@,F11.4,5X, 'F
RICTION COEFF. (SLIDING) .....@,F7.4/)
1006 FORMAT(3X,' X COORDINATE-SPRING (IN) ..... @,F6.4,5X,
1'X COORDINATE-C.G. (IN) .....@,F8.4)
1007 FORMAT(3X,' Y COORDINATE-SPRING (IN) ..... @,F6.4,5X,
1'Y COORDINATE-C.G. (IN) .....@,F8.4)
1008 FORMAT(3X,' SPRING WEIGHT (GM) ..... @,F6.4,5X,
1'SPRAG WEIGHT (GM) .....@,F8.4)
1009 FORMAT(3X,' NO. OF SPRINGS ..... @,F6.4,5X,
1'NO. OF SPRAGS ..... @,F7.4)
1010 FORMAT(3X,' INNER RACE O.D. ....@,F9.4,5X,
1'OUTER RACE I.D.(NOM.) .....@,F9.4)
1011 FORMAT(3X,' NUMBER OF INCREMENTS .....@,F9.4,5X,
1'SIGMA ANGLE (DEGREES) ....@,F8.4,'(MIN)....@,F9.4,'(MAX)@)
1012 FORMAT(3X,' SPRING DIA.-FREE (IN) ..... @,F6.4,4X,
1'EFFECTIVE SPRAG LENGTH (IN) .....@,F8.4)
1013 FORMAT(3X,' SPRING CONST (LB/IN) .....@,F8.4/)
1014 FORMAT(/17X,' COORDINATES@,9X,'RADIUS OF@,8X,'SIGMA ANGLE@)
1015 FORMAT(15X,' X@,11X,'Y@,9X,'CURVATURE@,10X,'(DEGREES)@)
1016 FORMAT(/3X,' INNER@,4X,F9.5,3X,F9.5,5X,F9.5,10X,F9.5)
1017 FORMAT(3X,' RACE@,5X,F9.5,3X,F9.5,5X,F9.5,10X,F9.5)
1018 FORMAT(13X,F9.5,3X,F9.5,5X,F9.5,10X,F9.5)
1019 FORMAT(/3X,' OUTER@,4X,F9.5,3X,F9.5,5X,F9.5,10X,F9.5)
1020 FORMAT(3X,' RACE@,5X,F9.5,3X,F9.5,5X,F9.5,10X,F9.5)
1021 FORMAT(13X,F9.5,3X,F9.5,5X,F9.5,10X,F9.5)

```

```

1022 FJRMAT(3X,' INNER RACE I.D. ....@,F9.4,5X,
1' OUTER RACE O.D. ....@,F9.4)
1023 FJRMAT(3X,' X COORDINATE-SPRING FRNT FACE (IN) ..... @,F5.4,5X,
1' X COORDINATE-SPRING EACK FACE (IN) .....@,F8.4)
1024 FJRMAT(3X,' Y COORDINATE-SPRING FRONT FACE (IN) ..... @,F5.4,5X,
1' Y COORDINATE-SPRING EACK FACE (IN) .....@,F8.4)
1025 FJRMAT(3X,' SPRAG CONTACT ANGLE-FRONT FACE (DEG.) .... ',F7.4,5X,'
1' X COORDINATE-C.G. (IN) .....',F8.4)
1026 FJRMAT(3X,' SPRAG CONTACT ANGLE-BACK FACE (DEG.) .... ',F7.4,5X,'
1' Y COORDINATE-C.G. (IN) .....',F8.4)
1027 FJRMAT(3X,' SPRING HEIGHT-FREE (IN) ..... @,F5.4,4X,
1' EFFECTIVE SPRAG LENGTH (IN) .....',F8.4)
1033 FJRMAT(1/10X,' FLAT PLATE DIMENSICNS@,3X,' CURVED SURFACE DIMENSIONS
1a)
1034 FJRMAT(10X,' ----- 0
1' OUTER')
1035 FJRMAT(2X,' SIGMA@,13X,' INNER STRUT@,8X,' STRUT ANGLE@,11X,' RACE@,
17X,' CG',5X,' DIFF')
1036 FJRMAT(2X,' ANGLE@,3X,' J PRIME@,6X,' ANGLE@,9X,' INNER@,7X,' OUTER@,8X
1,' I.D.',6X,' ANGLE ANGLE')
1037 FJRMAT(1X,F8.4,1X,F8.4,3X,F8.4,6X,F8.4,4X,F8.4,5X,F8.4,4X,F6.3,2X,
1F6.3)
1038 FJRMAT(1X,F8.4,' *@,F7.4,3X,F8.4,6X,F8.4,4X,F8.4,5X,F8.4,4X,F6.3,2
1X,F6.3)
1039 FJRMAT(2X,' (DEG)',4X,' (IN)',8X,' (DEG)',9X,' (DEG)',7X,' (DEG)',8X,' (
1IN)',6X,' (DEG) (DEG)')
1045 FJRMAT(1/40X,' OVERRUN + DIFFERENTIAL SPEED POINT VALUES')
1046 FJRMAT(40X,' -----@/)
1047 FJRMAT(3X,' SIGMA ANGLE (DEGREES) .....@,1X,1F8.4
1,6X,' DEFLECTED OUTER RACE I.D. (IN) .....@,1X,1F8.4)
1048 FJRMAT(3X,' INNER STRUT ANGLE (DEGREES) .....@,2X,1F7.4
1,6X,' OUTER STRUT ANGLE (DEGREES) .....@,2X,1F7.4)
1051 FJRMAT(1/35X,' INNER CUTEN@,33X,' SPRAG@,12X,' SPRING FILM FILM
1a)
1052 FJRMAT(' PERCENT P V P-V RACE RACE DRAG
1 PRS PRS-V CENTRIF. SPRING CENTRIF. THK. THK.@)
1053 FJRMAT(1X,' SPEED@,29X,' SPEC SPEED TORQUE@,23X,' FORCE FOR
1CE FORCE HYD. EHD.@)
1054 FJRMAT(10X,' (PPI) (FPM) (PPI-FPM) (RPM) (RPM) (IN-LB) (
1PSI) (PSI-FPS) (LB) (LB) (MICRO-IN)@)
1055 FJRMAT(2X,F6.2,2X,F6.2,2X,F6.0,2X,F7.0,3X,F6.0,2X,F6.0,2X,F7.2,3X,
1F7.0,2X,F8.0,2X,F6.1,3X,F5.2,3X,F5.2,3X,F7.2,1X,F5.2)
1057 FJRMAT(1X,' -----@/)
1' -----@/)
1059 FJRMAT(2X,F6.2,2X,F6.2,2X,F6.0,2X,F7.0,3X,F6.0,2X,F6.0,2X,F7.2,3X,
1F7.0,2X,F8.0,2X,F6.1,3X,F5.2,3X,F5.2,3X,' -----@,1X,' -----@)
1060 FJRMAT(1X,' MAX. SPEED NOT CALCULATED, EQUATION CONTAINS A NEGATIV
1E SQUARE ROOT@)
1062 FJRMAT(55X,' WITH SPRING@)
1063 FJRMAT(1/53X,' WITHOUT SPRING@)
1075 FJRMAT(1/51X,' LOAD POINT VALUES@)
1076 FJRMAT(51X,' -----@)
1077 FJRMAT(1/3X,' SIGMA ANGLE (DEGREES) .....@,1X,1F8.
14,6X,' DEFLECTED OUTER RACE I.D. (IN) .....@,1X,1F8.4)
1078 FJRMAT(3X,' INNER STRUT ANGLE (DEGREES) .....@,2X,1F7.4
1,6X,' OUTER STRUT ANGLE (DEGREES) .....@,2X,1F7.4)
1079 FJRMAT(1/20X,' ROTATIONAL COMPONENT@,16X,' PRESSURE COMPONENT@,27X
1,' TOTAL@)
1080 FJRMAT(15X,' -----@,5X,' -----@)
1' -----@,5X,' -----@)

```

```

1081 FORMAT(15X,' RACIAL    TANGENTIAL    RADIAL    RADIAL    TANGENT
      1IAL    RADIAL    RADIAL    TANGENTIAL    RADIAL)
1082 FORMAT(1X,' DIAMETER    STRESS    STRESS    DEFLECTION    STRE
      1SS    STRESS    DEFLECTION    STRESS    STRESS    DEFLECTION)
1083 FORMAT(3X,' (IN)2,9X,'(PSI)    (PSI)    (IN)2,9X,'(PSI)
      1 (PSI)    (IN)2,9X,'(PSI)    (PSI)    (IN)2)
1084 FCORMAT(//53X,' INNER RACE)
1085 FCORMAT(3X,1F7.4,3(5X,F8.C,4X,F8.C,3X,F8.6))
1086 FCORMAT(//53X,' OUTER RACE)
1089 FORMAT(/2X,' OUTER RACE I.D. HOOP STRESS MAX. (PSI) .....
      1.....2,1X,1F8.0,7X,' DEFLECTION (IN) .....2,1X,1F8.6)
1090 FORMAT(/2X,' INNER RACE)4X,'COMPRESSIVE STRESS MAX. - HERTZ (PSI)
      1 .....2,1X,1F8.0,7X,' DEFLECTION (IN) .....2,1X,1F8.6)
1091 FORMAT(2X,' OUTER RACE)4X,'COMPRESSIVE STRESS MAX. - HERTZ (PSI)
      1.....2,1X,1F8.0,7X,' DEFLECTION (IN) .....2,1X,1F8.6)
1092 FCORMAT(/2X,' NORMAL LOAD PER SPRAG AT OUTER RACE CONTACT POINT (LB
      1) ...',1F6.0/)
1100 FORMAT(1H1)
1101 FCORMAT(1X)
      END

```

APPENDIX III
RAW DATA, OVERRIDE TEST

CLUTCH DESIGN A

<u>Oil Flow (gpm)</u>	<u>Inner Race Speed (rpm)</u>	<u>Shaft Torque (in. - lb)</u>	<u>Reaction Torque (in. - lb)</u>	<u>Oil ΔT ($^{\circ}$ F)</u>	<u>Btu/hr</u>	<u>Torque Calculated Using Oil ΔT (in. - lb)</u>
2.4	26,500	11.0	8.4	37	19,350	18.1
	25,000	9.9	8.0	33	17,250	17.1
	20,000	8.8	7.4	34	17,800	22.0
	20,000	8.2	5.9	23	12,000	19.8
	10,000	4.0	4.4	17	8,900	22.0
	5,000	2.3	2.6	13	6,800	33.0
1.6	26,500	8.3	8.1	34	11,900	11.0
	25,000	7.4	7.6	31	10,000	10.7
	20,000	7.5	7.1	26	9,100	11.3
	15,000	6.0	5.8	19	6,600	10.9
	10,000	4.5	4.6	14	4,900	12.1
	5,000	3.1	3.6	5	1,740	8.4
.8	26,600	7.4	5.7	38	6,600	6.2
	25,000	7.1	5.4	33	5,800	5.8
	20,000	5.8	4.9	25	4,400	5.5
	15,000	5.3	4.8	21	3,700	6.1
	10,000	4.6	4.3	19	3,300	8.2
	5,000	3.4	3.4	9	1,570	7.5
.54	26,500	7.5	4.6	50	5,850	5.5
	25,000	7.6	4.7	42	4,900	4.9
	20,000	5.4	3.9	30	3,500	4.3
	15,000	3.8	3.3	14	1,640	2.7
	10,000	3.9	3.6	12	1,400	3.5
	5,000	2.8	2.8	3	350	1.7

CLUTCH DESIGN B

<u>Oil Flow (gpm)</u>	<u>Inner Race Speed (rpm)</u>	<u>Shaft Torque (in. -lb)</u>	<u>Reaction Torque (in. -lb)</u>	<u>Oil ΔT ($^{\circ}$ F)</u>	<u>Btu/hr</u>	<u>Torque Calculated Using Oil ΔT (in. -lb)</u>
2.4	26,500	8.6	10.2	30	15,700	14.7
	25,000	7.9	9.3	22	11,500	11.4
	20,000	6.4	7.4	15	7,800	9.7
	15,000	5.4	5.9	10	5,200	8.6
	10,000	4.1	4.4	6	3,100	7.7
	5,000	2.9	3.3	4	2,100	10.4
1.6	26,500	7.9	9.2	30	10,500	9.8
	25,000	7.6	8.5	28	9,800	8.7
	20,000	6.1	6.4	15	5,200	6.4
	15,000	6.1	5.2	5	1,750	2.9
	10,000	3.9	3.8	6	2,100	5.2
	5,000	2.7	2.4	5	1,750	8.7
.8	26,500	4.0	8.4	50	8,700	8.1
	25,000	3.9	8.0	45	7,800	7.7
	20,000	4.6	6.2	30	5,200	6.4
	15,000	4.7	5.1	17	3,000	5.0
	10,000	3.9	4.4	8	1,400	3.5
	5,000	2.7	3.0	3	520	2.6
.54	26,500	1.9	6.7	66	7,700	7.2
	25,000	2.0	6.1	53	6,200	6.2
	20,000	2.4	5.1	34	4,000	5.0
	15,000	2.7	3.9	21	2,500	4.1
	10,000	2.5	3.3	11	1,300	3.2
	5,000	1.7	2.3	3	350	1.7
.26	26,500	5.2	4.4	76	4,400	4.1
	25,000	4.8	4.1	66	3,800	3.8
	20,000	3.9	3.6	46	2,600	3.2
	15,000	2.9	3.1	28	1,600	2.6
	10,000	2.6	2.6	16	920	2.3
	5,000	2.1	2.1	-	-	-

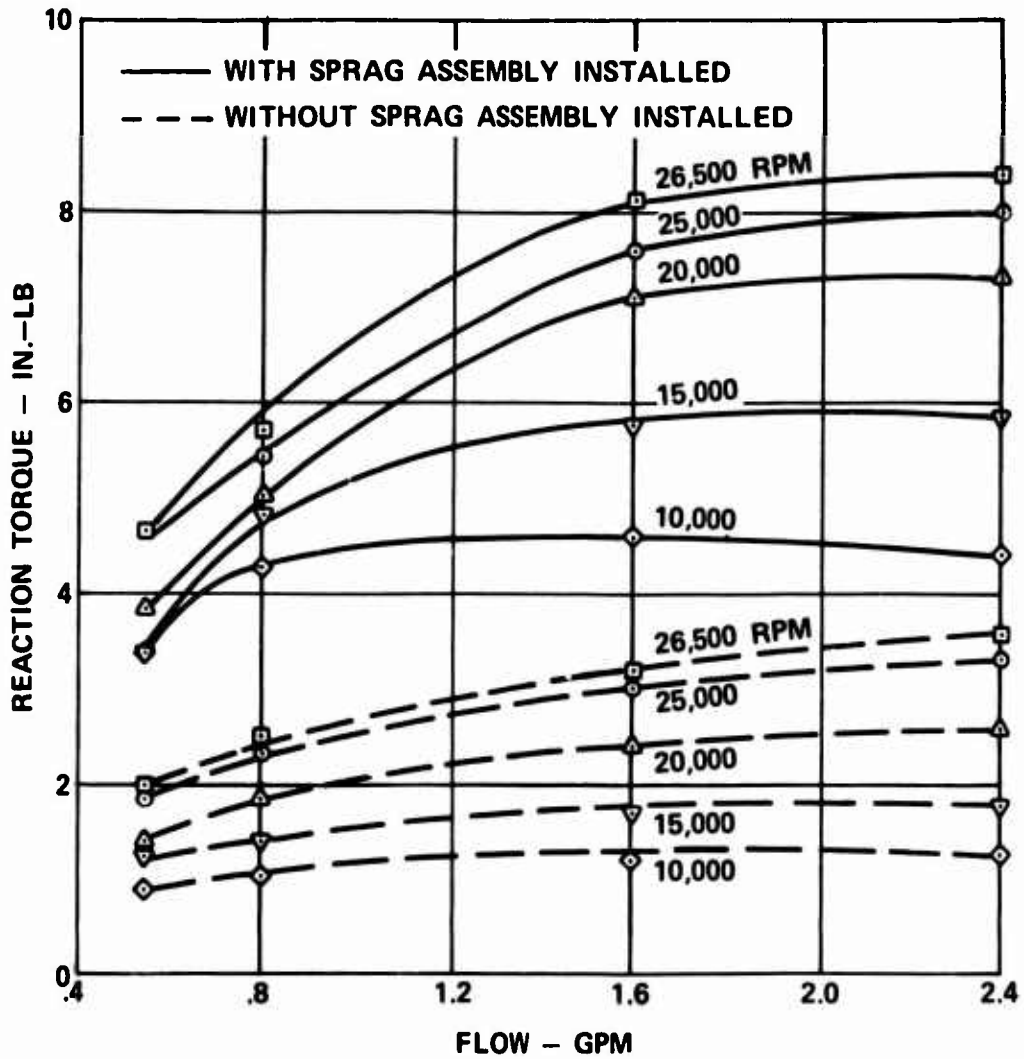


Figure 70. Reaction Torque Versus Oil Flow at Various Speeds, Design A Full-Speed Override (Input Stationary).

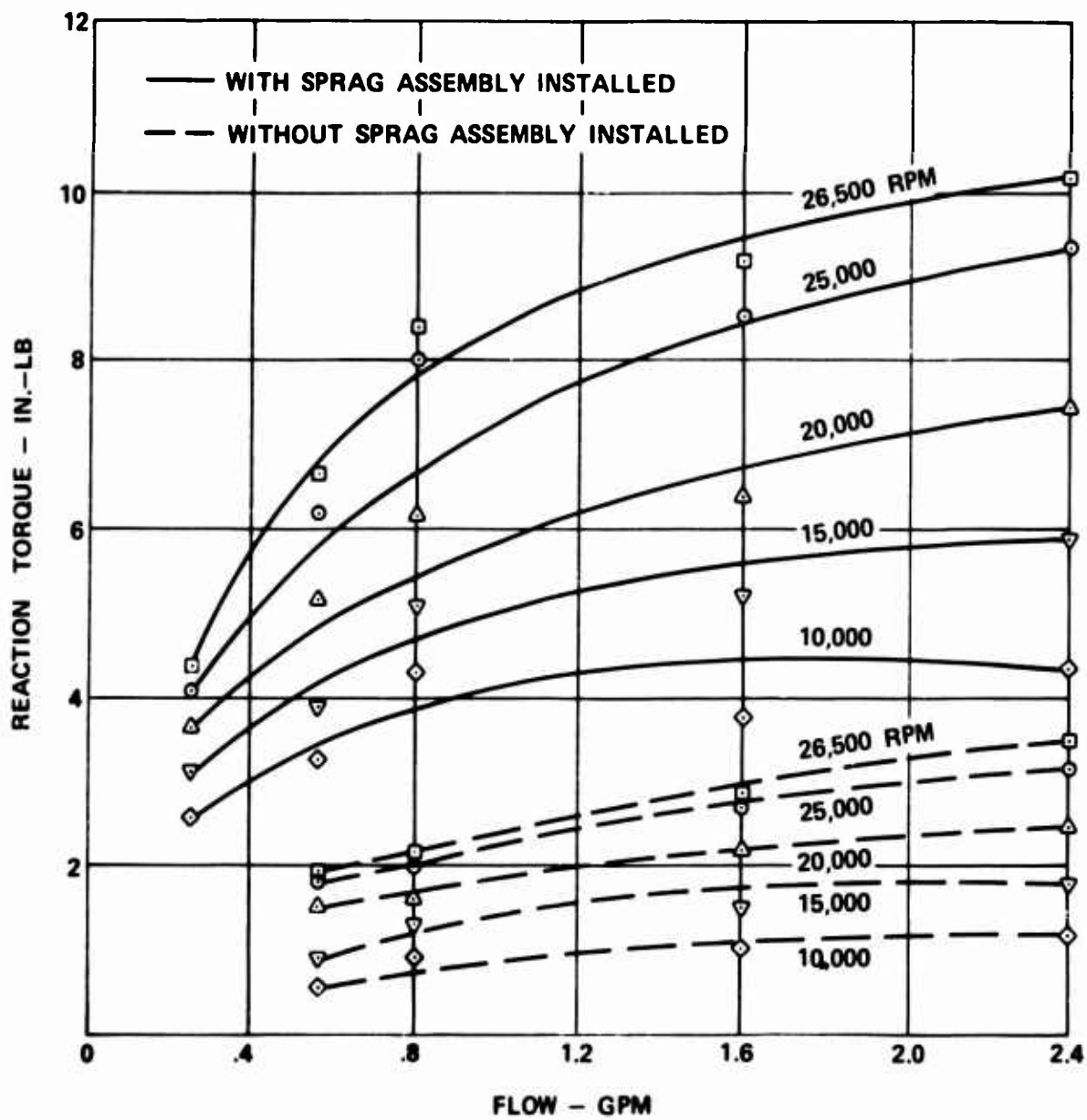


Figure 71. Reaction Torque Versus Oil Flow at Various Speeds, Design B Full-Speed Override (Input Stationary).

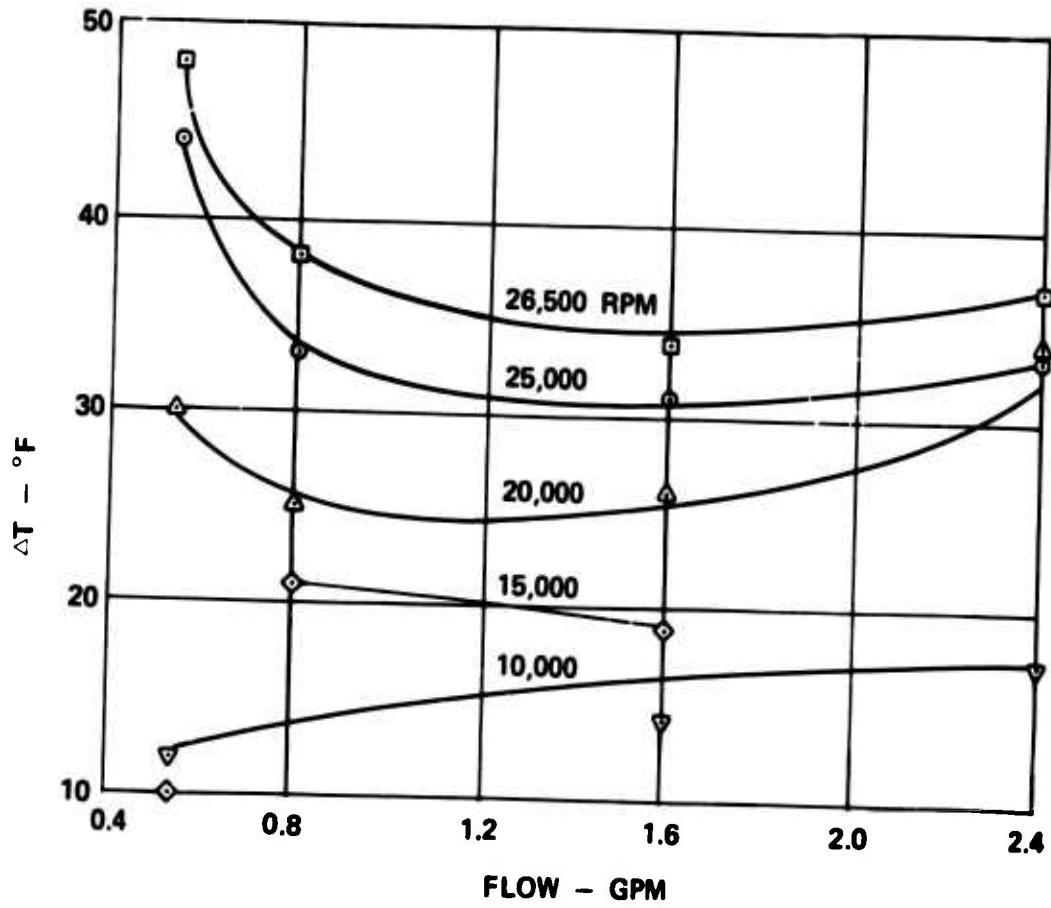


Figure 72. Oil ΔT Versus Flow at Various Speeds, Design A Full-Speed Override (Input Stationary).

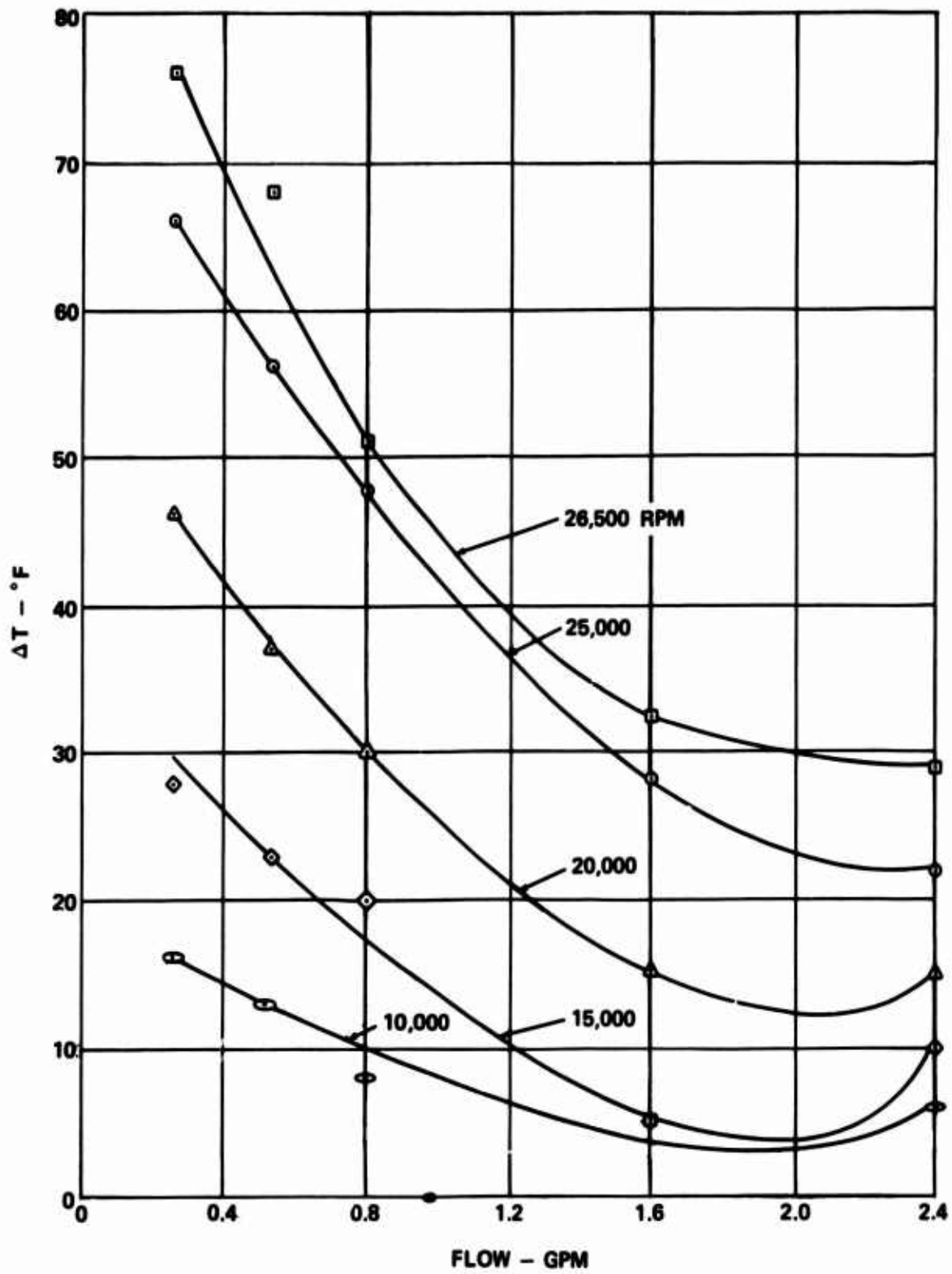


Figure 73. Oil ΔT Versus Flow at Various Speeds, Design B Full-Speed Override (Input Stationary).